NORTHERN STATES POWER COMPANY

MONTICELLO NUCLEAR GENERATING PLANT

SECOND RELOAD SUBMITTAL

NOVEMBER 1973

Prepared By

Northern States
Power Company

Information Supplied By

General Electric
Company

NORTHERN STATES POWER COMPANY

MONTICELLO NUCLEAR GENERATING PLANT

SECOND RELOAD SUBMITTAL

NOVEMBER 1973

Prepared By

Northern States
Power Company

Information Supplied By

General Electric
Company

LIST OF ILLUSTRATIONS

Table of Contents

1. INTRODUCTION

This document provides the technical basis of the license submittal for the second reload of Northern States Power/Monticello Unit 1. Presented herein is a description of the new fuel and the results of the evaluation of the refueled core for the February, 1974 outage.

The fuel at the site available for loading at the outage will be 116 Reload-2 fuel bundles, which are 8x8 bundles with an average enrichment of 2.62 wt% of U-235. There will also be available for reinsert 7 initial core bundles discharged at the end of Cycle 1 with an average exposure of about 7400 MWd/t.

The objective of this outage is to remove the 44 temporary control curtains which remained in the core during Cycle 2 and to load the core so as to assure the availability of the plant at high power for approximately an annual cycle.

Sections 3, 4, 5 and 6 of this document, dealing with the subjects of reload fuel mechanical design and reloaded core thermal-hydraulic and nuclear characteristics, and safety analysis, present descriptions of design criteria, methods and results from design calculations and safety evaluations and represents complete information for the review of fuel assembly and core design.

LIST OF ILLUSTRATIONS (Continued)

3. MECHANICAL DESIGN

3.1 GENERAL DESIGN DESCRIPTION

The 8x8 fuel bundle contains 63 fueled rods and one spacer-capture water rod which are spaced and supported in a square (8x8) array by the upper and lower tie plates (see Figure 3-1). The lower tie plate has a nosepiece which has the function of supporting the fuel assembly in the reactor. The upper tie plate has a handle for transferring the fuel bundle from one location to another. The identifying assembly number is engraved on the top of the handle, and a boss projects from one side of the handle to aid in assuring proper fuel assembly orientation. Both upper and lower tie plates are fabricated from Type-304 stainless steel castings.

Each fuel rod consists of high-density (95% TD) UO_2 fuel pellets stacked in a Zircaloy-2 cladding tube which is evacuated, backfilled with helium, and sealed by welding Zircaloy end plugs in each end. The fuel rod cladding thickness is adequate to be "free-standing," i.e., capable of withstanding external reactor pressure without collapsing onto the pellets within. Although most fission products are retained within the UO_2, a fraction of the gaseous products are released from the pellet and accumulate in a plenum at the top of the rod. Sufficient plenum volume is provided to prevent excessive internal pressure from these fission gases or other gases liberated over the design life of the fuel. A plenum spring, or retainer, is provided in the plenum space to prevent movement of the fuel column inside the fuel rod during fuel shipping and handling.

Three types of rods are employed in a fuel bundle: tie rods, a water rod, and standard rods. The eight tie rods in each bundle have threaded end plugs which thread into the lower tie plate casting and extend through the upper tie plate casting. A stainless steel hexagonal nut and locking tab are installed on the upper end plug to hold the assembly together. These tie rods support the weight of the assembly only during fuel handling operations when the assembly hangs by the handle; during operation, the fuel rods are supported by the lower tie plate. One rod in each fuel bundle (see Figure 3-2) is a hollow water tube used to position seven Zircaloy-4 fuel rod spacers vertically in the bundle.

2. SUMMARY

The Monticello Unit I Reload-2 fuel will employ an 8x8 fuel assembly configuration instead of the previously used 7x7. The pellet diameter, pellet length, cladding diameter, and rod pitch are changed from 7x7 design; however, the assembly exterior dimensions remain unchanged. The basic materials and fuel fabrication process used for the Reload-2 fuel assemblies are the same as those used on the 7x7 design.

The design reference core configuration for this license submittal consists of 116 Reload-2 new fuel bundles with an average enrichment of 2.62 wt% U-235, 20 Reload-1 fuel bundles with an average exposure about 5550 MWd/t and 348 Initial fuel bundles with an average exposure about 10,300 MWd/t. All temporary control curtains are removed from the core. The Reload-2 fuel bundle uses gadolinium for reactivity control augmentation. The relative location of the Reload-2 fuel bundles is shown in Figure 2-1. The design reference core was developed from an extrapolation from expected cycle 2 operation to the end of cycle and it contains extensive shuffling of irradiated fuel assemblies. At the time of the outage the final core loading will be analyzed and compared to the design reference case to insure that the core meets license requirements.

Shutdown calculations have been made on the full use of all Reload-2 bundles. Ample shutdown margin for the most reactive condition in the cycle has been calculated for the design reference core.

These results indicate that the reactor will be able to operate safely at 1670 MWt after the outage and satisfy all license requirements.

Table 2-1

FUEL TYPE AND NUMBER

Fuel Type	Number
Initial	348
Reload 1	20
Reload 2	116
Total	484

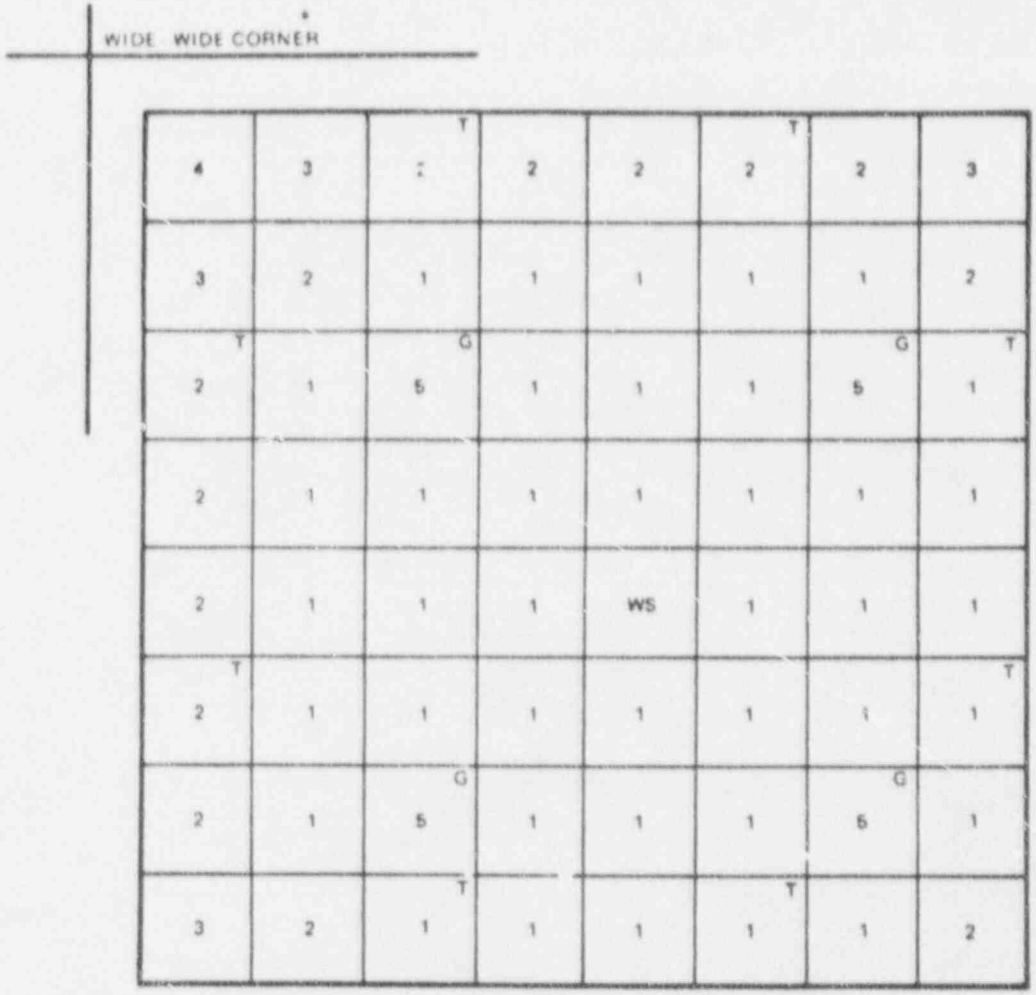

ROD TYPE	ENRICHMENT wt % U-235	NUMBER OF RODS
1	2.87	40
2	2.14	14
3	1.87	4
4	1.45	1
5	2.87	4
WS	–	1

WS – SPACER CAPTURE WATER ROD
T – TIE RODS
G – GADOLINIUM RODS

Figure 3-2. Monticello R2 Reload Fuel Lattice

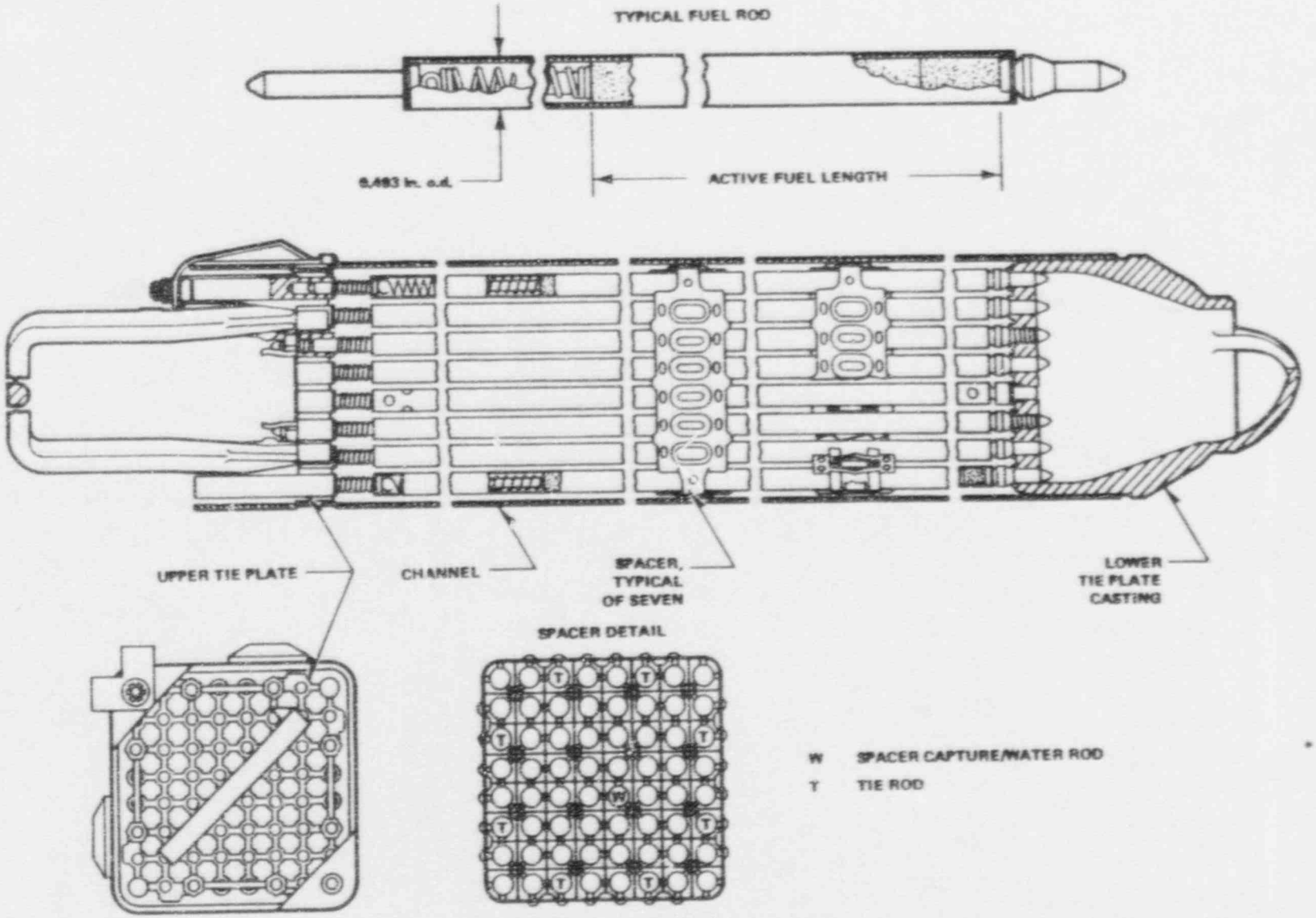

Figure 3-1. 8x8 Reload Fuel Assembly

Table 3-1 presents a summary of 8x8 design dimensions and a comparison to initial core and R1 fuel, and Figure 3-2 shows the location of the various fuel rod types within the Reload-2 assembly.

3.2 MECHANICAL DESIGN BASES

In meeting the power generation objectives, the nuclear fuel shall be used as the initial barrier to the release of fission products. The fission product retention capability of the nuclear fuel shall be substantial during normal modes of reactor operation so that significant amounts of radioactivity are not released from the reactor fuel barrier.

The nuclear fuel shall be designed to assure (in conjunction with the core nuclear characteristics, the core thermal and hydraulic characteristics, the plant equipment characteristics, and the capability of the nuclear instrumentation and reactor protection system) that fuel damage limits will not be exceeded during either planned operation or abnormal operational transients caused by any single equipment malfunction or single operator error.

3.2.1 Basis for Fuel Damage Analysis

Fuel damage is defined as a perforation of the fuel rod cladding which would permit the release of fission products to the reactor coolant.

The mechanisms which could cause fuel damage in reactor operational transients are: (1) rupture of the fuel rod cladding due to strain caused by relative expansion of the UO_2 pellet; and (2) severe overheating of the fuel rod cladding caused by inadequate cooling.

A value of 1% plastic strain of the Zircaloy cladding has traditionally been defined as the limit below which fuel damage due to overstraining of the fuel cladding is not expected to occur. The 1% plastic strain value is based on General Electric data on the strain capability of irradiated Zircaloy cladding segments from fuel rods operated in several BWRs.[3] None of the data obtained fall below the 1% plastic strain value; however, a statistical distribution fit to the available data indicates the 1% plastic strain value to be approximately

The water rod is a hollow Zircaloy-2 rod equipped with a square bottom end plug to prevent rotation and assure proper location of the water rod within the fuel assembly. Several holes are drilled around the circumference of the water rod at each end to allow coolant water to flow through the rod. The spacers are equipped with Inconel-X springs and maintain rod-to-rod spacing. The remaining 55 rods in a bundle are standard rods the same active fuel length as the tie rods. The end plugs of the standard rods have pins which fit into anchor holes in the tie plates. An Inconel-X expansion spring located over the top end plug pin of each fuel rod keeps the fuel rods seated in the lower tie plate and allows them to expand axially and independently by sliding within the holes of the upper tie plate.

The fuel pellets consist of high-density ceramic uranium dioxide manufactured by compacting and sintering uranium dioxide powder into cylindrical pellets with chamfered edges. The average UO_2 pellet immersion density is approximately 95% of theoretical density.

Four different U-235 enrichments are used in the fuel assemblies to reduce the local power peaking factor (see Figure 3-2). Fuel element design and manufacturing procedures have been developed to prevent errors in enrichment location within a fuel assembly. The fuel rods are designed with characteristic mechanical end fittings, one for each enrichment. End fittings are designed so that it is not mechanically possible to completely put together a fuel assembly with any high enrichment rods in positions specified to receive a lower enrichment. As in the 7x7 assembly design, the 8x8 bundle incorporates the use of small amounts of gadolinium as a burnable poison in selected fuel rods. The gadolinia-urania fuel rods are designed with characteristic extended end plugs. These extended end plugs permit a positive, visual check on the location of each gadolinium-bearing rod after bundle assembly.

Most aspects of the 8x8 bundle design are similar to the current 7x7 design. Specifically, the upper and lower tie plates, the fuel rod spacers, the upper and lower end plugs, and other associated bundle hardware are geometrically similar to the 7x7 except for modeling down in size to be compatible with the increased number of rods per bundle and the reduced rod diametral wall thickness. The 8x8 fuel assembly outline dimensions are the same as the current 7x7 dimensions.

Table 3-1

INITIAL CORE AND RELOAD FUEL ASSEMBLY DESIGN SPECIFICATIONS

	Initial Core Fuel	Reload Fuel R1	Reload Fuel R2
Fuel Assembly			
Geometry	7x7	7x7	8x8
High Enrichment Rods	22	32	44
Medium High Enrichment Rods	19	10	14
Medium Low Enrichment Rods	8	6	4
Low Enrichment Rods	0	1	1
Poison Rods	0	3	4
Water-Spacer Capture Rods	0	0	1
Rod Pitch (in.)	0.738	0.738	0.640
Water to Fuel Volume Ratio	2.47	2.53	2.60
Heat Transfer Area (ft^2)	86.5	86.5	97.6
Fuel Rod			
Active Fuel Length (in.)	144.0	144.0	144.0
Gas Plenum Length (in.)	11.25	11.0	11.24
Fill Gas	helium	helium	helium
Getter	no	yes	yes
Fuel			
Material	sintered UO_2	sintered UO_2	sintered UO_2
Initial Enrichment, wt/% U-235			
Average for Bundle	2.25	2.30	2.62
High	2.95	2.56	2.87
Medium High	1.91	1.94	2.14
Medium Low	1.13	1.69	1.87
Low	-	1.33	1.45
Pellet Diameter (in.)	0.487	0.477	0.416
Pellet Immersion Density (% TD)	95.0	95.0	95.0
Cladding			
Material	Zr-2	Zr-2	Zr-2
Thickness	0.032	0.037	0.034
Outside Diameter (in.)	0.563	0.563	0.493
Fuel Channel			
Material	Zr-4	Zr-4	Zr-4
Outside Dimension (in.)	5.438	5.438	5.438
Wall Thickness (in.)	0.080	0.080	0.080
Channel Length (in.)	162-1/8	162-1/8	162-1/8

Table 3-1 (Continued)

	Initial Core Fuel	Reload Fuel R1	Reload Fuel R2
Spacers			
Material	Zr-4 with Inconel Springs	Zr-4 with Inconel Springs	Zr-4 with Inconel Springs
Number per Bundle	7	7	7

the 95% point in the total population. This distribution implies, therefore, a small (<5%) probability that some cladding segments may have plastic elongation less than 1% at failure.

For design purposes, critical heat flux (the onset of the transition from nucleate boiling to film boiling) is conservatively defined as a design limit for fuel damage, although fuel damage is not expected to occur until well into the film boiling regime. Severe overheating of the fuel rod cladding is assumed to occur at a condition of minimum critical heat flux ratio (MCHFR - the minimum ratio of the critical heat flux correlation value at the corresponding fluid conditions to the actual heat flux at a given point in the fuel assembly) less than 1.0. If MCHFR remains above 1.0 no fuel damage occurs as a result of inadequate cooling. The steady-state MCHFR and the resulting MCHFR during transients are discussed in more detail in Sections 4 and 6.

3.2.2 Effects of Radiation and Fuel Swelling

Irradiation affects both fuel and cladding material properties. The effects include an increased cladding strength and a reduced cladding ductility. In addition, irradiation in a thermal reactor environment results in the buildup of both gaseous and solid fission products within the UO_2 fuel pellet which tend to increase the pellet diameter, i.e., fuel irradiation swelling. Pellet internal porosity and pellet-to-cladding gap have been specified in such a way that the thermal expansion and irradiation swelling are accommodated for the worst-case dimensional tolerances throughout life. The irradiation swelling model is based on data reported in References 1 and 2, as well as an evaluation of applicable high exposure data.[3]

Observations and calculations based on this refined model for relative UO_2 fuel-cladding expansion indicate that the as-fabricated UO_2 pellet porosity is adequate (without pellet dishing) to accommodate the fission-product-induced UO_2 swelling out to and beyond the peak exposures anticipated for this reload.[3]

The primary purpose of the gap between the UO_2 fuel pellet and Zircaloy cladding is to accommodate differential diametral expansion of fuel pellet and

cladding and, thus, preclude the occurrence of excessive gross diametral cladding strain. A short time after reactor startup, the fuel cracks radially and redistributes out to the cladding. Experience has shown that this gap volume remains available in the form of radial cracks to accommodate gross diametral fuel expansion.[4]

The thermal conductance across the pellet/clad gap, in theory, depends upon the gas conductivity and the distance of the pellet from the cladding when pellet and clad are not in contact, and upon the pressure of the fuel on the cladding if they are in contact. Initially, the gap is filled with helium. As the fuel accumulates exposure, a number of phenomena which can influence the pellet-clad thermal conductance can become important. Fission gases are released from the fuel and dilute the helium gas to form a mixture of He, Kr, Xe and UO_2 impurity volatiles with lower thermal conductivity than pure helium in the free volume within the fuel rods. In addition, it has been postulated that the phenomenon of fuel densification may tend to cause an increase in the pellet-to-cladding gap with an attendant feedback on pellet-clad thermal conductance. The important observation in this regard is that there is a phenomenon which tends to counteract the adverse effects of fission gas dilution and fuel densification. Specifically, it has been observed that for high power BWR fuel rods, the fuel pellet-to-cladding gap closes progressively with exposure in spite of any effect of densification on pellet diameter, with the result that the pellets and cladding achieve intimate contact with increasing exposure, thus reducing the importance of the gas conductivity to good thermal conductance.[4]

This qualitative discussion serves merely to describe the phenomena influencing pellet-clad thermal conductance with increasing exposure. In the integral models employed in the detailed mechanical design analysis of BWR fuel, the value of pellet-clad thermal conductance is held constant for convenience. The constant value employed is 1000 Btu/h-ft^2-°F. The use of this constant value has been found to be a conservative assumption when applied in conjunction with the integral fuel design models employed by General Electric. Specifically, the design fission gas release model employed in the determination of fuel rod plenum size and cladding wall thickness has been shown to overpredict available data on fission gas release when applied with a pellet-clad thermal conductance value of

1000 Btu/h-ft^2-°F. Similarly, the design model for relative fuel-cladding expansion (pellet-to-cladding interaction) also has been shown to be very conservative relative to available data when a value of 1000 Btu/h-ft^2-°F is used for pellet-cladding thermal conductance. The basis for these integral fuel design models is described in more detail in Reference 3.

Fission-product buildup also tends to cause a slight reduction in fuel melting temperature. The melting point of UO_2 is considered to reduce with irradiation at the rate of 32(°C)/10,000 (MWd/Te).

In the temperature range of interest (>500°C) the fuel thermal conductivity is not considered to be significantly affected by irradiation.

A small fraction of the gaseous fission products (approximately 20%) are released from the fuel pellets to produce an increase in fuel rod internal gas pressure. In general, such irradiation effects on fuel performance have been characterized by available data and are considered in determining the design features and performance. Thus, the irradiation effects on fuel performance are inherently considered when determining whether or not the stress intensity limits and temperature limits are satisfied.

3.2.3 Maximum Allowable Stresses

The strength theory, terminology, and stress categories presented in the ASME Boiler and Pressure Vessel Code, Section III, are used as a guide in the mechanical design and stress analysis of the reactor fuel rods. The mechanical design is based on the maximum shear stress theory for combined stresses. The equivalent stress intensities used are defined as the difference between the most positive and least positive principal stresses in a triaxial field. Thus, stress intensities are directly comparable to strength values found from tensile tests. Table 3-2 presents a summary of the basic stress intensity limits that are applied for Zircaloy-2 cladding:

Table 3-2

STRESS INTENSITY LIMITS

Categories	Yield Strength (Sy)	Ultimate Tensile Strength (Su)
Primary Membrane Stress	2/3	1/2
Primary Membrane Plus Bending Stress Intensity	1	1/2 to 3/4
Primary Plus Secondary Stress Intensity	2	1.0 to 1.5

In the design of BWR Zircaloy-clad UO_2 pellet fuel, no continuous functional variations of mechanical properties with exposure are employed since the irradiation effects become saturated at very low exposure. At beginning of life, the cladding mechanical properties employed are the unirradiated values. At subsequent times in life, the cladding mechanical properties employed are the saturated irradiated values. The only exception to this is that unirradiated mechanical properties are employed above the temperatures for which irradiation effects on cladding mechanical properties are assumed to be annealed out. It is significant that the values of cladding yield strength and ultimate tensile strength employed represent the approximate lower bound to data on cladding fabricated by General Electric, i.e., approximately two standard deviations below the mean value.

Design analyses have been performed for the 8x8 reload fuel which show that the stress intensity limits given in the above table are not exceeded during continuous operation with linear heat generation rates up to the operating limit of 13.4 kW/ft, nor for short-term transient operation up to 16% above the peak operating limit of 13.4 kW/ft, i.e., 15.6 kW/ft. Stresses due to external coolant pressure, internal gas pressure, thermal effects, spacer contact, flow-induced vibration, and manufacturing tolerances were considered. Cladding mechanical properties used in stress analyses are based on test data of fuel rod cladding for the applicable temperature.

3.2.4 Capacity for Fission Gas Inventory

A plenum is provided at the top of each fuel rod to accommodate the fission gas released from the fuel during operation. The design basis is to provide sufficient volume to limit the fuel rod internal pressure so that cladding stresses do not exceed the limits given in Table 3-2 during normal operation and for short-term transients of 16% or less above the peak normal operating conditions.

3.2.5 Maximum Internal Gas Pressure

Fuel rod internal pressure is due to the helium which is backfilled at one atmosphere pressure during rod fabrication, the volatile content of the UO_2, and the fraction of gaseous fission products which are released from the UO_2. The most limiting combination of dimensional tolerances is assumed in defining the hot plenum volume used to compute fuel rod internal gas pressure. A quantity of 1.35×10^{-3} gram moles of fission gas are produced per MWd of power production. In fuel rod pressure and stress calculations, 4.0% of the fission gas produced is calculated to be released from any UO_2 volume at a temperature less than 3000°F and 100% from any UO_2 above 3000°F. The above basis has been demonstrated by experiment to be conservative over the complete range of design temperature and exposure conditions. The calculated maximum fission gas release fraction in the highest design power density rod is <20%. This calculation is conservative because it assumes the most limiting peaking factors applied to this rod. The percentage of total fuel rod radioactivity released to the rod plenum is less than 20% because of radioactive decay during diffusion from the UO_2.

3.2.6 Internal Pressure and Cladding Stresses During Normal Conditions

The maximum internal pressure is applied coincident with the minimum applicable coolant pressure to compute the resulting cladding stresses which, combined with cladding stresses from other sources, must satisfy the stress limits described in Table 3-2. The maximum internal pressure generally does not exceed 1800 psia.

3.2.7 Cycling and Fatigue Limits

The design basis for fuel fatigue limits consists of the linear cumulative damage rule (Miner's hypothesis)[5] and the Zircaloy fatigue design basis of Reference 6. The fatigue life analysis is based on the estimated number of temperature, pressure, and power cycles. During fuel life, less than 5% of the allowable fatigue life is consumed.

Cyclic Condition	Estimated Cycles
Room temperature to 100% power	~4/yr
Hot standby to 100% power	~12/yr
50% power to 100% power	~60/yr
75% power to 100% power	~250/yr
100% power to 116% power	~1/2 yr

3.2.8 Deflection

The operational fuel rod deflections considered are the deflections due to:

1. Manufacturing tolerances
2. Flow-induced vibration
3. Thermal effects
4. Axial load

There are two criteria that limit the magnitude of these deflections. One criterion is that the cladding stress limits must be satisfied; the other is that the fuel rod-to-rod and rod-to-channel clearances must be sufficient to allow free passage of coolant water to all heat transfer surfaces. Thermal hydraulic testing has demonstrated that allowing a statistical minimum clearance of 0.060 inch at two standard deviations away from the nominal clearance is sufficient to assure a very low probability of local rod overheating due to occurrence of critical heat flux.

3.2.9 Flow Induced Fuel Rod Vibrations

Flow-induced fuel rod vibrations depend primarily on flow velocity and fuel rod geometry. For the range of flow rates and geometrical variations for the plant, vibrational amplitude does not exceed 0.002 inch. The maximum vibrational amplitude occurs midway between spacers due to the constraint of the spacer. The stress levels resulting from the vibrations are negligibly low and well below the endurance limit of all affected components.

3.2.10 Fretting Corrosion

Fretting wear and corrosion have been considered in establishing the fuel mechanical design basis. Individual rods in the fuel assembly are held in position by spacers located at intervals along the length of the fuel rod. Springs are provided in each spacer cell so that the fuel rod is restrained to avoid excessive vibration. Tests of this design have been conducted both out of reactor as well as in reactor prior to application in a complete reactor core basis. All tests and post-irradiation examinations have indicated that fretting corrosion does not occur. Post-irradiation examination of many fuel rods indicates only minor fretting wear. Excessive wear at spacer contact points has never been observed with the current spacer configuration.

3.2.11 Potential for Hydriding

The design basis for fuel in regard to the cladding hydriding mechanism is to assure, through a combination of engineering specifications and strict manufacturing controls, that production fuel will not contain excessive quantities of moisture or hydrogenous impurities. An engineering specification limit on moisture content in a loaded fuel rod is defined which is well below the threshold of fuel failure. Procedural controls are utilized in manufacturing to prevent introduction of hydrogenous impurities such as oils, plastics, etc., to the fuel rod. Hot vacuum outgassing (drying) of each loaded fuel rod just prior to final end-plug welding is employed to assure that the level of moisture is well below the specification limit. As a further assurance against possible fuel rod perforation resulting from inadvertent admission of moisture or hydrogeneous

impurities into a fuel rod, General Electric is now using a zirconium alloy hydrogen getter material in all fuel rods. This getter material has been proven effective by both in-pile and out-of-pile tests.

3.2.12 Dimensional Stability

The fuel assembly and fuel components have been designed to assure dimensional stability in-service. The fuel cladding and channel specifications include provisions to preclude dimensional changes due to residual stresses. In addition, the fuel assembly has been designed to accommodate dimensional changes that occur in-service due to thermal differential expansion and irradiation effects: for example, the fuel rods are free to expand lengthwise independent of each other, and the channel is free to expand relative to the fuel bundle.

3.3 RESULTS FROM MECHANICAL DESIGN EVALUATIONS

3.3.1 Steady-State Mechanical Performance

Reload fuel is designed to operate at core rated power with sufficient design margin to accommodate reactor operations and satisfy the mechanical design bases discussed in detail in Section 3.2. In order to accomplish this objective, the 8x8 reload fuel is designed under the most limiting conditions at 100% of rated power, to operate at a maximum steady-state linear heat generation rate of $\leq$13.4 kW/ft.

Thermal and mechanical analyses have been performed which demonstrate that the mechanical design bases are met for the maximum operating power and exposure combination throughout fuel life.

3.3.2 Fuel Damage Analysis

For fresh UO_2 fuel the calculated linear heat generation rate (LHGR) corresponding to 1% diametral plastic strain of the cladding is approximately 25.4 kW/ft. Later in life the calculated linear heat generation rate corresponding

to 1% diametral plastic strain decreases to approximately 23.8 kW/ft at 25,000 MWd/t and approximately 21.1 kW/ft at 39,500 MWd/t. However, due to a depletion of fissionable material, the high exposure fuel has less nuclear capability and will operate at correspondingly lower powers; therefore, a wide margin is maintained throughout life between the operating LHGR and the LHGR calculated to cause 1% cladding diametral strain.

The addition of small amounts of gadolinia to UO_2 results in a reduction in the fuel thermal conductivity and melting temperature. The result is a reduction in the LHGRs calculated to cause 1% plastic diametral strain for gadolinia-urania fuel rods. However, the gadolinia-urania fuel rods are designed to operate at lower power to compensate for this and provide margins similar to standard UO_2 rods.

For the 8x8 reload fuel design analysis has shown that the power required to produce 1% plastic strain throughout life for all rod types in the assembly is equal to or greater than 180% of the maximum steady-state power.

3.3.3 Incipient UO_2 Center Melting

For the 8x8 reload fuel, incipient center melting is expected to occur in fresh UO_2 fuel rods at a linear heat generation rate of approximately 20.4 kW/ft. This condition corresponds to the integral:

$$\int_{32°F}^{T_{melt}} k\,dT = 93 \text{ w/cm}$$

where

$$k = \left[\frac{3978.1}{692.61+T}\right] + 6.02366 \times 10^{-12} (T + 460)^3 \text{ Btu/h-ft-°F},$$

and T is in °F.

The value of the above integral decreases slightly with burnup, as a result of the decrease in fuel melting temperature with increasing exposure.

3.4 FUEL OPERATING AND DEVELOPMENTAL EXPERIENCE

3.4.1 Fuel Operating Experience

The peak linear heat generation rate design limit for steady-state operation is 13.4 kW/ft which corresponds to a heat flux of 354,250 Btu/h-ft^2. This condition is well within the bounds of available production and developmental fuel experience.

The fuel operating limit and the fuel damage limit have been established based on operating experience and experimental tests covering the complete range of design power and exposure levels. Tables 3-3 and 3-4 present a summary of power reactor production fuel experience. Tables 3-5 and 3-6 show the ranges of development fuel irradiations which have already been completed or are in progress. This experience has been used in establishing design features and in the analysis of performance characteristics. A large volume of experience has been obtained over the past 10 to 15 years with production fuel in commercial power BWRs and numerous developmental irradiations.

The large volume of production experience, starting with the first load of fuel in Dresden 1 Nuclear Power Station in 1960, has provided feedback on the adequacy of the design for, and the effects of, operation in a commercial power reactor environment. Production fuel experience has also provided feedback on the incidence and effect of flaws and impurities which occur statistically in large volume production processes.

The production Zircaloy-clad UO_2 pellet fuel experience is supplemented by a large amount of in-pile and out-of-pile developmental work. The developmental work to date has been employed to test a wide range of design characteristics, to investigate various mechanisms affecting the performance of the fuel rod, and to extend irradiation experience to higher local combinations of fuel rod power and exposure than covered by production fuel.

Table 3-3

SUMMARY OF LEADING EXPERIENCE ON CURRENTLY OPERATING PRODUCTION ZIRCALOY-CLAD UO_2 PELLET FUEL AS OF OCTOBER 1, 1971

Reactor	Exposure Peak Pellet (MWd/Te)	Exposure Average Assembly (MWd/Te)	Time Incore (Years)	Design Max Heat Flux(a,b) (Btu/h-ft^2)	Design Peak LHGR(a,b) (kW/ft)	Fuel Rod Dia (in.)	Clad Thickness (mils)	Pellet-to-Clad Gap (Nominal) (mils)	Active Fuel Length (in.)	Fission Gas Plenum (Vol Per Unit Fuel Vol)	Number of Segments or Rods Still in Core
Dresden I Type III B	25,800	16,450	5.45	360000	15.4	0.555	35	7.5	109.0	0.040	3,780
Dresden I Type III F	28,200	19,480	4.45	360000	15.5	0.5625	35	10	108.25	0.048	2,592
Dresden I Type V	21,320	13,250	2.45	360000	15.5	0.5625	35	10	108.25	0.048	3,492
Garigliano Type A	26,120	15,180	7.35	252000	10.3	0.534	30	5	105.7	0.031	6,804
Garigliano Type SA & SB	15,160	7,270	2.95	320000	14.6	0.593	37	11	107.0	0.030	7,936
Consumers (BRP) Type B(e)	35,380	23,430	4.95	434000	15.0	0.449	34	8	70.0	0.048	242
Consumers (BRP) Type E(e)	15,500	8,730	2.75	410000	17.7	0.5625	40	11	70.0	0.048	1,386
Consumers (BRP) Type EG(d,e)	15,559	7,930	2.00	410000	17.7	0.5625	40	11	70.0	0.048	2,079
Consumers (BRP) Type F			0.75	410000	17.7	0.5625	40	11.5	70.0	0.048	1,771
Humboldt Type II	21,598	13,230	4.00	325000	12.1	0.486	33	10	79.0	0.043	3,724
Humboldt Type III	14,332	6,615	2.00	389000	16.8	0.563	32	11	79.0	0.062	3,384
KRB	22,409	14,634	4.45	367000	15.8	0.5625	35	10	130.0	0.058	5,784
KRB-KD	11,124	7,050	1.15	367000	15.8	0.563	32	11	130.0	0.058	648
Tarapur I	13,738	8,337	1.80	365000	15.8	0.5625	35	10.5	144.0	0.059	10,224
Tarapur II	13,407	7,818	2.00	365000	15.8	0.5625	35	10.5	144.0	0.059	10,224
Oyster Creek I	11,976	8,307	2.35	400000	17.5	0.570	35.5	11	144.0	0.078	27,440
Nine Mile Point	8,412	5,106	2.05	400000	17.5	0.570	35.5	11	144.0	0.078	26,068
Dresden II	4,825	2,900	2.00	405000	17.5	0.563	32	12	144.0	0.078	34,941
Dresden II (reload)	1,600	970	0.50	405000	17.5	0.563	32	12	144.0	0.078	10,535
Dresden III	575	290	0.25	405000	17.5	0.563	32	12	144.0	0.078	35,476
Tsuruga	12,037	7,107	1.75	400000	17.5	0.570	35.5	12	144.0	0.078	34,700
Millstone	5,293	3,065	0.85	400000	17.5	0.570	35.5	12	144.0	0.078	28,420
Fukushima-I	4,410	3,300	0.85	400000	17.5	0.570	35.5	12	144.0	0.078	19,600
Monticello	2,945	1,582	0.75	405000	17.5	0.563	32	12	144.0	0.078	23,716
Nuclenor	2,070	1,290	0.60	400000	17.5	0.570	35.5	12	144.0	0.078	19,600
KKM	500	500	0.10	428000	18.5	0.563	32	12	144.0	0.11	11,172
BWR/4(c)	45,000	27,500	5.00	428000	18.5	0.563	37	12	144.0	0.11	
8x8 Reload(c)	45,000	28,000	5.00	354000	13.4	0.493	34	9	144.0	0.08	

a = at rated power
b = license limit
c = typical design as opposed to proven performance in preceding entries
d = includes 15 assemblies with 2 rods per bundle of plutonium
e = values as of February 11, 1971

Table 3-4

SUMMARY OF PRODUCTION FUEL EXPERIENCE

ZIRCALOY-CLAD UO_2 PELLET FUEL AS OF OCTOBER 1, 1971

Identification	Weight of Fuel (lb U)	Number of Fuel Assemblies	Number of Fuel Rods or Segments (S=Segments)	Design or Warranted Exposure (MWd/Te)	Average Assembly Exposure (MWd/Te)	Maximum Assembly Exposure (MWd/Te)	Years of Operation In Reactor
Dresden 1							
Type I	132,400	534	77,184(S)	7,400	9,100	23,100	1960-1969
Type III-B	43,500	192	6,912	14,900	16,750	20,650	1964-1971
Type III-F	21,400	104	3,744	16,500	17,900	25,950	1965-1971
Type V	24,800	106	3,816	16,500	13,050	19,600	1967-1971
KWE-KAHL	16,100	100	7,200(S)	8,800	11,000	21,000	1960-?
Garigliano							
Type A	111,100	229	16,848	12,100	13,600	19,750	1963-1971
Type SA	29,380	66	4,224	19,300	15,200	17,900	1968-1971
Type SB	28,770	64	4,096		2,900	5,300	1970-1971
JDPR	9,800	76	5,472(S)	8,800	3,800	N/A	1963-?
Humboldt							
Type II	28,600	169	8,281	15,400	13,600	17,250	1965-1971
Type III	23,702	140	5,040	20,700	4,950	13,150	1971-
Consumers							
Type B	8,700	30	3,630	16,500	19,800	24,600	1966-1971
Type E	12,640	42	3,234	16,500	8,700	10,800	1968-1971
Type EG	11,617	38	2,926	16,500	7,700	10,800	1969-1971
Type F	6,977	23	1,771	22,000	-	-	1971-
KRB							
Type A	104,400	371	13,248	16,500	15,300	18,900	1966-1971
Type KD	5,110	18	648	16,500	7,050	8,450	1970-1971
Tarapur 1	185,120	284	13,916	16,500	8,300	10,450	1969-1971
Tarapur 2	185,120	284	13,916	16,500	7,800	9,900	1969-1971
Oyster Creek	242,900	560	27,440	16,500	8,300	8,550	1969-1971
Nine Mile Pt.	230,760	532	26,068	16,500	5,100	6,250	1969-1971
Tsuruga	136,200	314	15,092	16,500	7,100	9,300	1969-1971
Dresden 2	314,050	753	35,476	20,900	2,900	3,450	1970-1971
Dresden 2 Reload	87,420	215	10,535	20,900	1,000	1,300	1971-
Fukushima 1	172,484	400	19,600	20,900	3,300	3,400	1971-
Monticello	206,873	484	23,716	20,900	1,300	1,600	1971-
Millstone	250,625	580	28,420	20,900	3,100	3,700	1971-
Nuclenor	172,818	400	19,600	20,900	1,300	1,550	1971-
Dresden 3	314,050	724	35,476	20,900	300	350	1971-
KKM	97,017	228	11,172	20,900	<500	<500	1971-

Table 3-5
GENERAL ELECTRIC DEVELOPMENTAL IRRADIATIONS
ZIRCALOY-CLAD 95% TD UO_2 PELLET FUEL RODS

Name	Reactor	No. of Rods	Fuel Rod Dia. (in.)	Clad Wall Thickness (in.)	Pellet-to-Clad Gap (mils)	Peak Heat Flux ($Btu/h-ft^2$)	Peak LHGR (kW/ft)	Peak Exposure (MWd/Te)	Status
Dresden Prototype	VBWR	9	0.565	0.030	3.0-16.0	460,000	19.94	12,000	Completed
Fuel Cycle (R & D)	VBWR	144	0.424	0.022	2.0-8.0	509,000	16.6	13,800	Completed
Dresden Prototypes	VBWR	52	0.565	0.028	5.0-8.0	407,000	17.64	10,000	Completed
High Performance	GETR	12	0.565	0.030	4.0-6.0	630,000	27.0	1,500	Completed[h]
UO_2[b]						1,126,000	49.0		
High Performance UO_2[b]	GETR	2	0.565	0.030	4.0-11.0	1,355,000	58.0	14,000	Completed[e]
Sa-1[c]	Dresden 1	98	0.424	0.022	4.0-8.0	400,000	13.0	40,000	Completed
D-1,2,3[d]	Consumers	363	0.424	0.030	7.0	434,000	14.2	30,000	Completed
D-50[f]	Consumers	36	0.570	0.035	12.0	507,000	22.0	15,400	g,i
D-52,53	Consumers	58	0.700	0.040	13.0	525,000	27.0	4,600	i
GE-Halden	Halden	21	0.563	0.032-0.060	7.0-14.0	510,000	22.0	6,300	Continuing

a = USAEC Contract AT(04-3) - 189 Project Agreement 11
b = USAEC Contract AT(04-3) - 189 Project Agreement 17
c = USAEC Contract AT(04-3) - 189 Project Agreement 41
d = USAEC Contract AT(04-3) - 361
e = Hollow Pellet
f = USAEC Contract AT(04-3) - 189 Project Agreement 50
g = Eight fuel rods failed during second operating cycle due to abnormal crud and scale deposition
h = One rod failure @ 49 kW/ft
i = Fuel assemblies presently out of reactor pending approval for reinsertion

Table 3-6
GENERAL ELECTRIC DEVELOPMENTAL IRRADIATIONS
ZIRCALOY-CLAD 95% TD UO_2 PELLET CAPSULES
GENERAL ELECTRIC TEST REACTOR

Capsule	Number of Rods	Fuel Rod Diameter (in.)	Clad Wall Thickness (in.)	Pellet-to-Clad Gap (mils)	Peak Heat Flux (Btu/h-ft^2)	Peak LHGR (kW/ft)	Peak Exposure (MWd/Te)	Status
A	3	0.425	0.024-0.032	1.4-10.2	750,000	24.5	88,000	Complete
	1	0.488	0.032	11.2	785,000	29.4	34,000	Complete
B	6	0.489	0.034	7.8-11.6	504,000	18.9	65,000	Complete
C	5	0.557	0.036	2.0-15.0	475,000	20.3	59,000	Complete
D	5	0.557	0.036	2.0-14.0	540,000	23.0	36,500	Complete
E	5	0.250	0.015	6.5	735,000	14.1	100,000	Complete
F	3	0.443	0.030	3.0-13.0	480,000	16.3	29,000	Complete

More than 25 production fuel types have been designed, manufactured, and operated in more than 19 BWRs. When all production fuel types are considered, a total of more than 440,000 Zircaloy-2-clad UO_2 fuel rods have been operated in GE-designed BWRs. Out of this number of rods, ~180,000 of which went into operation during 1970 and 1971, only ~0.2% have been detected to have failure due to wall perforation, and this includes fuel which failed after having exceeded design performance conditions.

Peak linear heat generation rates (LHGR) from approximately 10 to 17 kW/ft have been experienced with the production fuel. Individual fuel assemblies have achieved average exposures greater than 23,500 MWd/Te and have operated more than 9 years in-core residence. In comparison, the 8x8 reload fuel has the following proposed operating characteristics:

13.4 kW/ft maximum LHGR (Operating Limits),
45,000 MWd/Te maximum local exposure, and
4-6 years in-core residence time.

Fuel rod diameters in the range of 0.425 to 0.570 inch o.d. with cladding wall thickness from 30 to 40 mils and pellet-to-cladding gaps from 3 to 11 mils have been used in production fuel. Rod-to-rod pitch has varied from 0.533 to 0.874 inch, with rod-to-rod spacing varying from 0.128 to 0.213 inch. Active fuel column lengths have varied from 59.8 to 144.0 inches with fission gas plenum volume per unit of fuel volume from 0.013 to 0.100. Such fuel rods have been licensed and operated in 6x6, 7x7, 8x8, 9x9, 11x11 and 12x12 fuel bundle configurations. In comparison, the design for this 8x8 reload fuel has the following physical characteristics:

Bundle geometry	= 8x8
Active fuel length	= 144 in.
Fission gas plenum volume (volume per unit fuel volume)	= 0.08
Fuel rod o.d.	= 0.493 in.
Pellet-to-cladding gap	= 0.009 in.
Rod pitch	= 0.640 in.
Rod spacing	= 0.147 in.

3.4.2 Fuel Developmental Experience

The production Zircaloy-clad UO_2 pellet fuel experience described in the previous section is supplemented by a large amount of in-pile and out-of-pile developmental work. The developmental work to date has been employed to test a wide range of design characteristics, to investigate various mechanisms affecting the performance of the fuel rod, and to extend irradiation experience to higher local combinations of fuel rod power and exposure than covered by production fuel. The following presents a discussion of the pertinent developmental fuel experience which, in combination with the production fuel experience, provides the basis for the current BWR fuel design and operating limits.

Tables 3-5 and 3-6 present a summary of design details and performance conditions for Zircaloy-clad UO_2 pellet fuel rods and capsules* irradiated under General Electric or USAEC-General Electric development test programs. These data complement the BWR production fuel experience by providing additional data at higher local combinations of fuel rod power and exposure. Overall, more than 800 fuel pins with design characteristics similar to the current BWR fuel have been irradiated under General Electric or USAEC-General Electric programs. The irradiations have been performed with BWR environment in both test reactors and in commercial power BWRs. Test reactors employed in General Electric developmental irradiations summarized in Tables 3-5 and 3-6 are the Vallecitos Boiling Water Reactor (VBWR), the General Electric Test Reactor (GETR) and more recently the Halden Reactor. Developmental fuel irradiations have also been performed in the Consumers Big Rock Point and Dresden Unit 1 commercial power BWRs.

The range of peak performance conditions covered by the various development irradiations goes beyond the design performance conditions for fuel in this class of reactor. The development performance conditions include:

13.0 - 58.0 kW/ft maximum LHGR, and

1500 - 100,000 MWd/Te maximum local exposure.

---

*A capsule, as used herein, refers to a test fuel rod, or group of rods combined, with all features similar to production fuel rods except for having reduced active fuel length (as low as approximately 3 in.).

The corresponding operating conditions for this reload fuel are:

13.4 kW/ft maximum LHGR, and
~45,000 MWd/Te maximum local exposure.

The range of design characteristics and dimensions covered by the various developmental irradiations also encompasses the characteristics and dimensions employed in the current BWR fuel design. The range of design characteristics and dimensions covered by the various developmental irradiations include the following:

Fuel rod o.d. - 0.250 to 0.700 in.,
Clad wall thickness - 0.025 to 0.060 in.,
Pellet-clad gap - 0.0014 to 0.016 in., and
Pellet length - 0.3 to 0.95 in.

The corresponding fuel design characteristics for this reload fuel are:

Fuel rod o.d. - 0.493 in.,
Clad wall thickness - 0.034 in.,
Pellet-clad gap - 0.009 in., and
Pellet length - 0.420 in.

Considering the range of power levels and peak fuel burnups attained in the broad base of operating and developmental fuel experience, it has been concluded that the current 8x8 fuel design is a conservative application of this experience. A more complete review of GE BWR fuel experience is provided in Reference 3.

3.4.3 Fuel Damage Experience

Although the incidence of failure in General Electric Zircaloy-clad UO_2 fuel has been quite low (~0.2% out of more than 440,000 fuel rods), fuel has been operated at Dresden Unit 1 and elsewhere with perforated cladding. Dresden Unit 1 has operated with some failures in the Type I Zircaloy-clad UO_2 fuel, in the Type II stainless-steel-clad UO_2 fuel, and more recently in fuel Types

III-B, IV-F, and V. The Humboldt Bay and Big Rock Point reactors have also operated with failures in stainless steel fuel (Humboldt Type I and Big Rock Type A). The Big Rock reactor has operated with some fuel failures in both the Type B and Type E Zircaloy-clad UO_2 fuel designs as well as a number of failed high power (22 to 27 kW/ft) fuel rods in the center-melt developmental fuel assemblies. KRB, Dresden 2, Tsuruga, and Fukushima have operated with some perforated fuel rods during initial operation. Failures have resulted from manufacturing defects, incompatibility of stainless steel as cladding material in the BWR core steam-water environment, inadequate volume for accommodation of fuel expansion and/or fission gas pressure for fuel operated beyond design exposures, cladding over-temperature caused by excessive deposits of crud on fuel rod surfaces resulting from materials in the feedwater system, fretting wear caused by foreign debris trapped in fuel rod spacers, local internal hydriding of the cladding, and local clad strains due to pellet/cladding interaction. In essentially all cases, the mechanisms causing the fuel rods to fail in service have been carefully identified. Appropriate corrections have been made to the manufacturing process and to the fuel or system design and operation to reduce the probability of future recurrence of such failures.

Operation with failed fuel rods has shown that the fission product release rate from defective fuel rods can be controlled by regulating power level. The rate of increase in released activity apparently associated with progressive deterioration of failed rods has been deduced from chronological plots of the offgas activity measurements in operating plants. These data indicate that the activity release level can be lowered by lowering the local power density in the vicinity of the fuel rod failure. These measured data also indicate that sudden or catastrophic failure of the fuel assembly does not occur with continued operation and that the presence of a failed rod in a fuel assembly does not result in propagation of failure to neighboring rods. Shutdown can be scheduled, as required, for repairing or replacing fuel assemblies that have large defects.

Evaluating the fission product release rate for failed fuel rods shows a wide variation in the activity release levels. Designers have attempted to relate the release rates to defect type, size, and specific power level. These data support the qualitative observations that fission product release rates are functions of power density and that progressive deterioration is a function of time.

A more detailed summary of General Electric experience with BWR Zircaloy-clad UO_2 pellet fuel, including recent production and development data, has been documented (see Reference 3).

3.4.4 Fuel Densification

The amount of in-pile fuel densification in BWR Zircaloy-clad UO_2 pellet fuel has been observed to be small and is not considered to have any significant effects on fuel performance. Detailed consideration of the occurrence and potential effects of in-pile fuel densification in General Electric BWRs is reported in Reference 4. The AEC staff has recently issued a model for analysis of densification effects in BWRs. This model is considered by General Electric to be overly conservative in light of observations on BWR fuel. A separate submittal will be provided to present the results of analysis employing the AEC staff model.

REFERENCES - SECTION 3

1. WAPD-TM-263, "Effects of High Burnup on Zircaloy-Clad, Bulk UO_2 Plate Fuel Element Samples," September 1962.

2. WAPD-TM-629, "Irradiation Behavior of Zircaloy-Clad Fuel Rods Containing Dished End UO_2 Pellets," July 1967.

3. Williamson, H. H., and Ditmore, D. C., "Experience with BWR Fuel Through September 1971," May 1972 (NEDO-10505).

4. Ditmore, D. C., and Elkins, R. B., "Densification Considerations in BWR Fuel Design and Performance," December 1972 (NEDM-10735).

5. Miner, M. A., "Cumulative Damage in Fatigue," Journal of Applied Mechanics, 12, Transactions of the ASME, 67, 1945.

6. O'Donnel, W. J., and Langer, B. F., "Fatigue Design Basis for Zircaloy Components," Nuclear Science and Engineering, 20, 1964.

4. THERMAL-HYDRAULIC CHARACTERISTICS

4.1 FUEL ASSEMBLY HYDRAULIC ANALYSIS

4.1.1 Core Pressure Drop, Hydraulic Loads, and Correlations

The flow distribution to the fuel assemblies is calculated on the assumption that the pressure drop across all fuel assemblies is the same. This assumption has been confirmed by measurements of the flow distribution in modern boiling water reactor as reported in References 1 and 2. The components of bundle pressure drop considered are friction, local, elevation, and acceleration. Pressure drop measurements made in operating reactors confirm that the total measured core pressure drop and calculated core pressure drop are in good agreement. There is reasonable assurance, therefore, that the calculated flow distribution throughout the core is in close agreement with the actual flow distribution of an operating reactor.

4.1.1.1 Friction Pressure Drop

Friction pressure drop is calculated using the model relation

$$\Delta P_f = \frac{w^2}{2g\rho} \quad \frac{fL}{D_H A_{ch}^2} \quad \phi_{TPF} \ ,$$

where

ΔP_f = friction pressure drop, psi,
w = mass flow rate,
g = acceleration of gravity,
ρ = water density,
D_H = channel hydraulic diameter,
A_{ch} = channel flow area,
L = length,
f = friction factor, and
ϕ_{TPF} = two phase friction multiplier.

This basic model is similar to that used throughout the nuclear power industry. The formation for the two-phase multiplier is based on data which compare closely to those found in the open literature.[3]

General Electric Company has taken significant amounts of friction pressure drop data in multirod geometries representative of modern BWR plant fuel bundles and correlated both the friction factor and two-phase multipliers on a best-fit basis using the above pressure drop formulation. Checks against more recent data are being made on a continuing basis to ensure that the best models are used over the full range of interest to boiling water reactors.

4.1.1.2 Local Pressure Drop

The local pressure drop is defined as the irreversible pressure loss associated with an area change such as the orifice, tie plates, and spacers of a fuel assembly.

The general local pressure drop model is similar to the friction pressure drop and is

$$\Delta P_L = \frac{w^2}{2g\rho} \quad \frac{K}{A^2} \quad \phi_{TPL} \ ,$$

where

ΔP_L = local pressure drop, psi,
K = local pressure drop loss coefficient,
A = reference area for local loss coefficient,
ϕ_{TPL} = two-phase local multiplier,

and w, g, and ρ are defined the same as for friction. This basic model is similar to that used throughout the nuclear power industry. The formulation for the two-phase multiplier is similar to that reported in the open literature[4] with the addition of empirical constants to adjust the results to fit data taken at General Electric Company for the specific designs of the BWR fuel assembly. Tests are performed in single-phase water to calibrate the orifice and lower tie

plate, and in both single- and two-phase flow to arrive at best-fit design values for spacer and upper tie plate pressure drop. The range of test variables is specified to include the range of interest to boiling water reactors. Full scale 8x8 tests have been performed to determine the local loss coefficients for upper and lower tie plates and fuel rod spacers. These loss coefficients are in turn used in hydraulic analyses of the core for determination of local pressure losses.

4.1.1.3 Elevation Pressure Drop

The elevation pressure drop is based on the well-known relation

$$\Delta P_E = \bar{\rho} L; \quad \bar{\rho} = \rho_f (1 - \alpha) + \rho_g \alpha;$$

where

ΔP_E = elevation pressure drop, psi,
L = length,
$\bar{\rho}$ = average water density,
α = void fraction, and
ρ_f, ρ_g = saturated water and vapor density, resp.

The void fraction correlation is similar to models used throughout the nuclear power industry and includes effects of pressure, flow direction, mass velocity, quality, and subcooled boiling. Checks against new data are made on a continuing basis to ensure that the best models are used over the full range of interest to boiling water reactors.

4.1.1.4 Acceleration Pressure Drop

The pressure drop component due to acceleration includes the pressure change experienced by the fluid at an area change and the pressure change resulting from density change, such as that which occurs in steam formation. The formulation for the acceleration pressure drop is as follows:

Acceleration Pressure Change due to Flow Area Change:

$$\Delta P_{ACC} = (1 - \sigma^2) \frac{w^2}{2g\rho A_2^2}; \quad \sigma = \frac{A_2}{A_1};$$

where

ΔP_{ACC} = acceleration pressure drop,
A_2 = final flow area,
A_1 = initial flow area,

and other terms are as previously defined.

Acceleration Pressure Change due to Density Change:

$$\Delta P_{ACC} = \frac{w^2}{g A_{ch}^2} \left[\left(\frac{1}{\rho_M} \right)_{OUT} - \left(\frac{1}{\rho_M} \right)_{IN} \right];$$

where

$$\frac{1}{\rho_M} = \frac{x^2}{\rho_g \alpha} + \frac{(1-x)^2}{\rho_f (1-\alpha)},$$

ρ_M = momentum density,
x = steam quality,

and other terms are as previously defined. The total acceleration pressure drop in boiling water reactors is on the order of less than 5 percent of the total pressure drop.

4.2 FUEL ASSEMBLY THERMAL-HYDRAULIC EVALUATION

4.2.1 Critical Heat Flux and Minimum Critical Heat Flux Ratio

The critical heat flux (CHF) condition (the onset of the transition from nucleate boiling to film boiling) is one of the important design considerations in boiling water reactors. It occurs whenever excessive heat is being transferred

to boiling or evaporating water and is usually accompanied by a rapid deterioration of the heat transfer process. The critical heat flux is a function of the local steam quality, mass flow rate, pressure, and flow area geometry.

Analyses of CHF are based on the concept of the minimum critical heat flux ratio (MCHFR). The steam quality distribution, calculated by means of energy balances between the fuel and coolant, is used with the CHF correlation[5] to calculate the spatial distribution of CHF values. Dividing these values by actual design reactor heat fluxes yields the design MCHFR.

4.2.2 Steady-State Thermal-Hydraulic Licensing Criteria

For purposes of maintaining adequate thermal margin during normal steady-state operation, the previously established license limits of MCHFR $\geq$ 1.9 and MLHGR $\leq$ 17.5 kW/ft were applied to the 7x7 initial core and reload fuel. For the 8x8 reload fuel, the limits of MCHFR $\geq$ 1.9 and MLHGR $\leq$ 13.4 kW/ft were employed. Results from safety analyses using these steady-state operating limits as initial conditions are discussed in Section 6. Results of full scale 8x8 CHF testing will be made available to the USNRC upon completion of this ongoing test program.[6]

4.3 RESULTS OF THERMAL-HYDRAULIC ANALYSIS

Analyses were performed for a variety of core loadings to fully assess the effect of the 8x8 reload assembly on core thermal-hydraulic characteristics. The five core configurations considered are described as follows:

1. Core loaded with 7x7 fuel (representative of initial core or Reload-1 core loading).

2. Core loaded with 7x7 fuel and a single 8x8 reload fuel assembly.

3. One-quarter of the core loaded with 8x8 reload assemblies and the remainder loaded with 7x7 fuel.

4. One half of the core loaded with 8x8 reload assemblies and the remainder loaded with 7x7 fuel.

5. Full core loaded with 8x8 reload assemblies.

The thermal-hydraulic analyses were performed for the following reactor conditions:

Reactor Power:	1670 MWt
Reactor Pressure:	1040 psia (steam dome)
Recirculation flow rate:	57.6×10^6 lb/h
Inlet enthalpy:	523 Btu/lb
Bypass flow:	10% of total core flow

The same design basis power distribution as was previously employed was used in the analysis. The power peaking factors are as follows:

Power Peaking Factor	7x7	8x8
Radial	1.47	1.47
Axial	1.57	1.57
Local	1.24	1.22

Table 4-1 presents a tabulation of significant thermal-hydraulic characteristics calculated for the identified cases. The results show that, irrespective of the number of 8x8 fuel assemblies loaded in the core, both the 7x7 and 8x8 fuel assemblies receive adequate coolant flow. The margin to CHF for the limiting assembly in an 8x8 core, or in a mixed 7x7-8x8 core, is always equal to or greater than the margin to CHF for the limiting assembly in a 7x7 core. Furthermore, due to the increased heat transfer area and correspondingly lower operating heat flux of the 8x8 assembly relative to the 7x7 assembly, the 8x8 fuel has greater margin to CHF than does the 7x7 fuel.

Table 4-1

RESULTS OF THERMAL-HYDRAULIC ANALYSES

Case Number	1	2		3		4		5
Core Average Void Fraction, %	27.4	27.4		27.4		27.5		27.5
Core Pressure Drop, psi	17.9	17.9		18.2		18.4		18.9
Water Rod Flow, % of Total Core Flow	N/A	0.0008		0.09		0.17		0.35
Assembly Type	7x7	7x7	8x8	7x7	8x8	7x7	8x8	8x8
Number	484	483	1	363	121	242	242	484
Hot Channel Coolant Flow, 10^3 lb/h	109	109	102	111	103	112	104	106
Hot Channel MCHFR	2.01	2.01	2.27	2.03	2.30	2.05	2.31	2.36

Case Description:

Case 1: Full core loading (484 assemblies) of 7x7 fuel.
Case 2: Same as case 1 with one 7x7 assembly replaced with an 8x8 assembly.
Case 3: One-quarter core load of 8x8 reload assemblies with the remainder 7x7 assemblies.
Case 4: One-half core load of 8x8 reload assemblies with the remainder 7x7 assemblies.
Case 5: Full core loading of 8x8 reload fuel.

REFERENCES - SECTION 4

1. "Core Flow Distribution in a Modern Boiling Water Reactor as Measured in Monticello," Licensing Topical Report, January 1971 (NEDO-10299).

2. Kim, H. T. and Smith, H. S., "Core Flow Distribution in a General Electric Boiling Water Reactor as Measured in Quad Citier Unit 1," Licensing Topical Report, December 1972 (NEDO-10722).

3. Martinelli, R. C. and Nelson, D. E., "Prediction of Pressure Drops during Forced Convection Boiling of Water," ASME Trans., 70, pp. 695-702, 1948.

4. Baroozy, C. J., "A Systematic Correlation for Two-Phase Pressure Drop," Heat Transfer Conference (Los Angeles), AIChE, Preprint No. 37, 1966.

5. Monticello Nuclear Generating Plant Safety Analysis Report, Docket No. 50-263.

6. Hinds, J. A. (General Electric Co.) letter to J. M. Hendrie (USAEC), March 30, 1973.

5. NUCLEAR CHARACTERISTICS

5.1 INTRODUCTION

The nuclear design of the 8x8 reload bundles described in this section has been performed with the same analytical models and design methods used for General Electric 7x7 reload cores licensed by the USAEC over the past several years. No changes have been made in the analytical models or in the design methods. The 8x8 reload bundles will be loaded into the cores that have been closely followed by GE using these same analytical models and design methods. A high degree of confidence can be expressed regarding the verification of GE nuclear models and methods for these plants. In addition, these same models and methods have been routinely used for cores having lattices in the range from 6x6 to 11x11, and in cores with mixtures of either 6x6 and 7x7 or 8x8 and 9x9.

The 8x8 fuel being licensed is well within the range of physical parameters of previous General Electric fuel designs, and no decrease in accuracy can be expected because of the change to an 8x8 fuel design.

5.2 BUNDLE NUCLEAR DESCRIPTIONS

The mechanical description and physical parameters of the 8x8 reload fuel have been given in Section 3. This section describes the calculated nuclear parameters of the 8x8 reload bundles and makes comparisons to previously licensed 7x7 fuel designs.

There are few real "limits" on the bundle design itself. The real limits are generally expressed in terms of core parameters (e.g., shutdown margin or maximum heat flux). The results of analyses involving core nuclear characteristics are discussed in Section 5.5. The intent herein is to describe the nuclear parameters and to show that for 7x7 and 8x8 bundles of the same average enrichment, the calculated nuclear parameters are either not remarkably different or are different in a manner that would be expected. The choice of some parameter (say hot reactivity) for reload fuel is dependent on the environment in which the reload fuel bundle will be used: that is, the reload bundle

requirements would be slightly different for a very early shutdown than for an outage following a period of operation beyond full power exposure capability. Generally, for reload fuel, the enrichments and reactivities of the bundles will be higher than for initial cores. Specifically, a much higher value of reactivity is allowable for the low exposure reload bundle than is allowable for the initial core bundle (at the same low exposure) because the reload fuel bundle is loaded into an environment of highly exposed bundles of generally lower average reactivity.

5.2.1 2.62 wt% U-235 8x8 Bundle Design

5.2.1.1 Reactivity

Figure 5-1 shows the hot average void reactivity of the 2.62 wt% U-235 bundle versus exposure and compares this bundle to a 7x7 bundle of 2.63 wt% U-235 enrichment used at Oyster Creek as the first reload batch. The Oyster Creek R-1 bundle has the same number of gadolinium-containing rods as the 8x8 bundle, but the average gadolinium concentration is about half that of the 8x8. The result of this difference is that the gadolinium is worth less and burns out faster in the 7x7 bundle than in the 8x8, and thus the 7x7 bundle has a higher initial reactivity than the 8x8. Following the gadolinium burnout, however, the reactivities of the bundles are essentially identical.

Table 5-1 compares some physical parameters for these two bundles, while Table 5-2 compares the zero exposure cold reactivities of the two bundles. As can be seen in Figure 5-1, while the initial reactivities of the bundles differ because of different gadolinium worths, after the gadolinium is gone the reactivities of the bundles are essentially identical.

5.2.1.2 Void Reactivity

The variation of reactivity with void is of importance in the stability of the reactor core while at normal power operation. There is no design criteria placed on the void coefficient except that the overall void coefficient be negative at every point in the operating cycle. Overall void coefficients refer to

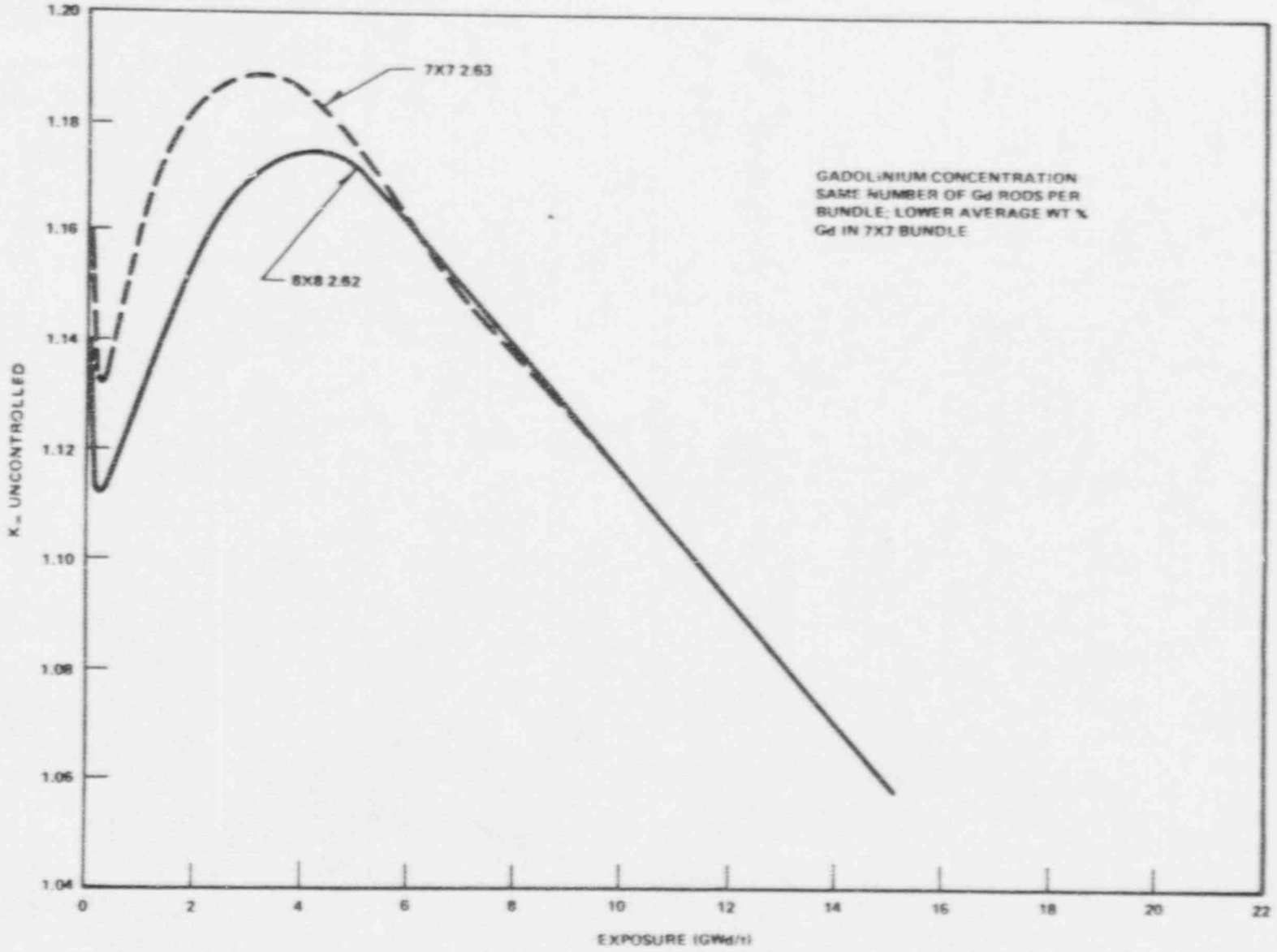

Figure 5-1. Hot Average Void Infinite Lattice K∞ versus Exposure

Table 5-1
PHYSICAL PARAMETERS OF 2.63 7x7 AND 2.62 8x8

	7x7	8x8
Pellet Outside Diameter (in.)	0.487	0.416
Rod Outside Diameter (in.)	0.563	0.493
Rod-to-Rod Pitch (in.)	0.738	0.640
Water-Fuel Ratio (cold)	2.43	2.60
U Bundle Weight (pounds)	427.8	404.6
Cladding Thickness (mils)	32	34

Table 5-2
COLD REACTIVITY COMPARISON
Zero Exposure

Condition	Controlled	7x7*	8x8**
k-infinity Cold	No	1.163	1.166
k-infinity Cold	Yes	0.988	0.981
Δk/k Control Strength		0.150	0.157

*2.63 wt% 7x7
**2.62 wt% 8x8

the core response. It will be sufficient here to give results of infinite lattice calculation of reactivity versus in-channel void fraction and to show that the same behavior is seen for both 8x8 and 7x7 fuel. Figure 5-2 compares the void reactivity of the same two bundles described above, and, as can be seen, the variation in reactivity with void is very close for both the controlled and uncontrolled states at zero exposure. Again, note that the value of the 7x7 bundle is lower than that of the 8x8 because an initially larger volume fraction of the bundle contains gadolinium. Figure 5-3 compares the lattice Δk_∞ going from 0.40 void to other voids as a function of exposure. As can be seen, the void reactivity characteristics are very similar.

5.2.1.3 Doppler Reactivity

The Doppler coefficient is of prime importance in reactor safety. The Doppler coefficient is a measure of the reactivity change associated with an increase in the absorption-of-resonance-energy neutrons caused by a change in the temperature of the material in question. The Doppler reactivity coefficient provides instantaneous negative reactivity feedback to any rise in fuel temperature, on either a gross or local basis. The magnitude of the Doppler coefficient is inherent in the fuel design and does not vary significantly among BWR reactor designs having low fuel enrichment. For most structural and moderator materials this effect is not significant, but in U-238 and Pu-240 an increase in temperature produces a comparatively large increase in the absorption cross section. The resulting nonfission absorption of neutrons causes a significant loss in reactivity. In BWR fuel, in which approximately 98% of the uranium in the UO_2 is U-238, the Doppler coefficient provides an immediate reactivity response that opposes fuel fission rate changes.

Although the reactivity change caused by the Doppler effect is small compared to other power-related reactivity changes during normal operation, it becomes very important during postulated rapid power excursions in which large fuel temperature changes occur. The most severe power excursions are those associated with rapid removal of control rods. A local Doppler feedback associated with a 3000 to 5000°F temperature rise is available for terminating the initial burst.

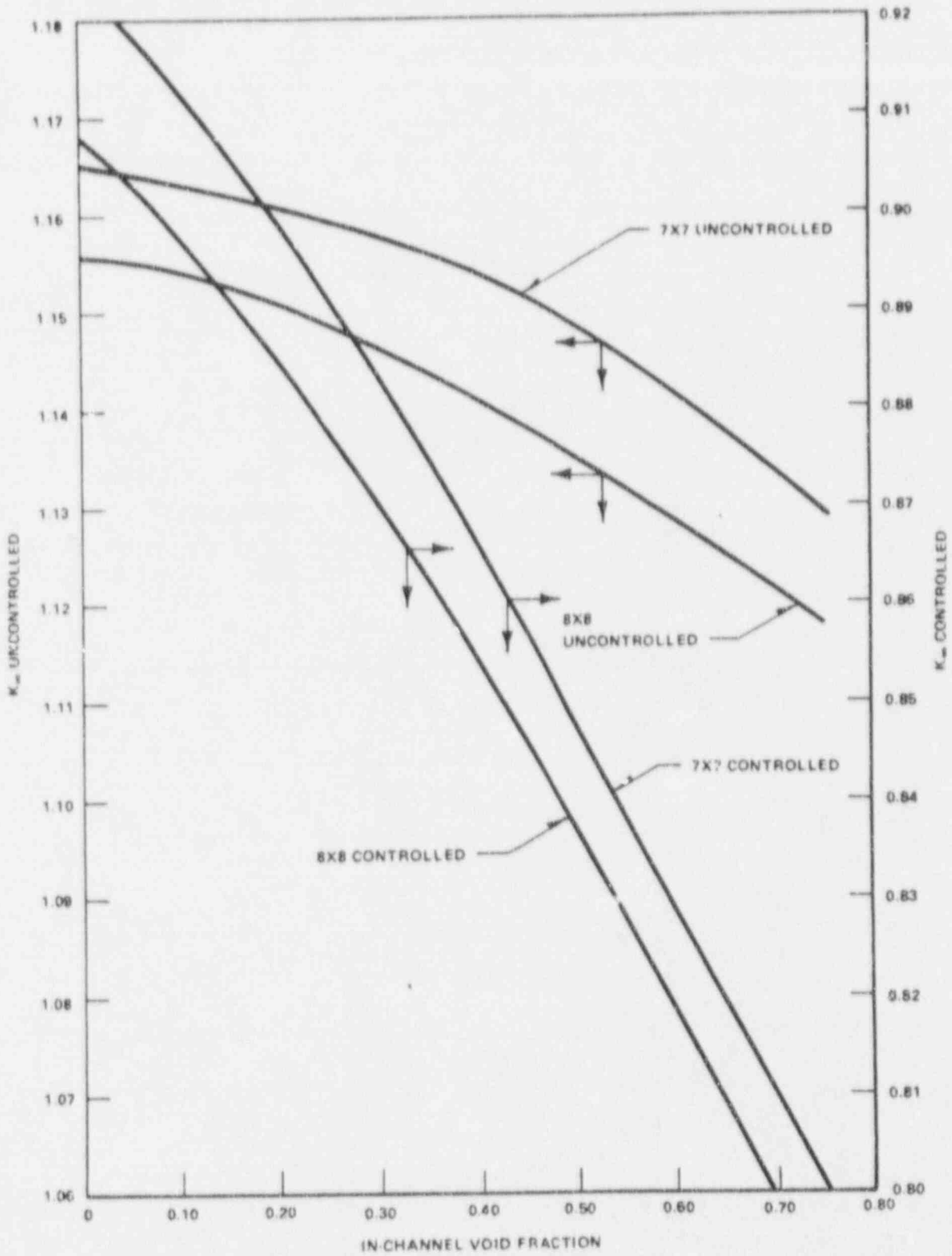

Figure 5-2. 2.63 7x7, 2.62 8x8 Infinite Lattice K^{∞} versus In-Channel Void Fraction Zero Exposure

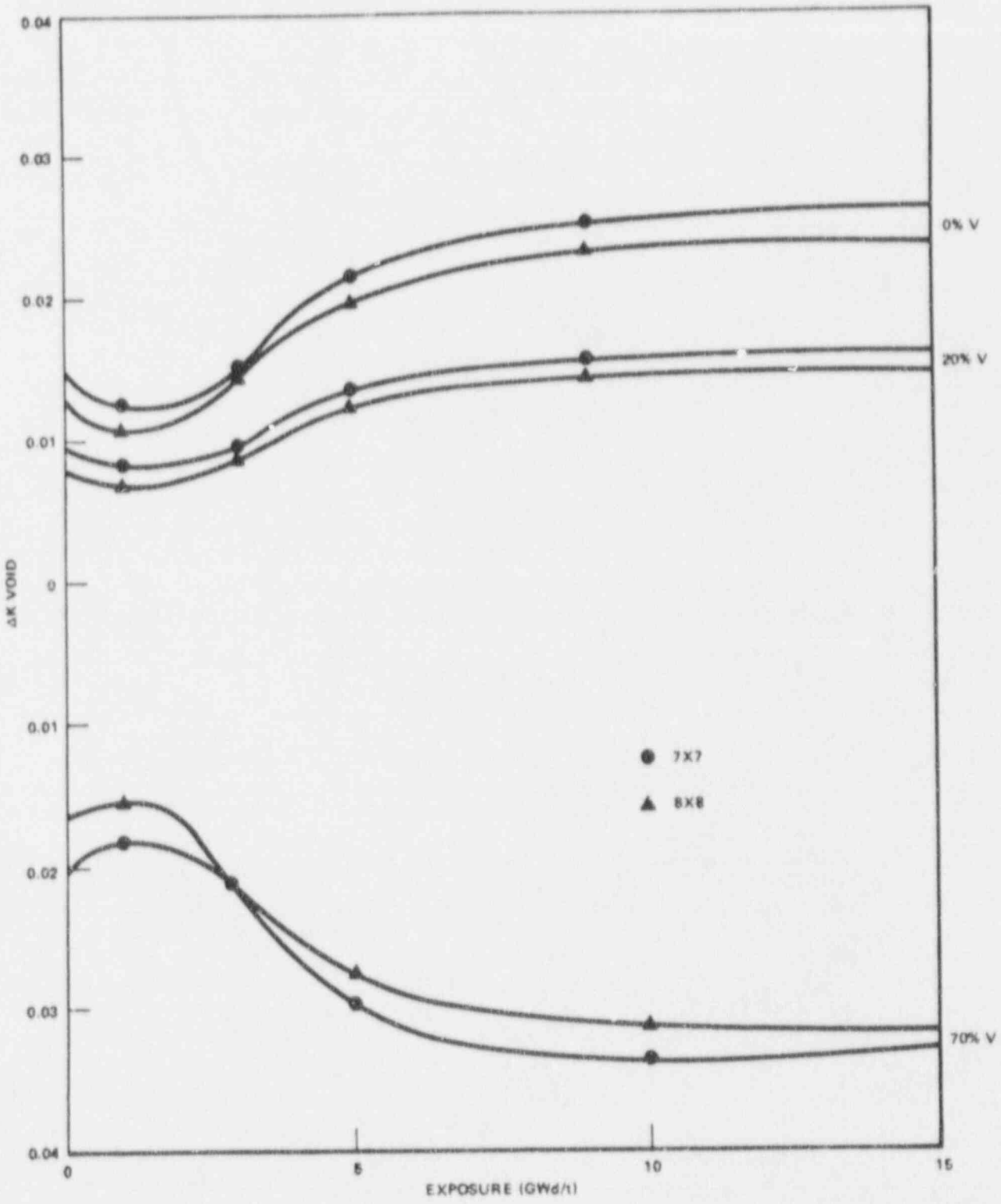

Figure 5-3. ΔK Void Comparison 7x7 versus 8x8 from 0.40 Void to Other Voids

The Doppler reactivity decrement is derived directly from the lattice calculations which are performed to generate the nuclear constants. The lattice methods currently being employed in the fast and resonance-neutron-energy regions are based on the method of Adler, Hinman and Nordheim[1] with the inclusion of the intermediate resonance approximation. This provides an adequate calculation of both the spatial and energy self-shielding for the resonance absorbers that explicitly includes temperature, moderator density, and geometry effects. A fine group B-1 slowing-down calculation of the fast and epithermal neutron spectrum provides the proper weighting of the resonance absorption to yield effective resonance integrals or cross sections that accurately represent the BWR environment.

The Doppler decrement is determined by doing the lattice calculations at several fuel temperatures holding all other input parameters constant. This results in a change in the neutron multiplication factor which is solely due to a change in the fuel temperature, which is the Doppler effect. From these analyses it has been determined that the Doppler defect, Δk_{Dop}, can be represented very accurately by the following expression:

$$\Delta k_{DOP} = CDOP\ (\sqrt{T_2} - \sqrt{T_1}).$$

Therefore, the Doppler reactivity decrement increases proportionally with the square root of fuel temperature, T, and CDOP is the constant of proportionality. The Doppler reactivity coefficient is derived using the same techniques described above. The following equation is used to calculate the Doppler reactivity coefficient:

$$\frac{1}{k}\frac{dk}{dT_2} = \frac{CDOP}{\left[k_1 + CDOP\left(\sqrt{T_2} - \sqrt{T_1}\right)\right] 2\sqrt{T_2}}$$

Figures 5-4 and 5-5 compare the Doppler coefficients for two 7x7 fuel designs o the Doppler coefficients for the 2.50 wt% U-235 8x8 bundle at 200 MWd/t and at 10,000 MWd/t, respectively. The Doppler coefficient of the 8x8 2.62 is essentially identical to that of the 8x8 2.50 bundle.

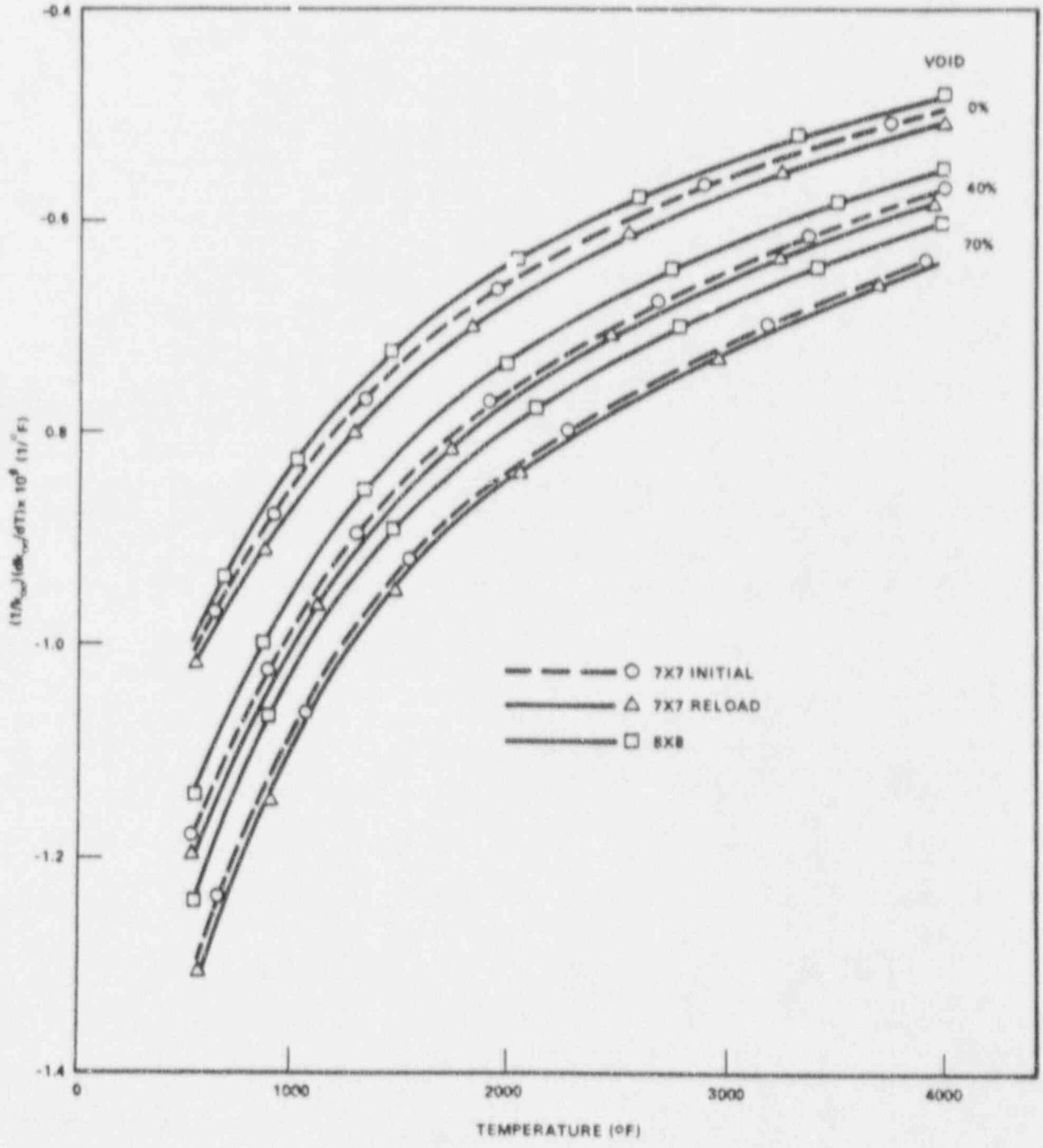

Figure 5-4. 200 MWd/t Doppler Coefficients Uncontrolled

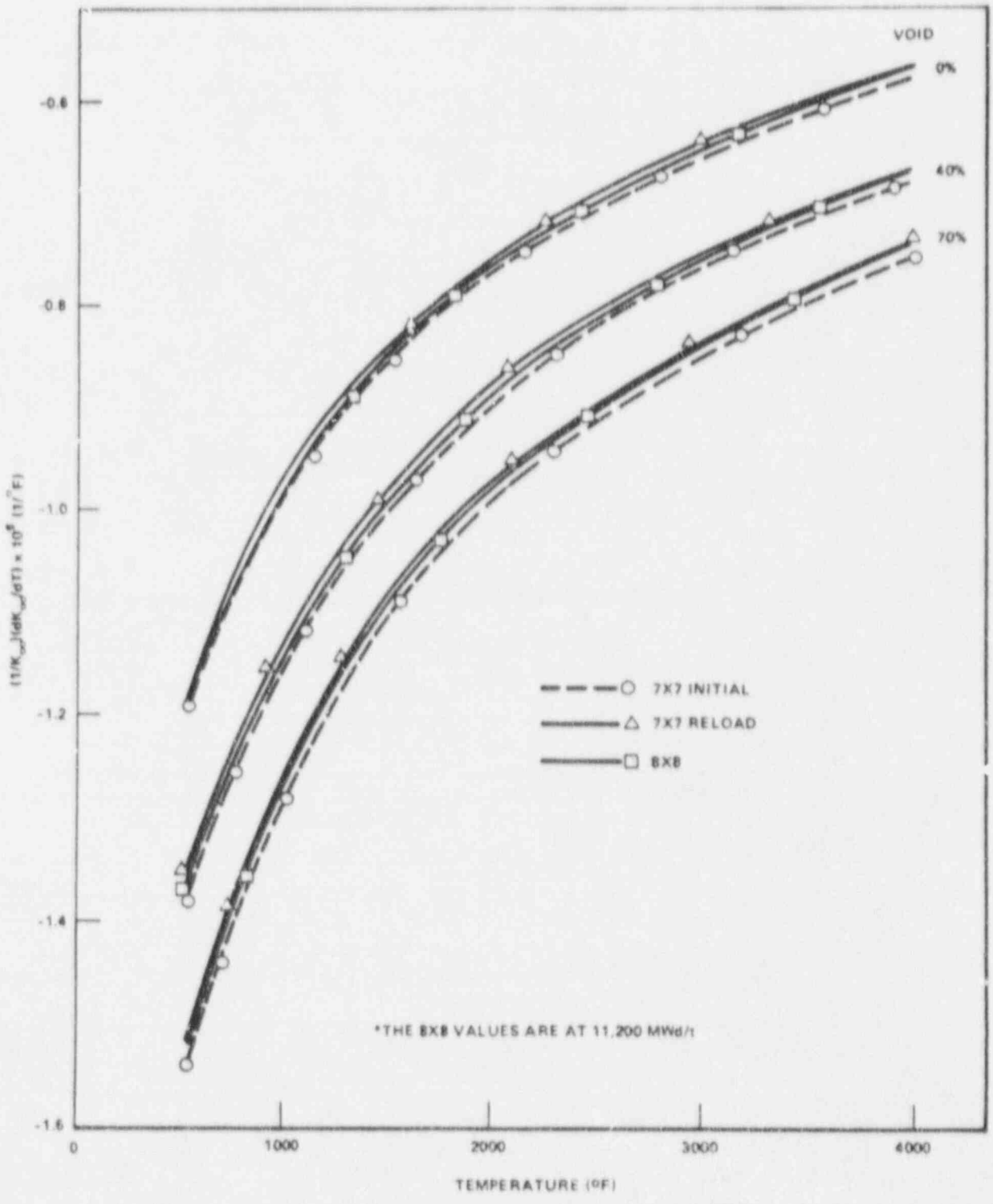

Figure 5-5. 10,000 MWd/t Doppler Coefficients Uncontrolled

It should be understood that the data presented in these figures are for an infinite lattice. In a finite reactor system the power distribution, and hence fuel temperature distribution, will vary spatially. This in turn results in a spatial variation in the Doppler feedback with larger Doppler reactivity decrements occurring in the high temperature and thus in high neutron flux regions of the reactor core. Therefore, high Doppler reactivity feedback can occur for relatively low core average power increases since the larger Doppler reactivity decrements will occur in the high flux, or importance weighting, regions of the core. Results of core calculations are reported in Table 5-3.

5.2.1.4 Delayed Neutron Fraction

Given in Figure 5-6 is a comparison of the delayed neutron fraction for the 2.62 8x8 bundle and the 2.63 7x7 bundle at hot average void conditions. As can be seen the differences are negligible.

5.2.1.5 Peaking Factors

The calculated maximum local peaking factors at average void for the 7x7 2.63 and 8x8 2.62 wt% U-235 bundles are compared in Figure 5-7. Of more importance to the reactor operator is the increased heat transfer area of the 8x8 bundle, leading to much lower peak kW/ft, as noted in Section

5.3 ANALYTICAL METHODS

The analytical methods and nuclear data used to determine the nuclear characteristics are similar to those used throughout the industry for water-moderated systems.[2]

The Lattice Physics Model is used to generate few-group-neutron cross sections for use in calculating lattice reactivities, relative fuel rod powers within assemblies, and averaged few-group cross sections. These cross sections and reactivities are calculated at various void and exposure conditions and are used for calculating two- and three-dimensional reactor power distributions. Local fuel rod powers are calculated for an extensive combination of parameters

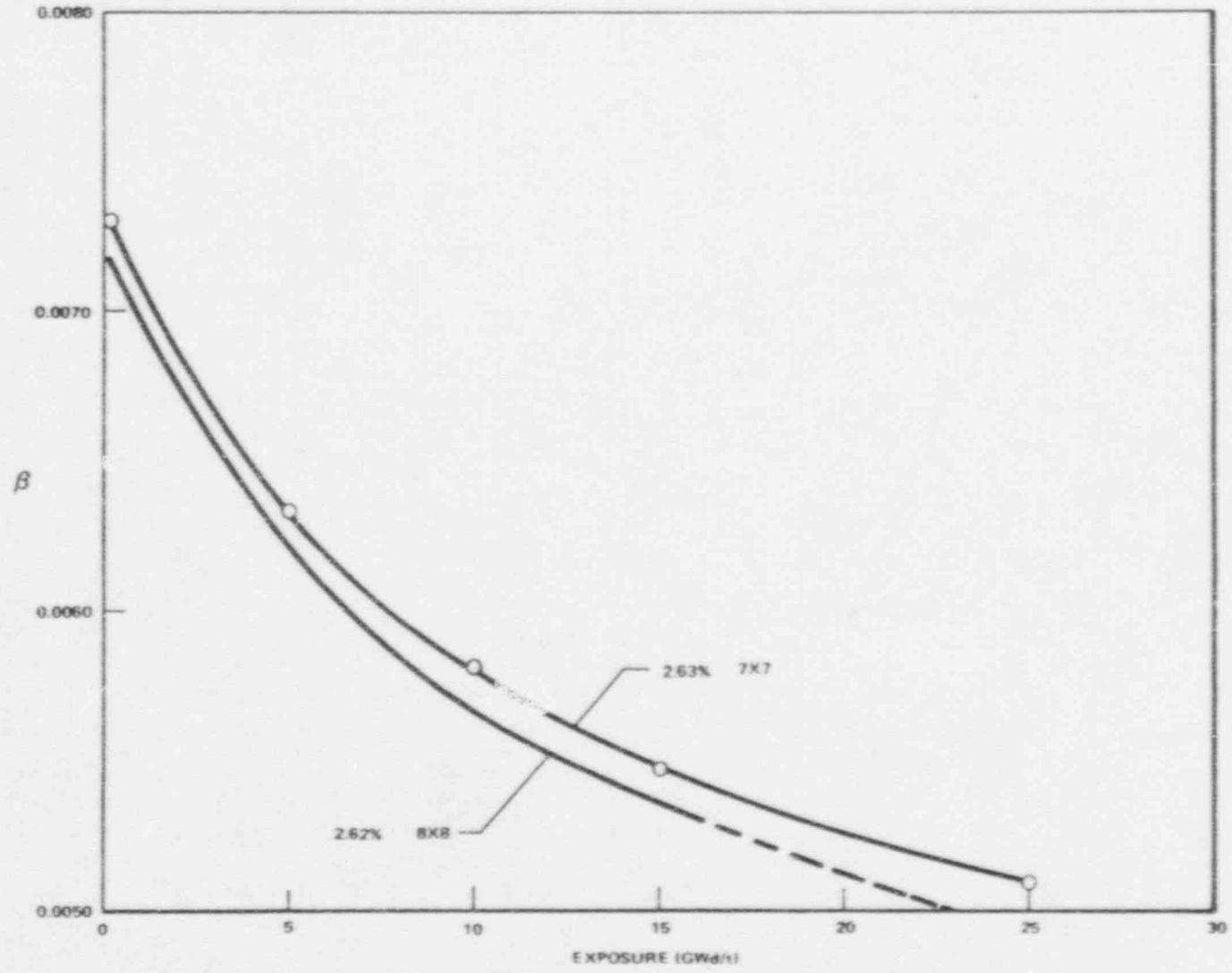

Figure 5-6. β versus Exposure Comparison 2.62 wt% 8x8, 2.63 wt% 7x7 Average Voids, Uncontrolled

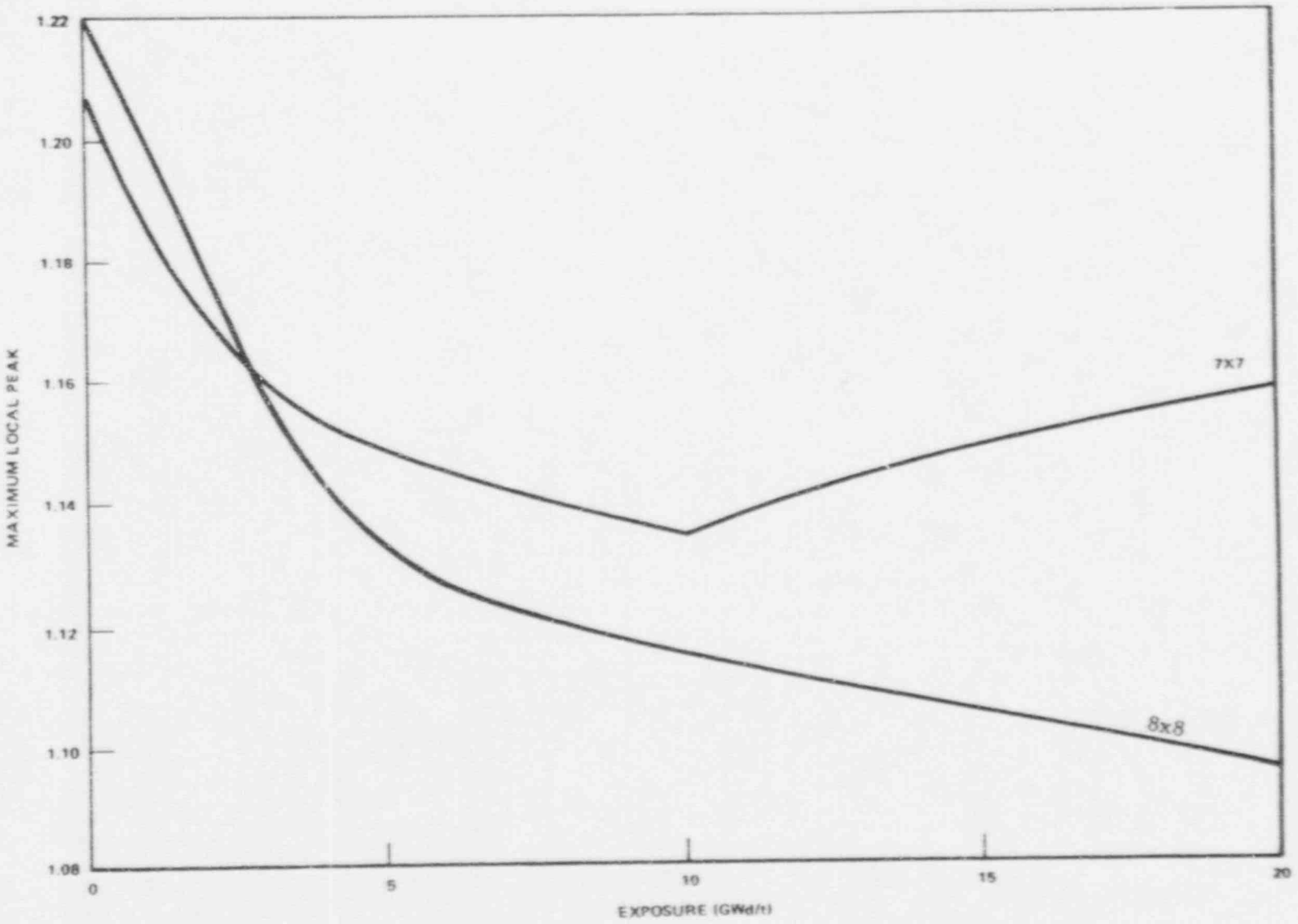

Figure 5-7. Maximum Local Peaking versus Exposure Comparison

including fuel and moderator temperatures, burnup, steam voids, and the presence or absence of adjacent control rods. These few-group calculations are performed over either single-bundle cells or groups of four bundles characteristic of repeating arrays in the loaded reactor core. The fast and resonance-energy cross sections are computed by GAM-type program.[1,3,4] The fast energies are treated by multigroup, integral collision probabilities to account for geometrical effects in fast fission. Resonance cross sections are computed using the intermediate resonance approximation, and the epithermal spectrum is obtained from a B-1 multigroup solution.[3] Account is taken of position and energy-dependent Dancoff factors. Changes due to concentration self-shielding and spectral effects of isotopic composition are recomputed as a function of fuel exposure. THERMOS-type calculations[5] are used to determine the spatially varying thermal spectrum throughout the fuel bundle. The effects of control blades on the cross sections of adjacent materials are calculated and accounted for. Power and flux distributions, infinite multiplication factors, and material and flux-weighted cross sections are calculated using two-dimensional, few-group diffusion theory on fuel assemblies and arrays of fuel assemblies. Burnup calculations are performed by integrating the secular equations describing the fuel depletion process with spatial neutron flux and energy distributions typical of reactor operating conditions. At selected burnup intervals, the nuclide concentrations are used to recalculate revised cross sections with the lattice model, and these are again recycled through two-dimensional diffusion theory.

A large three-dimensional boiling water reactor simulation code[6] providing for representation and calculation of spatially varying voids, control rods, burnable poisons, and other variables is used to compute power distributions, exposure, and reactor thermal-hydraulic characteristics at the beginning of core life and as burnup progresses. Gadolinia is distributed in a few rods within each fuel assembly for supplementary control. This feature makes it necessary to compute the radial space-time dependence of the Gd-155 and Gd-157 concentrations within the fuel rods. Experimentally, verification of the calculated reactivity effect as well as the calculated removal rate of the high cross-section isotopes has been accomplished. Observation of the operating control rod pattern during full power operation has shown the removal of the gadolinia control to be well matched to the fissionable isotope removal. The effective rate of depletion can be monitored by observing the operating reactivity status.

Thus, any trend toward an unacceptably small shutdown margin caused by faster-than-anticipated absorber removal could be detected and remedial action applied before any unsafe condition could be created. Any tendency toward slower removal rates would affect only cycle length and would be an economic problem unrelated to safety.

Operating reactor and critical experiments compared to theoretical data provide the precision necessary for reactor design.[7,8,9] The reactivity calculation of these analytical methods is frequently compared to the actual performance of operating reactors. Specific comparisons have been made for the Oyster Creek and Dresden 2 plants. The results of these comparisons show that the calculated and actual results agree within experimental and manufacturing tolerances. The design methods have been shown to be able to compute local powers to within ±3%, fuel assembly segment powers to within ±10%, Pu-U ratios versus exposure to within ±3%, and core reactivities and cold shutdown margin to within 0.005 Δk.

Experimental tests have also been used to verify the analytical calculations of both reactivity and isotopic composition for lattices in the range from 6x6 to 8x8. These tests give results nearly identical to the comparisons with the operating plants. The most recent experimental comparison is documented in Reference 9.

5.4 EXPERIENCE WITH GE NUCLEAR MODELS

The analytical methods described in Section 5.3 have been used by General Electric to design and follow cores having lattices in the range from 6x6 to 11x11 aside from the normal 7x7 reload cores. Of special interest in this regard are the Humboldt Bay and the Garigliano reactors. These cores are operating with mixed lattices and have operated successfully for some time. In the case of Humboldt, the core has operated since July of 1969 with a mixture of 6x6 and 7x7 reload fuel bundles in the core. This mixed lattice reload core has been licensed by the USAEC following General Electric analysis using the same analytical methods described above. Also of note in this regard is the Garigliano reactor which has operated since October of 1968 with a mixture of 8x8 and 9x9 fuel bundles. This reload core has been licensed by a regulatory agency

comparable to the USAEC following General Electric analysis. All nuclear license submittal information supplied by General Electric for the past several years has been developed using these same well proven analytical methods. There has been adequate experimental and operational verification of these methods to lattice designs of other than 7x7 fuel. No decrease in accuracy can be expected because of the change to an 8x8 fuel design.

5.5 NUCLEAR CHARACTERISTICS OF THE CORE

Earlier sections have discussed the infinite lattice steady-state reactivities and reactivity coefficients of the new 8x8 reload fuel bundles and have made comparisons to previously used 7x7 reload bundles. This section discusses the results of core calculations on shutdown margin (including the liquid poison system) and core average reactivity coefficients.

5.5.1 Core Effective Multiplication, Control System Worth and Reactivity Coefficients

A tabulation of the typical nuclear characteristics of the pre- and post-outage cores is provided in Table 5-3. Because the nuclear characteristics of the reload fuel are close to those of the initial fuel, the temperature and void dependent characteristics of the reload core will not differ significantly from the values previously reported.

5.5.2 Reactor Shutdown Margin

The refueled core fully meets criteria established for the initial core in that it may be maintained subcritical in the most reactive condition throughout the subsequent operating cycle with the most reactive control rod in its full-out position and all other rods fully inserted. The shutdown margin at BOC3 is 0.010, and with an R value of 0.00 in Cycle 3, this shutdown margin is the minimum Cycle 3 value.

Table 5-3
NUCLEAR CHARACTERISITCS OF THE DESIGN REFERENCE CORE

Core-Effective Multiplication and Control System Worth (0% Voids, 20°C)		Pre-Outage Core	Reload Core
K_{eff}	Uncontrolled	1.093	1.122
Δk	Poison Curtains	0.008	---
Δk	Control Rods	0.153	0.163
K_{eff}	Fully Controlled	0.932	0.959
K_{eff}	Strongest Rod Out	0.946	0.990
Increase in Core Reactivity with Exposure into Cycle		<0.0	<0.0
Reactivity Coefficients, Range During Operating Cycle for Reload Core			
Steam Void Coefficient at 40% Voids			
$(1/k)(\Delta k/\Delta V)$, 1/% Void		-10.1×10^{-4}	-10.3×10^{-4} to -10.0×10^{-4}
Power Coefficient at 1670 MWt and 524 Btu/lb Inlet Enthalpy;			
$(\Delta k/k)/(\Delta P/P)$		-0.051*	-0.062 to -0.053
Fuel Temperature Coefficient at 650°C;			
$(1/k)(\Delta k/\Delta T)$, 1/°F Fuel		-1.17×10^{-5}	-1.06×10^{-5} to -1.17×10^{-5}

*Reference power level about 1400 MWt at EOC2.

5.5.3 Liquid Poison System

The liquid poison system is designed to provide the capability to bring the reactor from full power (1670) to a cold xenon-free shutdown condition (K_{eff} <0.97) assuming none of the control rods can be inserted. The requirements of this system are dependent primarily on the reactor power level and on the reactivity effects of voids and temperature between full-power and the cold, xenon-free condition. The liquid poison system has been examined and has been found to be adequate since the reference power level of 1670 MWt has not changed and the core reactivity effects of voids and temperature have not been significantly altered by the introduction of reload fuel.

5.5.4 Reactivity of Fuel in Storage

There is no new safety implication with the spent fuel storage pool and the new fuel storage rack configuration, because the K_∞ of the reload fuel is less than the K_∞ of the initial fuel assemblies without temporary control curtains.

REFERENCES - SECTION 5

1. Carter, J. L., Jr., "Computer Code Abstracts, Computer Code-HRG," Reactor Physics Dept., Technical Activities Quarterly Report, July, August, September 1966, October 15, 1966 (BNWL-340).

2. Chernick, J., "Status of Reactor-Physics Calculations for U.S. Power Reactors " Reactor Technology, 13, 4, (Winter 1970-1971).

3. Wilcox, T. P. and Perkins, S. T., "AGN-GAM, an IBM 7090 Code to Calculate Spectra and Multigroup Constants," April 1965 (AGN-TM-407).

4. Carter, J. L., "HRG3 A Code for Calculating the Slowing Down Spectrum in the P_1 or B_2 Approximation," October 15, 1966 (BNWL-340).

5. Honeck, H. C., "THERMOS - A Thermalization Transport Theory Code for Reactor Design," June 1961 (BNL-5826).

6. Crowther, R. L., Petrick, W. P., and Weitzberg, G. A., "Three Dimensional BWR Simulation," ANS National Topical Meeting, April 1969.

7. Fuller, E. D., "Physics of Operating Boiling Water Reactors," Nuclear Applications and Technology, 19, November 1969.

8. Aline, P. G., et al., "The Physics of Non-Uniform BWR Lattice," BNES International Conference on the Physics Problems in Thermal Reactor Design, June 1967.

9. "Contained Burnable Neutron Absorber as Supplementary Control," Quad Cities Units 1 and 2 FSAR, Ammendment 9.

6. SAFETY ANALYSES

6.1 MODEL APPLICABILITY TO 8x8 FUEL

This section provides information on the applicability (to the 8x8 design) of existing models used for safety analysis. Where changes in fuel design affect model applicability, the capacity of the models to accommodate these changes is discussed.

6.1.1 Control Rod Drop Accident (RDA)

The postulated sequence of events for this the worst case accident involves an abnormally high worth rod becoming disconnected from its drive, being stuck in the fully inserted position, the drive being withdrawn and the control rod falling out of the core to the rod drive position. Analysis of this accident is performed at various reactor operating states; the key reactivity feedback mechanism affecting the shutdown of the initial prompt power burst is the Doppler coefficient. Final shutdown is achieved by scramming all but the dropped rod. The methods utilized to evaluate the rod drop accident have been updated on a continuing basis to reflect improvements in analytical capability.[1,2,3,]

The change from a 7x7 to an 8x8 fuel lattice has no effect on the excursion model used in the analysis of the RDA or on the reactivity feedback effect due to Doppler which is used in the analysis. The number of fuel pins failed due to the RDA is dependent on the fuel pin (local) power peaking factors in the bundle and final peak fuel enthalpy in the core. The local peaking factors and the peak fuel enthalpy are inherently known for an 8x8 lattice, the local peaking factors from the lattice design calculations,[1] and the peak fuel enthalpy from the RDA analysis.

Homogenized bundle cross sections and nuclear constants are calculated using standard lattice design techniques as noted in Section 5. Since the bundle cross sections, which are produced from the lattice calculations and which are used in the RDA excursion model, are homogenized, the RDA excursion model does not recognize the lattice type used to produce the bundle cross sections.

A mixture of 7x7 and 8x8 fuel bundles in a reloaded core present no analytical problem. The homogenized cross sections and nuclear constants used to represent each fuel bundle in the RDA analysis are calculated using methods which have previously been used for lattice designs from 6x6 to 11x11 geometry and in cores with mixtures of either 6x6 and 7x7 or 8x8 and 9x9 (refer to Section 5). Local power peaking at RDA conditions is explicitly calculated.

6.1.2 Loss-of-Coolant Accident (LOCA)

The Emergency Core Cooling System models which are used for the LOCA analysis for 8x8 fuel are essentially those which have been previously used for the 7x7 fuel designs. They are described and exemplified in Reference 5. The specific models as applied to the 8x8 fuel design will be discussed in the following paragraphs in their order of presentation in Reference 5.

6.1.2.1 Short-Term Thermal-Hydraulic Model

The significant parameters used by the short-term thermal-hydraulic model will remain essentially the same in changing fuel designs. The exceptions are:

1. Core pressure drop - the total core pre-transient pressure drop for a full 8x8 core is ~1 psi higher than for a full 7x7 core. Since maximization of the core pressure drop is conservative, a partial 7x7/partial 8x8 core is assumed to be fully 8x8.

2. Core heat flux - the core heat flux versus time is consistent with 8x8 fuel operating LHGR and stored energy as well as 8x8 geometry. As in the case of core pressure drop the effect is small. The most significant parameters, the core thermal power, the maximum steam flow, and the recirculation flow, remain unchanged with this change in fuel design. The changes listed above result in only a small change in core flow and pressure responses.

6.1.2.2 Long-Term Thermal-Hydraulic Model

The only significant change to the long-term thermal-hydraulic model is the change in bundle geometry and therefore a small change in the core total hydraulic diameter of the core. The long-term thermal-hydraulic model has the capacity to model various geometries; therefore, such small changes resulting from the change in fuel design do not represent an "extrapolation" in the model. The important parameters, e.g., core power, steam flow, recirculation flow and basic reactor geometry, remain unchanged.

6.1.2.3 Transient Critical Heat Flux Model

The transient critical heat flux model will change only in that the bundle geometry and LHGR will change. Test data taken in the new ATLAS loop with full power 8x8 bundles is being provided to the AEC by General Electric to verify the applicability of the existing model. If modification of the model is required, it will be made based on the results of these extensive tests.

6.1.2.4 Core Heatup Model

The core heatup model used for 8x8 analyses is essentially that described in Reference 5 with the incorporation of the modifications described in Reference 6 and the obvious change to the 8x8 bundle geometry and LHGR. The model has been used to predict the results of a number of ECCS transient tests of a full scale stainless steel clad 8x8 heater rod bundle. These tests fully confirm the applicability of the Core Heatup Model as modified for 8x8 fuel. Full scale ECCS tests with pressurized Zircaloy heaters were conducted in October of 1973 for further demonstration of the applicability of the Core Heatup Model.

6.1.2.5 Total LOCA Analysis

The total LOCA analysis which includes the four above models will not change in procedure. The only changes in the results will be due to changes in fuel geometry and linear heat generation rate, which are handled by the existing

models without modification with the possible exceptions noted in 6.1.2.3. General Electric is presently discussing the applicability of current LOCA models for licensing 8x8 fuel with the AEC, and confirmation is expected shortly.

6.1.3 Transient Analysis and Core Dynamics

A complete range of single failure caused events which are abnormal but reasonably expected during the life of the plant were analyzed for 7x7 fuel as a part of the original plant licensing. Results from these analyses were included in the FSAR and subsequently reviewed for 7x7 reload fuel. A reanalysis of these events has been carried out incorporating 8x8 reload fuel and planned modifications to the reactor pressure relief system. The purpose of this section is to demonstrate the applicability of the current analytical models to 8x8 fuel and mixed core analysis.

6.1.3.1 Transient Analysis Model Applicability to 8x8 Fuel

The documentation of transient analysis methods for General Electric BWRs is provided in Reference 7. This document includes not only the equations of the transient model, but also a parameter study and comparison of safety analyses applying the model to plant startup data. The mathematical model described in Reference 7 is applied to both new and reloaded cores. The model as presently constituted is a "lumped" thermodynamic model with single bundle representations for average and hot channels. The neutron kinetics representation is a point reactor using the point reactor kinetics equations. This brief model review serves as a basis to point out that the model, which is very generally defined, does not change or lose validity due to a mixture of 7x7 and 8x8 or a total core of 8x8 fuel. Parts of the model lump or average system components for computation purposes. These model parts, such as thermodynamic regions or neutron kinetics, are affected by simple input parameter changes due to fuel changes.

The most affected part of the model is the actual fuel heat transfer model. There are several objectives in transient analysis which affect the fuel model. Briefly these can be broken down as: (1) computation of fuel thermal margins,

(2) conservative heat flux computation for the system transients, and (3) computation of average fuel temperature for Doppler. If the system contains a complete load of either 7x7 or 8x8 fuel, the fuel model input is straightforward because the entire core is represented by the same fuel parameters. In the case of mixed 7x7 and 8x8 core fuel loading, the average core thermal calculations are not completely characterized by either the 7x7 or 8x8 fuel type. The mixed fuel loading can be adapted conservatively to the model however. This is achieved by doing three things for input to the dynamic model: (1) using the fuel type conservative for the fuel thermal margin as the hot channel fuel type in the transient analyses; (2) since mixed load core dynamic performance is the average of 7x7 and 8x8 fuel, choosing the conservative fuel type for plant transients to yield overall system conservative results in the dynamic analysis; and (3) using Doppler coefficient input data which is conservative to the overall core design when coupled with the conservative fuel design of (2) above. The use of the dynamic model as outlined above will allow a totally conservative dynamic analysis for any fuel loading.

6.1.4 Rod Withdrawal Error (RWE)

The rod withdrawal error reactivity insertion event is normally included in the Transient Analysis portion of reload fuel safety analysis submittals. However, since the event is analyzed by methods other than the transient mathematical models referred to in 6.1.3, the model applicability of analysis of this event to 8x8 fuel or mixed cores is discussed separately.

Analysis of the rod withdrawal error is performed on the assumption that the maximum worth rod is fully inserted and adjacent rods are withdrawn in a manner which will allow full design reactor power with operating limits attained near the inserted rod. This is an abnormal rod pattern which is not normally employed, but it maximizes the rod worth of the inserted rod for purposes of the conservative analysis. The maximum worth rod is then inadvertently withdrawn until rod block occurs, initially assuming the worst allowable LPRM bypass conditions. The results depend primarily on the capability of the flux monitors to detect the local change in the fuel around the control rod as it is withdrawn and to stop the control rod before damage limit conditions occur.

It should be noted that there are two rod block systems currently in use in GE BWRs. The first is described in Reference 8 and is employed in Oyster Creek Unit 1 and Nine Mile Point Unit 1. All other GE BWRs utilize the rod block system described in Reference 9.

The Oyster Creek 1/Nine Mile Point 1 system uses the APRMs on a quadrant basis[8] and the other system uses the LPRM strings surrounding the control rod being withdrawn. In both cases the sensors in the system are reading neutron flux. Also in both cases, analysis of the transient is performed assuming worst case allowable LPRM bypass conditions.

The total analysis of the RWE transient utilizes the three-dimensional coupled nuclear-thermal-hydraulic representation of the core as described in Section 5.2 for determination of neutron flux levels at instrumented locations and for determination of fuel assembly flow rate. The responses by instruments to changes in flux levels is independent of the fuel type.

6.2 RESULTS OF SAFETY ANALYSIS

6.2.1 Core Safety Analyses

Use of the Hench-Levy correlation to determine the safety limit and to establish margins from the normal operating points to the safety limit was established in previous licensing submittals. The same considerations, margins, and damage limits described in detail before, have been applied in evaluating the reloaded core. The operating limit on LHGR for the reload fuel is lower than previously loaded fuel. A further discussion of these controlling factors in the core safety analyses is presented below.

6.2.1.1 Fuel Damage Limits

Fuel damage from perforation of the cladding and a subsequent release of fission products can result from overheating or excessive strain of the cladding. The former is assumed to occur when MCHFR reaches 1.0 based on the Hench-Levy correlation and the latter is assumed to occur when MLHGR reaches 25.4 kW/ft

(see Section 3). The mechanical design of the reload fuel is to the same design criteria and bases as the initial core fuel and the same damage limits are applicable.

6.2.1.2 Operating Limits

The R-2 bundles are designed to operate with the same MCHFR limit as the irradiated fuel in the same environment and with a lower MLHGR. That is, MCHFRs will be greater than 1.9 and MLHGRs will not be greater than 13.4 kW/ft. The limiting values of MCHFR for the reload fuel during normal operation are the same as for the initial core fuel based on the similar design conditions established for the fuels. The limiting value of MLHGR is lower for the reload fuel since it has 63 rods instead of 49 rods in the initial core fuel with approximately the same bundle power.

6.2.1.3 Operating Margins

With the previously given damage limits and design limits for the reload fuel, operating margins between the two limits for the reload fuel are expected to be greater than the previously loaded fuel. However, this is based on the maximum design condition. Actual reload fuel operating conditions of MCHFR and MLHGR are expected to be well below the design limits as has been the experience for previously loaded fuel. Thus, actual operating margins will continue to be greater than the minimum allowable values used in the analyses discussed below.

6.2.1.4 Abnormal Conditions

The minimum allowable operating margins described above are conservatively used in analyses of events such as abnormal operational transients and uncertainties concerning steady-state fuel operating conditions. Since these margins are not reduced with the reload fuel, the results of these analyses are not expected to change appreciably with the insertion of reload fuel except where dynamic changes are occurring on the reactor and its characteristics have been changed by the reload fuel in such a way as to significantly affect the transient results. These considerations involve the transient analyses which are covered separately below.

6.2.2 Accident Analyses

6.2.2.1 Main Steam Line Break Accident

The analysis of the main steam line break accident depends on the operating thermal-hydraulic parameters of the overall reactor, such as the pressure, and the overall factors affecting the consequences, such as primary coolant activity. Insertion of 8x8 reload fuel will not change any of these parameters so the previously reviewed results of this analysis will not change.

6.2.2.2 Refueling Accident

The analysis of the refueling accident depends on mechanical damage caused by a fuel bundle falling back onto the top of the core while it is being removed, which will not change with the use of the reload fuel. The consequences depend on the fission product inventory in the fuel and various factors affecting the amount and kind of releases to the atmosphere. The fission product inventory is not expected to increase even with the large number of rods in the 8x8 reload fuel bundle. Thus, even if more rods were damaged, the total fission product inventory is not increased, but there will be slight changes in the relative amounts of different constituents because of the slight differences in enrichment and gadolinia concentration. The effects of these small differences will be inconsequential in terms of the releases caused, and undetectable when the various reduction factors are applied to determine offsite consequences. Therefore, the prevously reviewed results of this accident analysis will not change.

6.2.2.3 Control Rod Drop Accident

6.2.2.3.1 Identification of Causes

There are many ways of inserting reactivity into a boiling water reactor. However, most of them result in a relatively slow rate of reactivity insertion and therefore pose no threat to the system. It is possible, however, that

rapid removal of a high worth control rod could result in a potentially significant excursion. Therefore, the accident which has been chosen to encompass the consequences of a reactivity excursion is the control Rod Drop Accident (RDA).

6.2.2.3.2 Starting Conditions and Assumptions

Before the control rod drop accident is poasible, the following sequence of events must occur:

1. The complete rupture, breakage or disconnection of a fully inserted control rod drive from its cruciform control blade at or near the coupling.

2. The sticking of the blade in the fully inserted position as the rod drive is withdrawn (worst case).

3. The falling of the blade after the rod drive is fully withdrawn (worst case).

This unlikely set of circumstances makes possible the rapid removal of a control rod. The dropping of the rod results in a high local k_∞ in a small region of the core. For large, loosely coupled cores, this would result in a highly peaked power distribution and subsequent shutdown mechanisms. Significant shifts in the spatial power generation would occur during the course of the excursion. Therefore, the method of analysis must be capable of accounting for any possible effects of the power distribution shifts.

In order to limit the worth of the rod which could be dropped, the rod worth minimizer system or a second operator controls the sequence of rod withdrawal. This assures no movement of an out of sequence rod before the 50% rod density configuration is achieved and limits movement of rods to in-sequence segments beyond the 50% rod density configuration during startups. The 50% rod density configuration occurs during each reactor startup and corresponds to the condition in which 50% of the rods are fully inserted in the core and 50% are fully withdrawn.

6.2.2.3.3 Accident Description

The accident is defined as:

1. The highest worth rod that can be developed at any time in core life under any operating condition drops from fully inserted position to fully withdrawn position (rod increments only beyond 50% rod density).

2. The rod drops.

3. The scram is that defined in the technical specifications.

The detailed analysis of this accident is discussed in References 1, 2, 3 and 4. A continuing effort is being made in the area of analytical methods to assure that nuclear excursion calculations reflect the latest "state-of-the-art."

The sequence of events and the approximate times of occurrence are as follows:

Event	Approximate Elapsed Time
(1) Reactor is at a control rod density pattern corresponding to maximum in-sequence rod worths	
(2) Rod worth minimizer or operators are functioning to restrict rod withdrawals to in-sequence rods or rod increments. Maximum worth in-sequence control blade becomes decoupled.	
(3) Operator selects and withdraws the control rod drive of the decoupled maximum worth in-sequence rod to its fully withdrawn position (rod increments only beyond 50% rod density).	
(4) Blade sticks in the full inserted position.	

Event	Approximate Elapsed Time
(5) Blade becomes unstuck and drops at the maximum velocity determined from experimental data (3.11 fps).	0
(6) Reactor goes prompt critical and initial power burst is terminated by the Doppler Reactivity Feedback.	<1 sec
(7) APRM 120% power signal scrams reactor.	
(8) Scram terminates accident.	<5 sec

6.2.2.3.4 Identification of Operator Actions

The termination of this excursion is accomplished by automatic safety features or inherent shutdown mechanisms. Therefore, no operator action during the excursion is required.

6.2.2.3.5 Analysis of Effects and Consequences

6.2.2.3.5.1 Methods, Assumptions and Conditions

The methods, assumptions, and conditions for evaluating the excursion aspects of the control rod drop accident are described in detail in References 1, 2, 3, and 4.

Reference (1) is the topical report on rod drop and is applicable to beginning of life conditions for curtained cores. Reference (2) is the first supplement to Reference (1) and is applicable to beginning of life conditions for Gadolinia cores. Reference (3) is the second supplement to Reference (1) and is applicable to exposed cores. Reference (4) is not a supplement to Reference (1), however, the information contained therein is supplemental since it is a direct expansion of the described methods applied to a parametric study of worst cased variables resulting in a boundary approach to rod drop accident evaluation.

The technical bases which are presented in Reference (4) were used to verify that the result of a rod drop excursion in the reloaded core would not exceed the design criteria, as described below.

Although there are many input parameters to the Rod Drop Accident Analysis, the resultant peak fuel enthalpy is most sensitive to three basic conditions. These are: 1) Doppler reactivity feedback, 2) accident reactivity characteristics, and 3) scram reactivity feedback.

If all other parameters remained unchanged, the rod drop excursion for exposed cores would be less severe than for initial cold clean cores under the same set of conditions since the Doppler reactivity feedback will be more negative. This is due to the fact that Pu^{240}, which has a large negative Doppler effect, builds up with exposure. Figure 6-1 shows the comparison between the actual Doppler coefficient and the Technical Bases Doppler (Reference 4) coefficient.

The accident reactivity characteristics have varying effects on the rod drop excursion results. These characteristics are accident reactivity shape, total control rod worth, local peaking factor, and the delayed neutron fraction. The total control rod reactivity worth (worth of the dropping rod) has a major effect on the accident results; this will not change substantially with the insertion of reload fuel. The local peaking factor and the delayed neutron fraction were inputs to the evaluation and were in the same range as those shown for actual plant experience in Reference(4). A comparison of the calculated accident reactivity shape function with the Technical Bases shape function is shown in Figure 6-2. Figures depicting hot startup conditions are not shown since the maximum in-sequence rod for that condition is not as limiting as for cold startup conditions.

The scram reactivity feedback function has a significant effect on the results of a rod drop excursion. The scram reactivity feedback shape was evaluated based on Technical Specification scram times and shown to be above that used in establishing the boundary in Reference (4). (See Figure 6-3).

The evaluation of each of these parameters by comparison to the boundary values presented in Reference (4) shows that the maximum rod worth is not as great as the

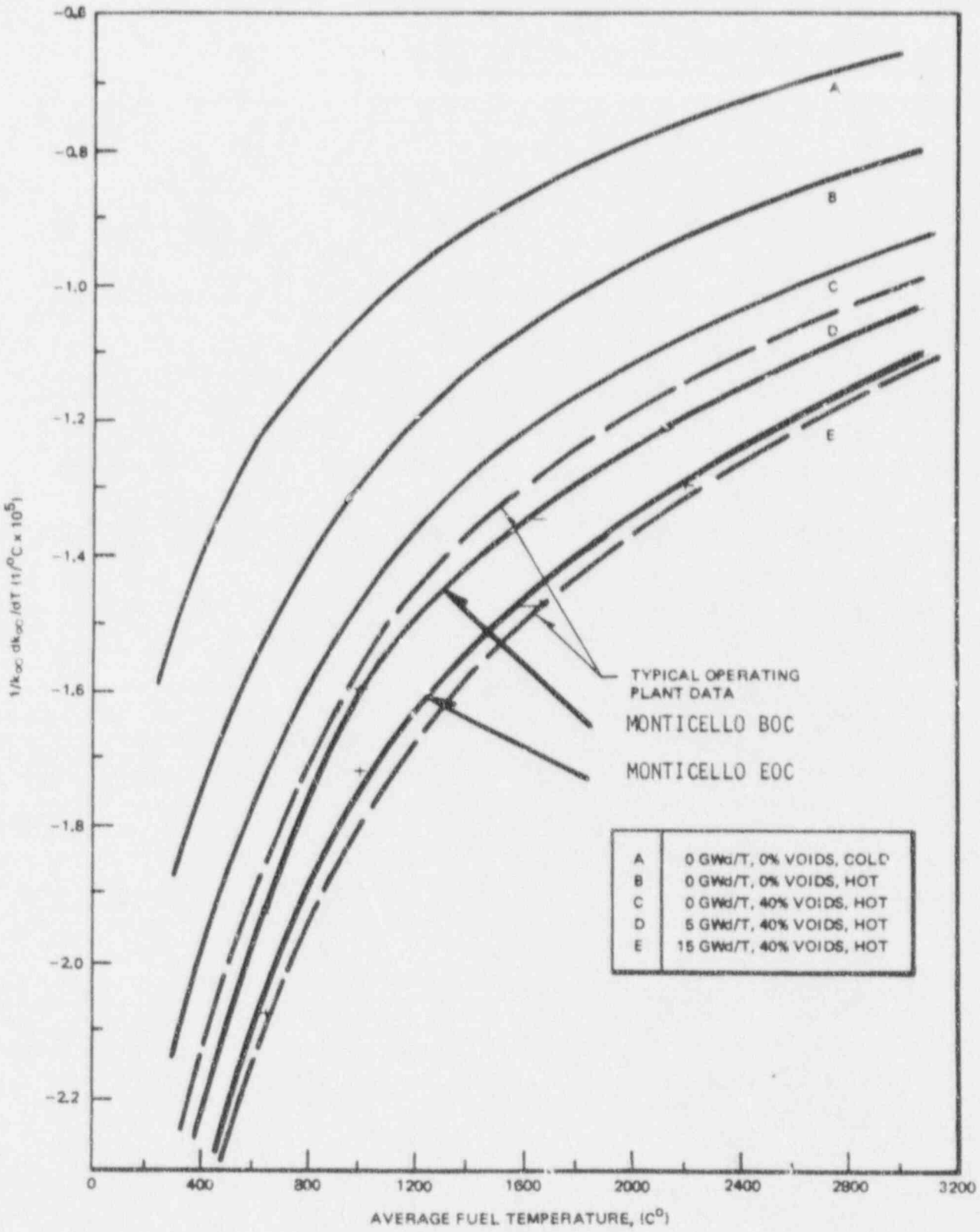

Figure 6-1. Doppler Reactivity Coefficient versus Average Fuel Temperature as a Function of Exposure and Moderator Condition for R2 Fuel

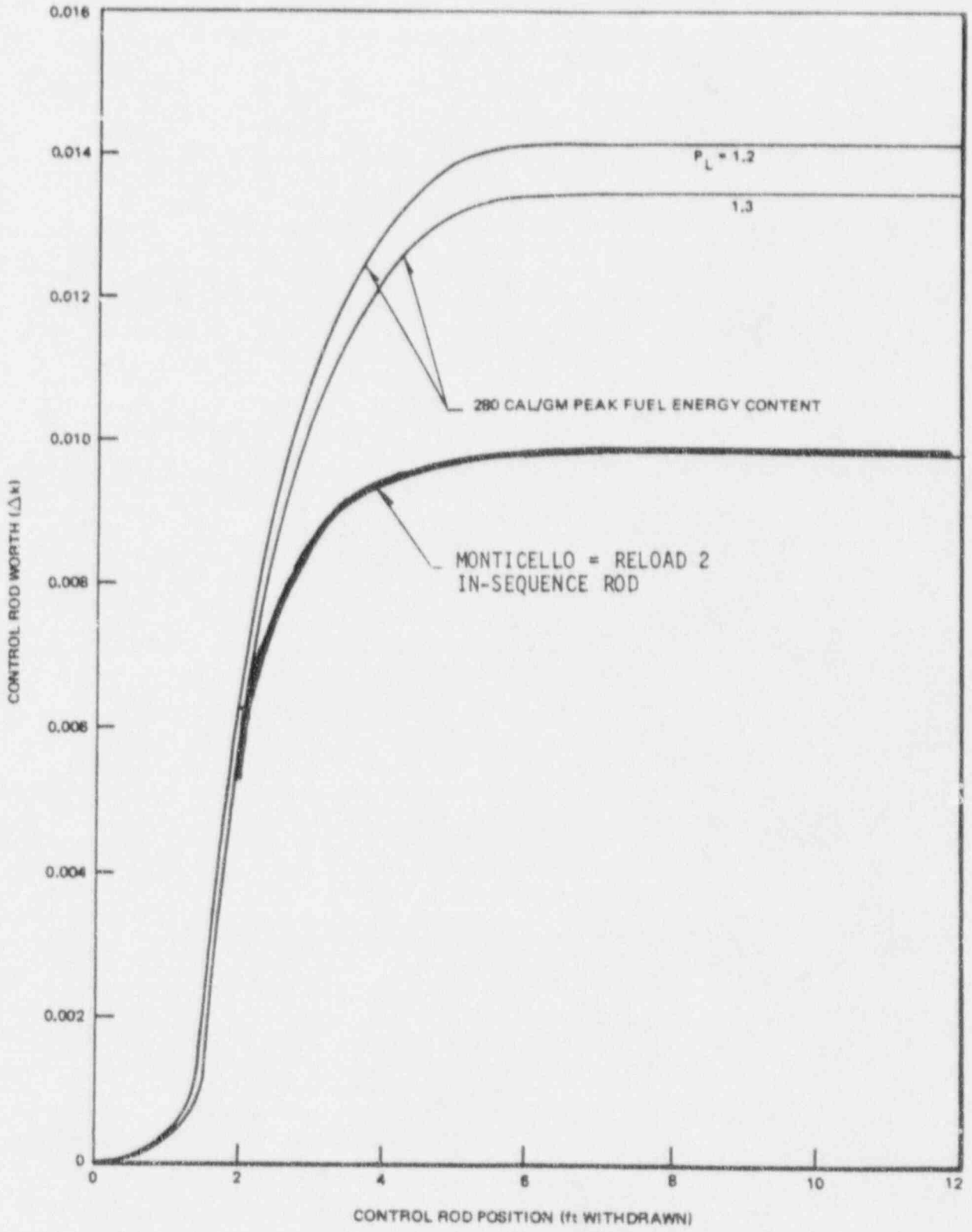

Figure 6-2. Accident Reactivity Shape Functions for Cold Startup β = 0.0054

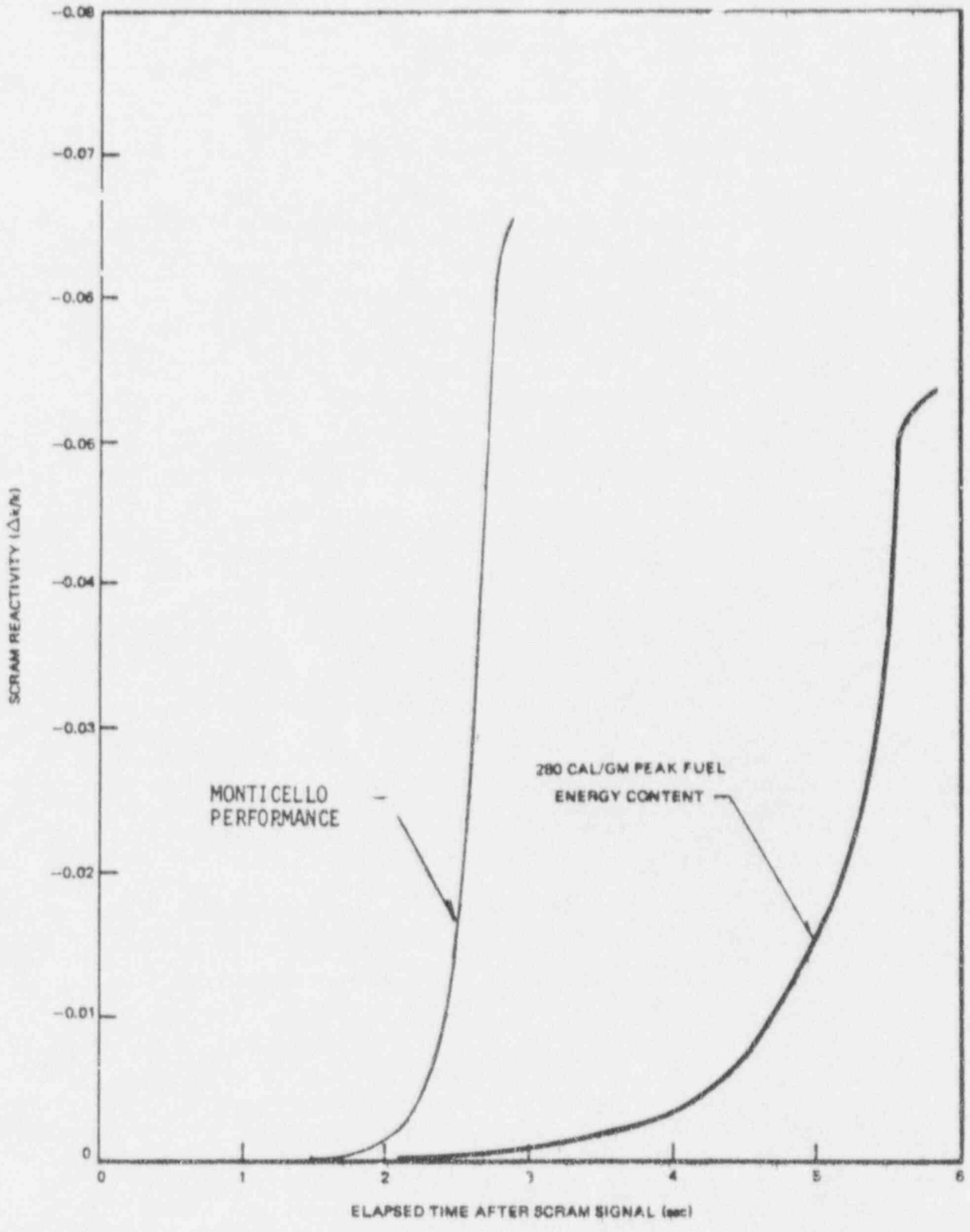

Figure 6-3. Scram Reactivity Function for Cold Startup

1.3% Δk derived. This verified that the consequences of a rod drop excursion from any in-sequence control rod would be below the 280 cal/gram design limit, since maximum in-sequence rod worths after this reload will be well below the 1.3% Δk allowable.

6.2.2.3.4.2 Fuel Damage

The fuel damage thresholds are based on both experimental and theoretical data. This information is discussed in Section 14 of Reference 10, and Section VI of Reference 11.

The rod drop accident analysis is sensitive to spatial variations in the core design such as fuel loading patterns, gadolinium distribution, etc. An estimate of the radiological exposures has been made and is based on the failure of all fuel rods above an energy content of 170 cal/gm assuming the maximum enthalpy reaches 280 cal/gm during the accident. This is consistent with the boundary approach established in Reference (4). The number of failed fuel rods and the released fission products are therefore approximately the same as those discussed in the boundary approach document. The resulting doses are well within the 10 CFR Part 100 guidelines.

6.2.2.4 Loss-of-Coolant Accident

The following evaluation is based on the 8x8 reload fuel. The results of the 7x7 fuel evaluation has not changed and can be found in previous submittals.

6.2.2.4.1 Design Bases

The objective of the emergency core cooling systems (ECCS), in conjunction with the containment, is to limit the release of radioactive materials following a loss-of-coolant accident so that resulting radiation exposures are within the values provided in published regulations.

Safety design bases and functional requirements for the emergency core cooling systems are given in the FSAR and have not changed.

6.2.2.4.2 System Design

The ECCS, comprising four separate subsystems, is designed to satisfy the following performance objectives:

1. To prevent fuel cladding melting as the result of any mechanical failure of the nuclear boiler system up to, and including, a break equivalent to the largest coolant recirculation system pipe.

2. To provide this protection by at least two independent, automatically actuated cooling systems.

3. To function with or without external (off-site) power sources.

4. To permit testing of all ECCS by acceptable methods including, wherever practical, testing during power plant operations.

5. To function under assumed seismic conditions described in Section 12 of Reference 10.

The operational capability of the various emergency core cooling systems to meet functional requirements and performance objectives is as follows.

During the first ten minutes following the initiation of operation of the ECCS, the functional requirements are satisfied for all combinations of single active component failure and single pipe breaks, including pipe breaks in any ECCS subsystem which might partially or completely disable that subsystem. After the first ten minutes, and in the event of an active or passive failure in the ECCS or its essential support system, long term core and containment cooling is provided by any one LPCI or core spray pump delivering water to the reactor vessel and by one RHR pump supported by one RHR heat exchanger with 100% service water flow.

The description and detailed design information on specific parts of the emergency core cooling system is presented in the FSAR (Reference 10).

6.2.2.4.3 Performance Evaluation

Summary. To achieve reliability, each emergency core cooling subsystem uses the minimum feasible number of components that are required to actuate. All equipment is testable during operation. Two different cooling methods - spraying and flooding - provide diversity.

Evaluation of ECCS controls and instrumentation for reliability and redundancy shows that a failure of any single initiating sensor cannot prevent or falsely start these cooling systems. No single control failure can prevent the combined cooling systems from adequately cooling the core. The controls and instrumentation are calibrated and tested to assure adequate response to conditions representative of accident situations.

The emergency core cooling systems are provided to remove the residual and decay heat from the reactor core so that fuel cladding temperature is kept below 2300°F. The intent of the ECCS temperature criterion is to prevent gross core meltdown and fuel cladding fragmentation. Under extreme conditions highly oxidized Zircaloy could fracture on cooling. Based on the AEC's model in the Interim Acceptance Criteria for ECCS, cladding fragmentation on cooldown is prevented (for the time scale of interest here) if the maximum cladding temperature is limited to less than 2300°F. This is therefore the design temperature criterion for ECCS system performance. The actual performance of the core cooling systems is such that peak temperatures much lower than 2300°F will be maintained throughout the complete break spectrum.

A summary of peak cladding temperatures calculated to occur in R-2 fuel for the worst intermediate break and the design-basis break is in Table 6-1.

Table 6-1

PEAK CLADDING TEMPERATURES

	Single Failure Assumed	Large Break Temperature (°F)	Intermediate Break Temperature (°F)	Intermediate Break Size (Ft^2)
AEC Index of Acceptability*	Worst Single Failure	2300	2300	X
Case				
1. AEC Assumptions	LPCI injection valve#	2030	X	X
2. AEC Assumptions	HPCI Failure†	X	1500	0.08

* Calculated metal-water reaction is less than 0.2% of cladding for all cases above. AEC acceptability index is 1%.

† Four LPCI pumps, two CS pumps, and ADS remaining.

X Does not apply.

Two CS pumps, one HPCI pump, and ADS remaining.

Evaluation Model. The performance analysis of the ECCS is based upon analytical models used to conservatively predict reactor vessel pressure, liquid inventory, and fuel cladding temperature variations with time after a break. These models are identified, exemplified, and fully explained in Reference 5. There have been no deviations from the evaluation model described in Appendix A, Part II of AEC Interim Policy Statement.

Fuel Clad Effects. Figure 6-4 shows peak cladding temperatures as a function of time for the worst single failure case which leaves 2CS + HPCI and the ADS operable. As shown, the maximum cladding temperature for this break, the most severe design-basis accident, is substantially limited by the emergency core cooling systems.

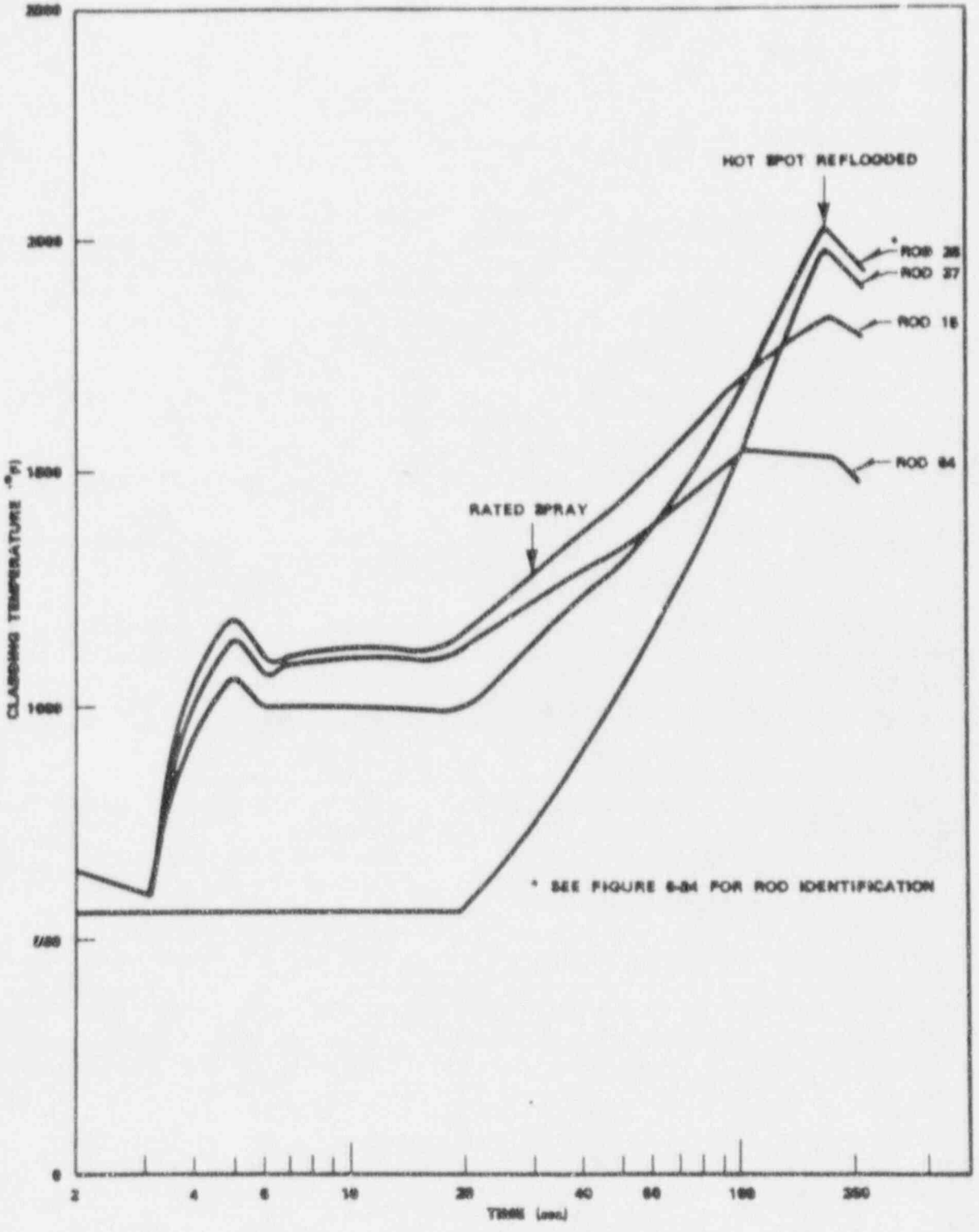

Figure 6-4. Cladding Temperature vs. Time for the Recirculation line Break with Failure of the LPCI Injection Valve (HPCI + ICS + ADS) ASC Assumptions

An example of the integrated system performance is shown in Figure 6-5 for a typical small size break with failure of HPCI. Peak cladding temperature for this case is shown in Figure 6-6.

Figure 6-7 is a break area spectrum analysis of the peak cladding temperature and percent metal-water reaction for the worst single failures. The single failures are the loss of the HPCI or the loss of the LPCI injection valve resulting in ECCS degradation to 4 LPCI + 2CS + ADS and HPCI + 2CS + ADS, respectively. Adequate cooling is maintained.

ECCS Performance

Individual System Performance. The capability of the individual subsystems of the ECCS is shown on the bar chart (Figure 6-8). A whole bar represents the capability of an individual system to protect the core without assistance from another subsystem. A half bar represents the range of break sizes for which a low pressure system must rely upon a high pressure system for additional inventory makeup and/or more rapid vessel depressurization. The ADS provides no inventory makeup and therefore cannot protect the core individually. The bar chart reveals subsystem characteristics but should not be applied to ECCS performance evaluations. No single failure could be hypothesized that would result in only one subsystem of the ECCS being available.

Integrated Operation of Emergency Core Cooling Systems. Two different methods and at least two independent core cooling systems are provided to limit fuel cladding temperature, over the entire spectrum of postulated reactor primary system breaks, as required by the design bases.

The following discussion is directed toward the integrated performance of the ECCS; that is, how the ECCS will actually operate to provide core cooling for the entire spectrum of loss-of-coolant accidents. The discussion is subdivided based on the two types of loss-of-coolant accidents; a break of a liquid line and a break of a steam line.

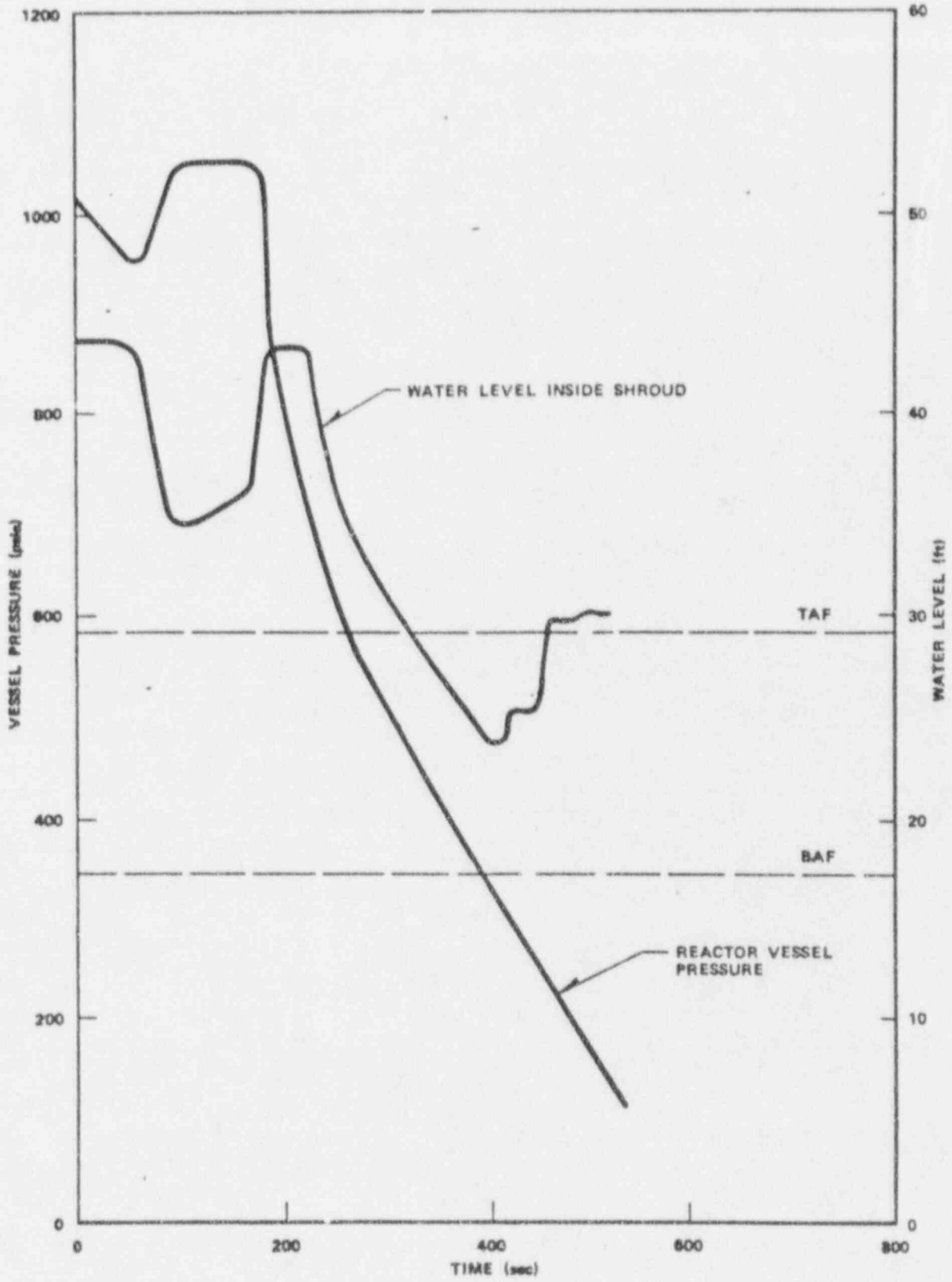

Figure 6-5. Performance of ECCS with Failure of HPCI for Small (0.02 ft^2) Liquid Break (2CS + 4LPCI + ADS) AEC Assumptions

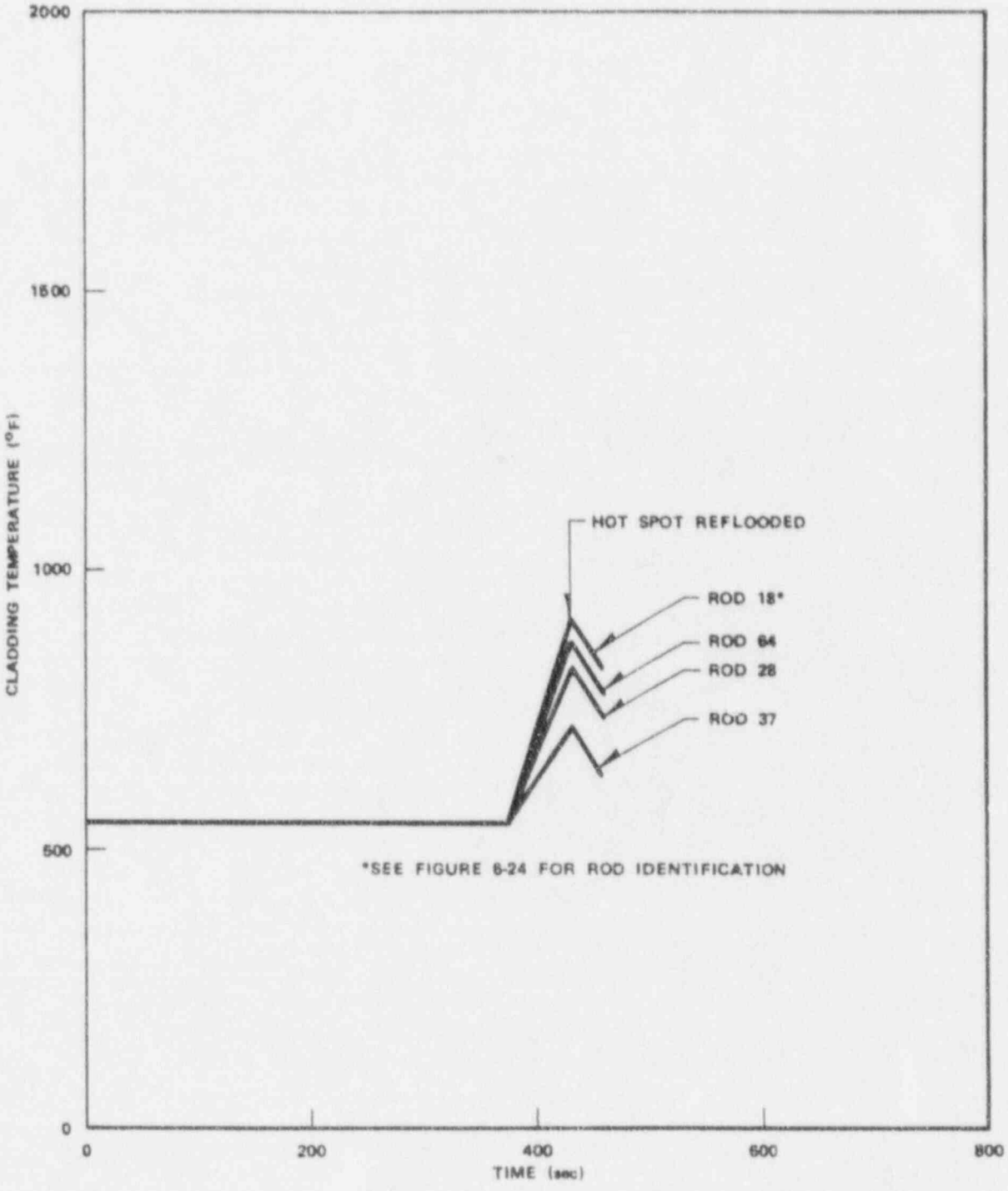

Figure 6-6. Cladding Temperature vs. Time for a Small Break with Failure of HPCI (0.02 ft^2 Break) (4LPCI + 2CS + ADS) AEC Assumption

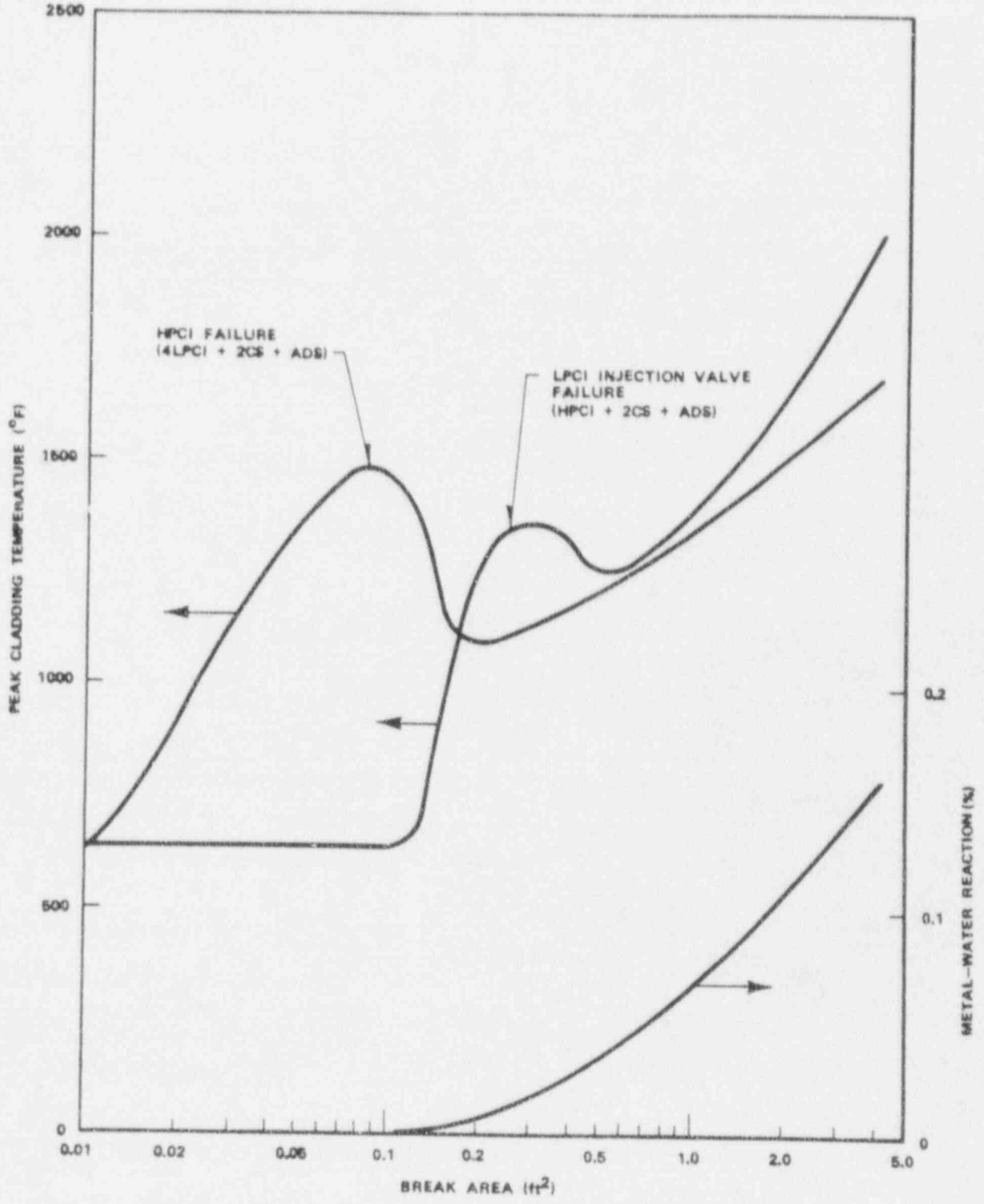

Figure 6-7. Peak Cladding Temperature Spectrum for Single Failure Conditions AEC Assumptions

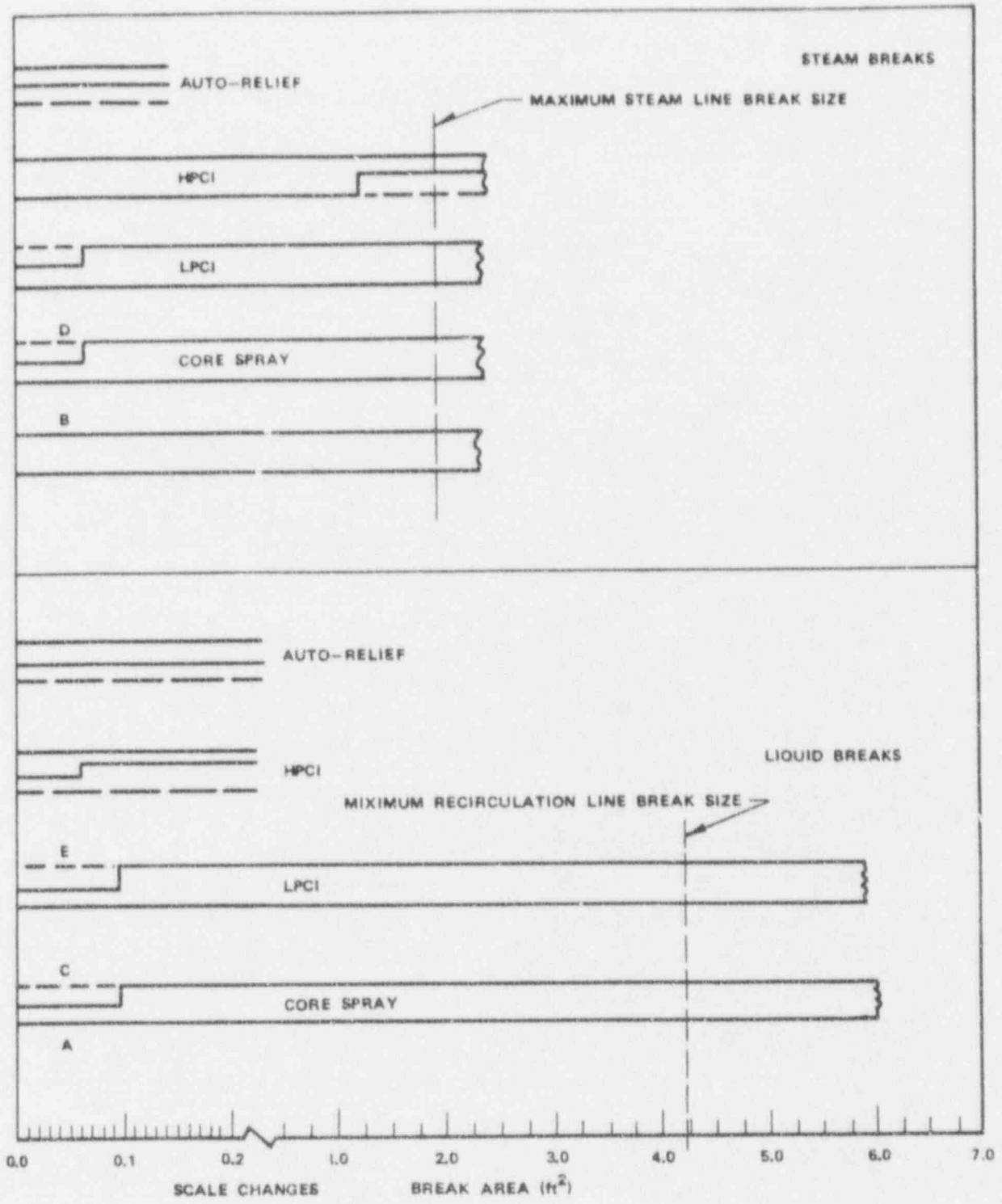

Figure 6-8. Emergency Core Cooling System–Performance Capability

For convenience, the breaks are classified according to the location of the penetration on the reactor vessel. The break types will fall into one of three categories. These, along with the lines that fall into these categories, are described below:

1. Steam Type Breaks. These are breaks in which the reactor vessel penetration is exposed to the steam regions inside the vessel.

   a. Steam Lines
   b. Some Instrument Lines

2. Steam/Liquid Type Breaks. These are breaks in which the reactor vessel penetration is either exposed to the two-phase regions inside the vessel or to regions which are exposed to liquid, but are near the water level and would therefore turn into steam breaks very shortly after the break occurred. These are located above the core.

   a. Feedwater Lines
   b. Core Spray Lines
   c. Some Instrument Lines

3. Liquid Type Breaks. These are breaks in which the reactor vessel penetration is well below the vessel water level and below the top of the core.

   a. Recirculation Pump Suction Lines
   b. Recirculation Pump Discharge Line
   c. Drain Line
   d. CRD Housing
   e. Incore Housing
   f. Jet Pump Instrument Line

For a given size break, the lower the line penetration is located on the vessel, the higher the peak clad temperatures; i.e., the peak clad temperature for a given size break will be higher for those lines in liquid type breaks than

in steam/liquid type breaks and those in steam/liquid type breaks will be higher than those in steam type breaks. In demonstrating the performance and capability of the ECCS, recirculation line breaks are analyzed since these will result in the highest ECCS peak clad temperatures for a given break size. The rupture and consequences of a main steam line break have also been analyzed since this is the most severe case with regard to containment performance.

For purposes of core performance and cladding integrity the most severe accident (design basis accident) is the loss-of-coolant accident (recirculation line break). By analyzing breaks in the main steam line, the effects of all other steam type breaks are covered. For liquid type breaks, the spectrum analysis performed on the recirculation line breaks covers the effects of all other type liquid breaks such as the RHR suction and return lines, and recirculation riser lines.

The peak clad temperatures for the steam/liquid type breaks will be less than for the comparable size liquid breaks. This was shown in part in Millstone Unit 1, AEC Docket No. 50-245 Amendment 14[12] in which the effects of various size feedwater breaks were analyzed.

Steam Line Breaks. The most severe steam pipe break is one that occurs inside the drywell, upstream of the flow limiters. Although the isolation valves close within 10.5 seconds (10-second valve action time plus 0.5-second instrument response), such a break permits the pressure vessel to continue to depressurize. For purposes of analysis, pre-accident conditions assumed are the reactor operating at design power, steam dome at maximum design operating pressure, scram low water level in the pressure vessel, and loss of auxiliary power coincident with the steam pipe break.

The accident sequence starts with an instantaneous, guillotine severance of the steam pipe upstream of the steam flow restrictors. The steam flow accelerates to its limiting critical flow value in the break at the pressure vessel end and at the flow-limiter end. Steam loss exceeds the generation rate and results in rapid depressurization of the pressure vessel and steam pipes. The first 10 seconds of this accident are similar to the break outside the drywell. However,

for the break inside the drywell, closure of the isolation valves reduces the blowdown rate but does not prevent the vessel from depressurizing. The vessel continues to depressurize causing sufficient voids to immediately shut down the reactor.

A scram is initiated by a position switch in each isolation valve (at approximately 10% closure) so control rod insertion begins within 1.5 seconds after the break. Low water level or high drywell pressure also initiate a scram.

Loss of reactor coolant through blowdown from the double-ended break consists of three intervals: first steam blowdown, then mixture blowdown, and finally steam blowdown again. As the reactor vessel depressurizes, flashing causes the water level to rise. When the level reaches the steam pipes, the break flow changes from a steam blowdown to a steam-water mixture blowdown. Mass flow rate through break increases sharply. At 10.5 seconds the isolation valves are closed, which reduces the blowdown rate. As coolant is expelled and pressure decreases, the water level outside the shroud drops below the steam pipe elevation and steam blowdown begins again. The long term pressure transient and level elevation transient are shown in Figure 6-9.

Approximately 40 seconds after the break occurs, both core spray systems and the LPCI system start to inject coolant into the vessel. For this analysis the normal situation where all ECCS pumps are operating is assumed. Analyses of degraded situations in which only a portion of ECCS operates also show that the core remains covered and cooled throughout the entire blowdown transient, with cladding integrity maintained.

Liquid Line Breaks. The double-ended recirculation line break is the design basis accident for the emergency core cooling systems. The reactor is assumed to be operating at design power when a complete circumferential rupture instantly occurs in one of the two recirculation system suction lines. Normal a-c power supply to the recirculation pumps is assumed to fail at the time of the accident. Core inlet flow and vessel pressure following the accident are shown in Figure 6-10.

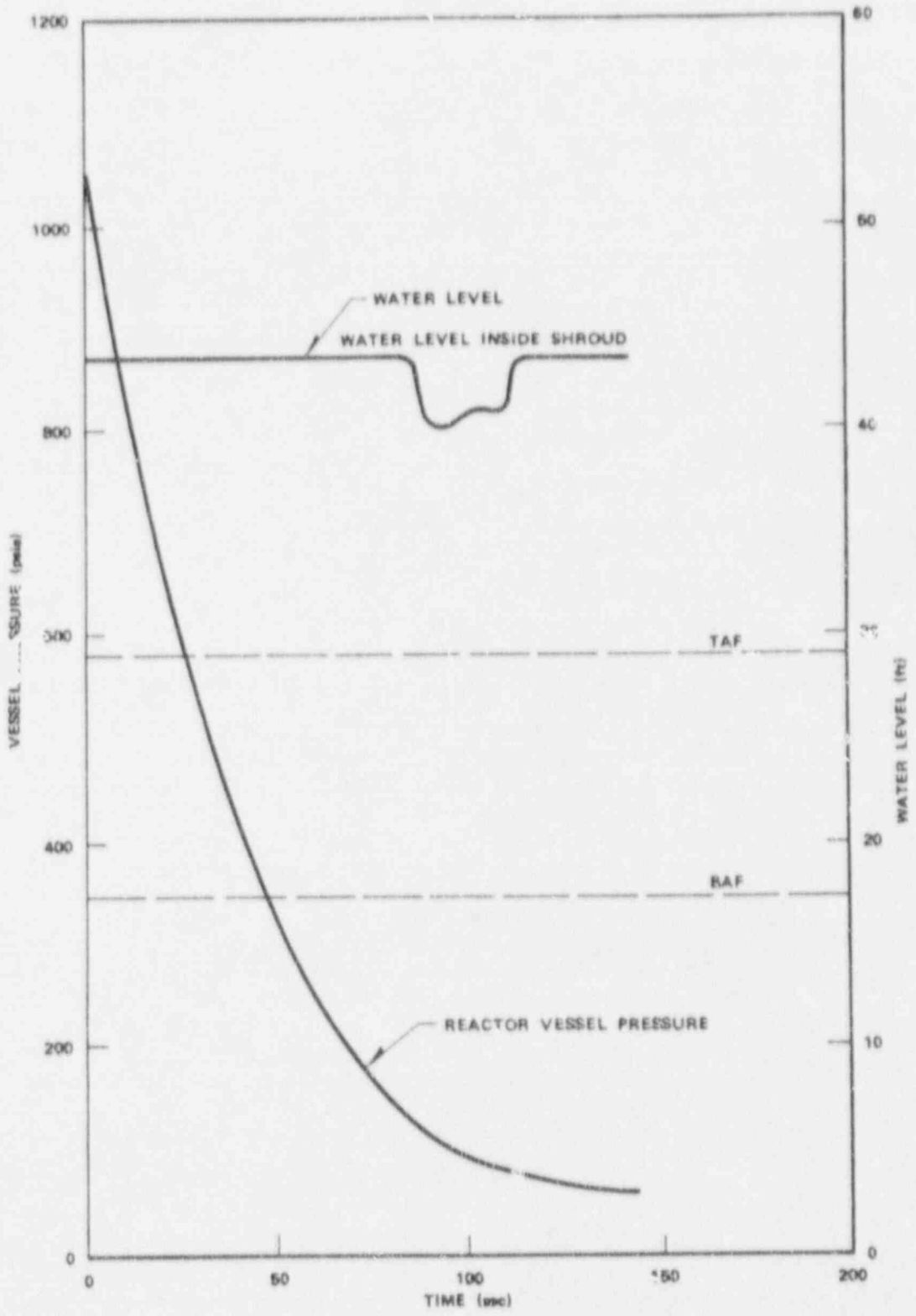

Figure 6-9. Performance of ECCS for Main Steam Line Break Inside the Drywell with all ECCS Operating (HPCS + 2CS + 4LPCI + ADS) AFC Assumptions

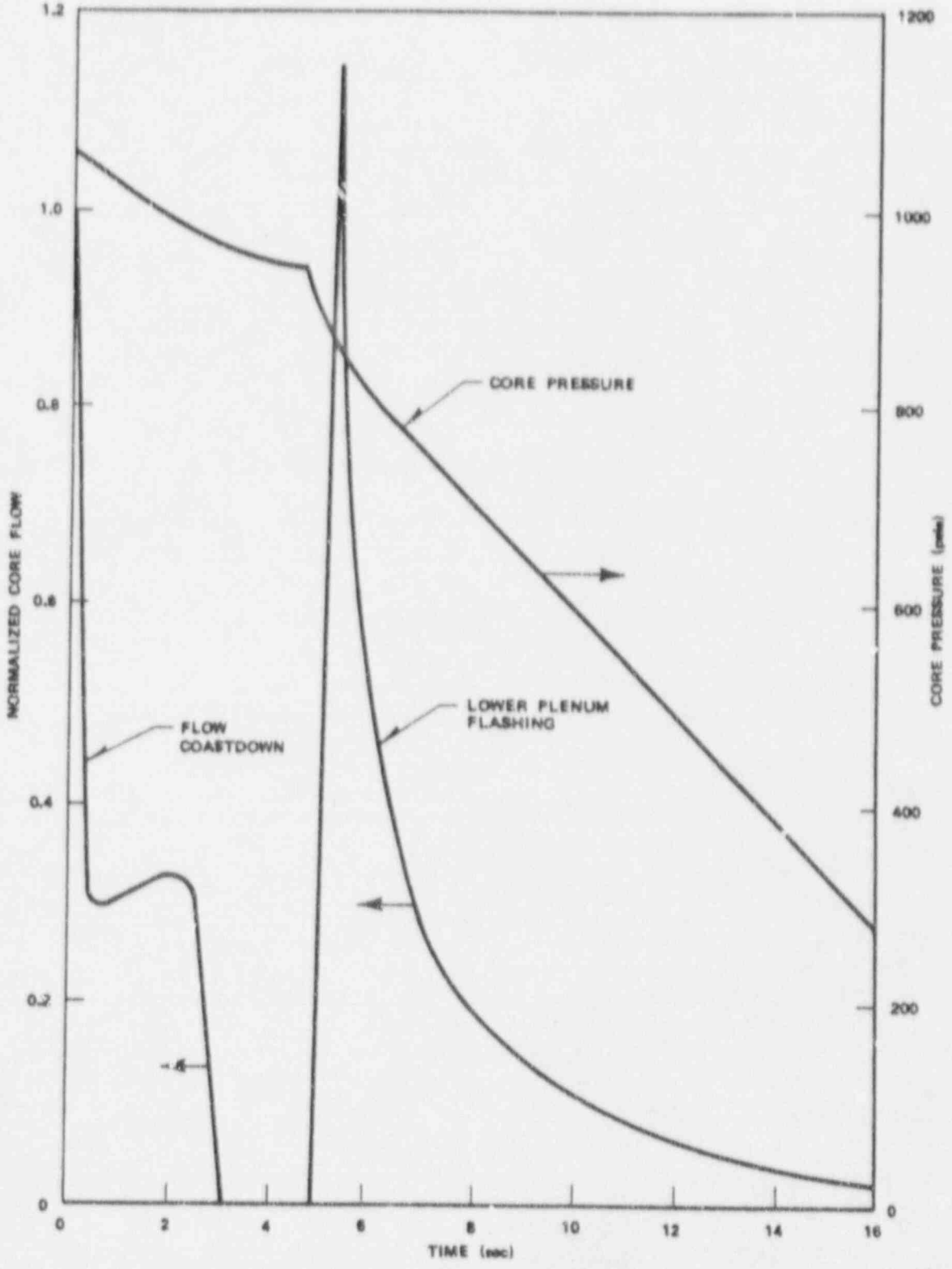

Figure 6-10. Core Flow and Pressure Following a Recirculation Line Break

Initially, the rotating energy stored in the pump and motor of the unbroken recirculation system line provides continuing flow into the lower plenum, maintaining a relatively high level of core flow. The flow is assumed to cease when the falling level in the downcomer reaches the jet pump suction level.

When the break flow in the severed recirculation line changes to steam, the associated high vessel depressurization rate causes the water in the lower plenum to vigorously and immediately flash to steam. This will force a two-phase flow up through the core and through the jet pump diffusers. As the lower plenum inventory is depleted, the mass flow rate into the core diminishes.

Calculations indicate that the reactor vessel depressurizes in approximately 40 seconds. The ECCS is initiated by either the low water level sensors in the reactor vessel or high drywell pressure sensors. The ECCS begins delivering flow to the vessel at ~30 seconds after the accident. Figure 6-11 shows the vessel pressure and water inventory transient following the accident.

The transient minimum critical heat flux ratio (MCHFR) for the highest powered fuel bundle during the blowdown is shown in Figure 6-12. The axial power shape was chosen to assure that the fuel bundle was initially operating at thermal limits.

As is evident from the figure, the MCHFR decreases initially after the accident occurs, increases slightly, and then decreases to less than 1.0 when core flow stagnates due to the uncovering of the jet pumps. Steam then blankets the reactor core and film boiling is established. However, this heat transfer is conservatively neglected for this analysis (i.e., the heat transfer coefficient is set to zero).

MCHFR becomes greater than unity when the high core flow rates caused by water in the lower plenum flash to steam. This flashing forces large quantities of water through the core and jet pumps. (See Figure 6-10.) With MCHFR greater than unity, reestablished nucleate boiling would quickly cool the cladding to near saturation temperature. However, no credit for rewetting is taken. The Groeneveld film boiling correlation (AECL-3281) is used to determine the convection coefficient as instructed by the AEC Interim Acceptance Criteria (IAC).

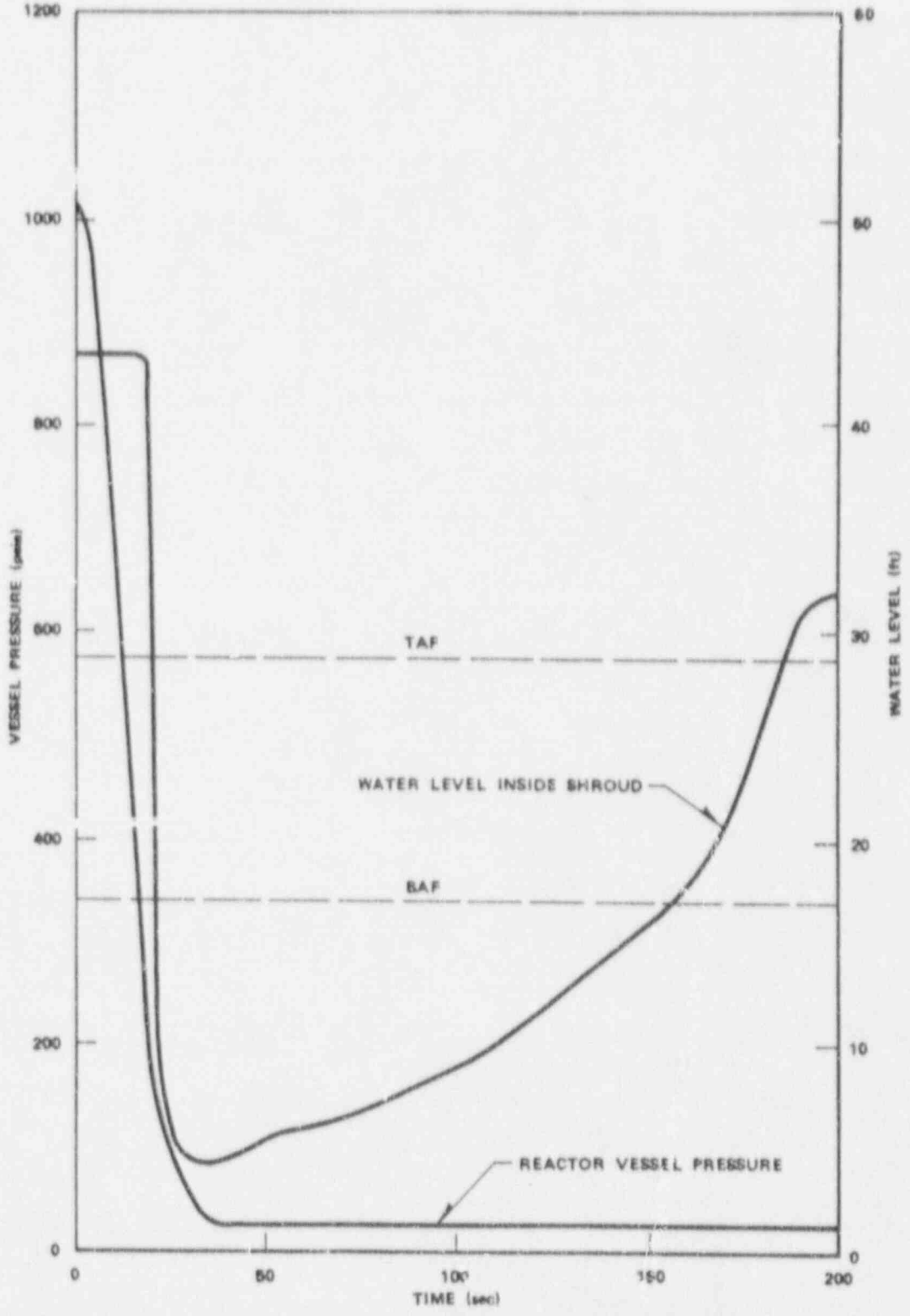

Figure 6-11. Performance of ECCS with Failure of LPCI Injection Valve for the Design Basis Recirculation Line Break (HPCS + 2CS + ADS) AEC Assumptions

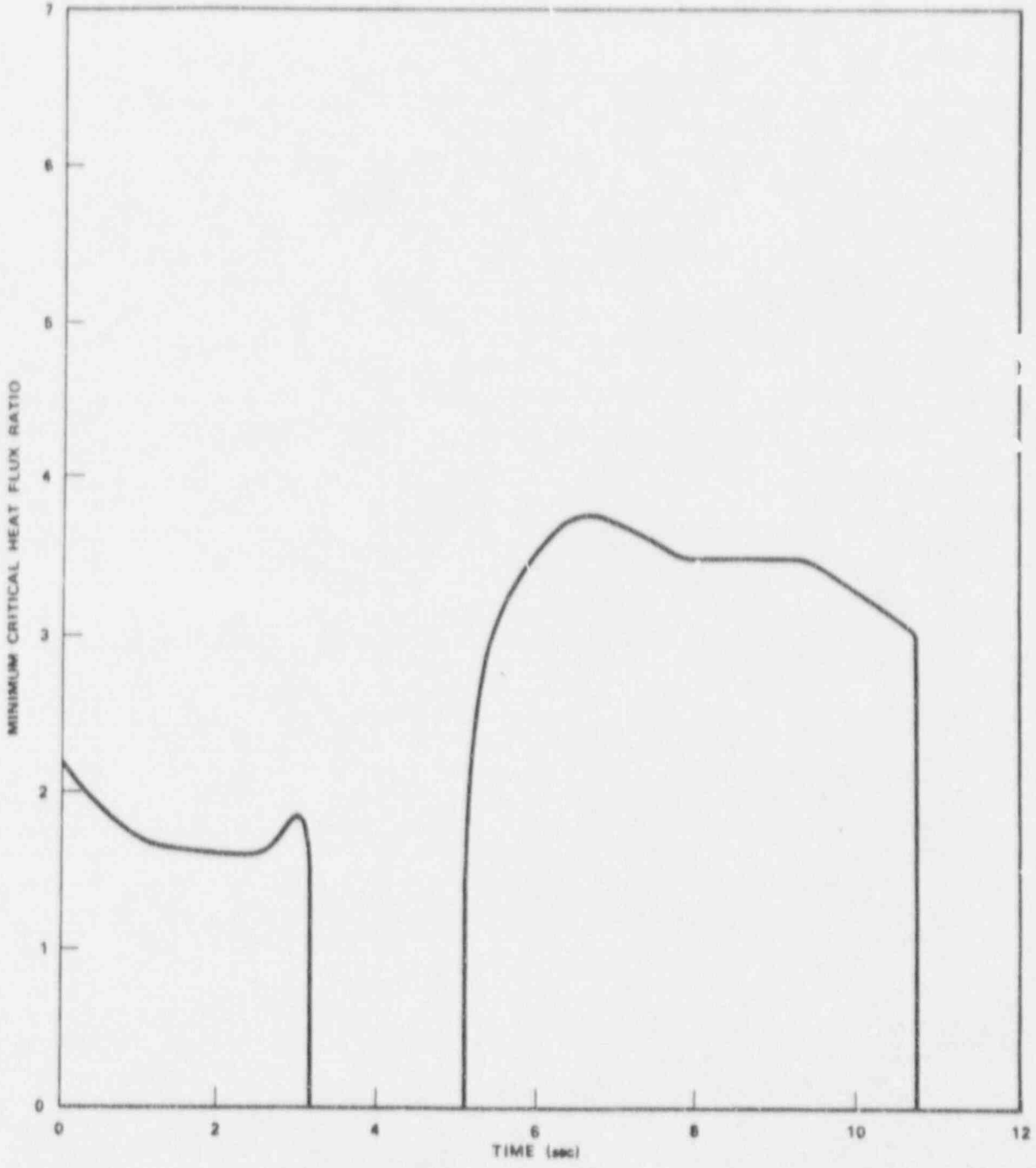

Figure 6-12. Minimum Critical Heat Flux Ratio for DBA at Monticello

When the core uncovers, it is assumed to be insulated. A drywell high pressure or reactor vessel low water level signal starts the HPCI and LPCI, the LPCS, and the standby a-c power supply. When the core spray flow reaches rated value or when the core is reflooded, the appropriate coefficients are applied.

Figures 6-6 and 6-13 show the peak cladding temperatures for four rod groups for a small and intermediate break, respectively. The intermediate break size shown is one that results in high peak cladding temperature in the smaller break size range.

Figure 6-14 shows core inlet and outlet quality versus time for the DBA. The curve is shown for only the DBA, because quality affects the film boiling heat transfer coefficient. For small and intermediate size breaks, nucleate boiling is assured as long as the core is covered. Nucleate boiling heat transfer coefficients are independent of fluid quality. When the core is uncovered, the heat transfer coefficient is assumed to be zero, even though a significant steam cooling coefficient would exist.

Figures 6-15, 6-16, and 6-17 show the heat transfer coefficient versus time for the small break, intermediate break, and design basis accident, respectively.

Figures 6-5 and 6-18 show the reactor vessel (RPV) water level versus time for the small break and intermediate break, respectively.

Figure 6-12 shows the minimum critical heat flux ratio (MCHFR) versus time for the design basis LOCA. Because the flow transient for the small and intermediate break sizes is mild compared to the LOCA, it is not shown. As long as the core is covered, the MCHFR for smaller breaks is always greater than unity, and nucleate boiling is always assured.

Figure 6-19 shows the assumed power generation following a design basis accident.

System Capacity. System capacity description and detailed information is contained in the FSAR and has been shown to be adequate to keep peak cladding temperatures <2300°F.

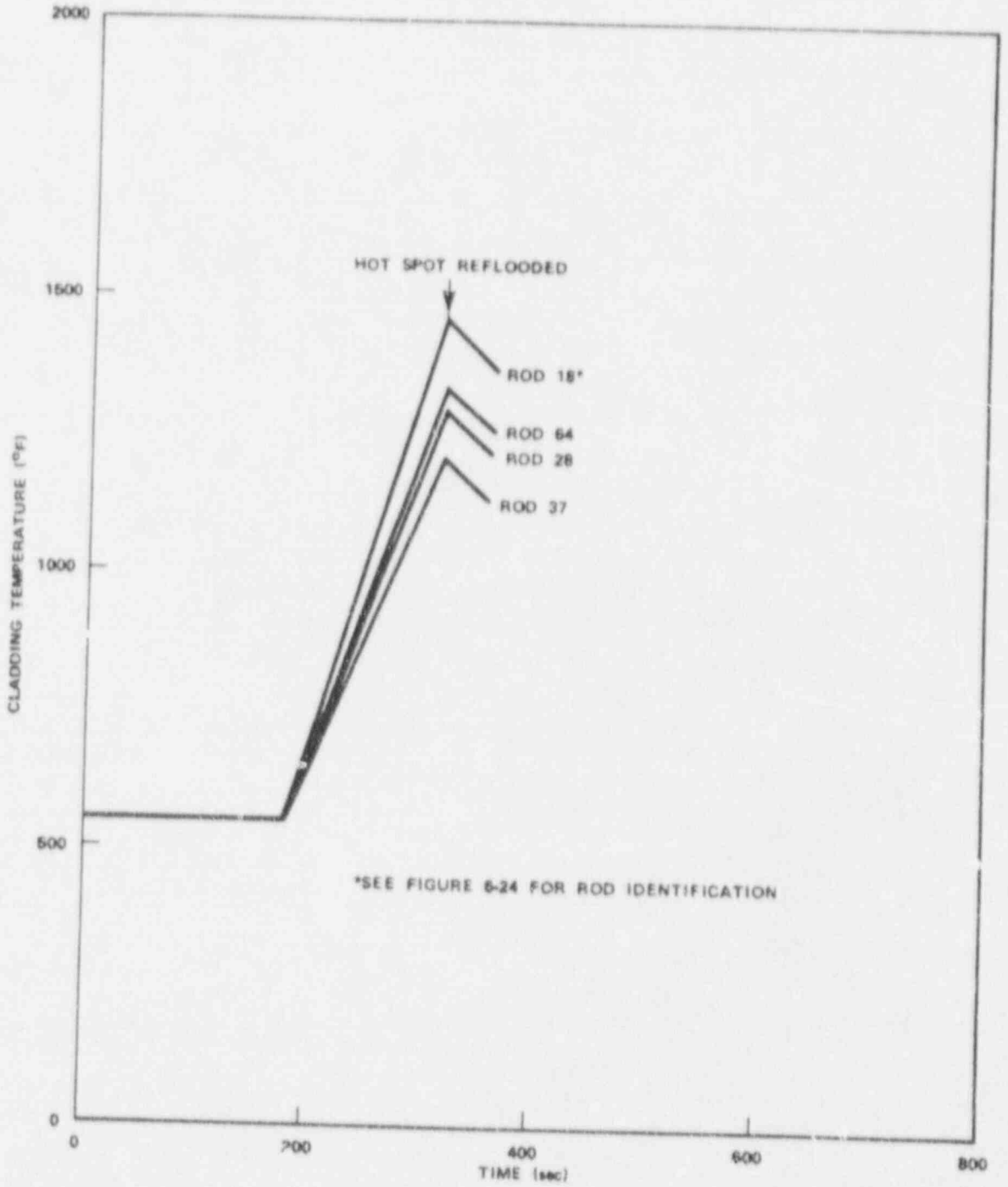

Figure 6-13. Cladding Temperature vs. Time for an Intermediate Break with Failure of HPCI (0.1 ft^2 Break) (4LPCI + 2CS + ADS) AEC Assumptions

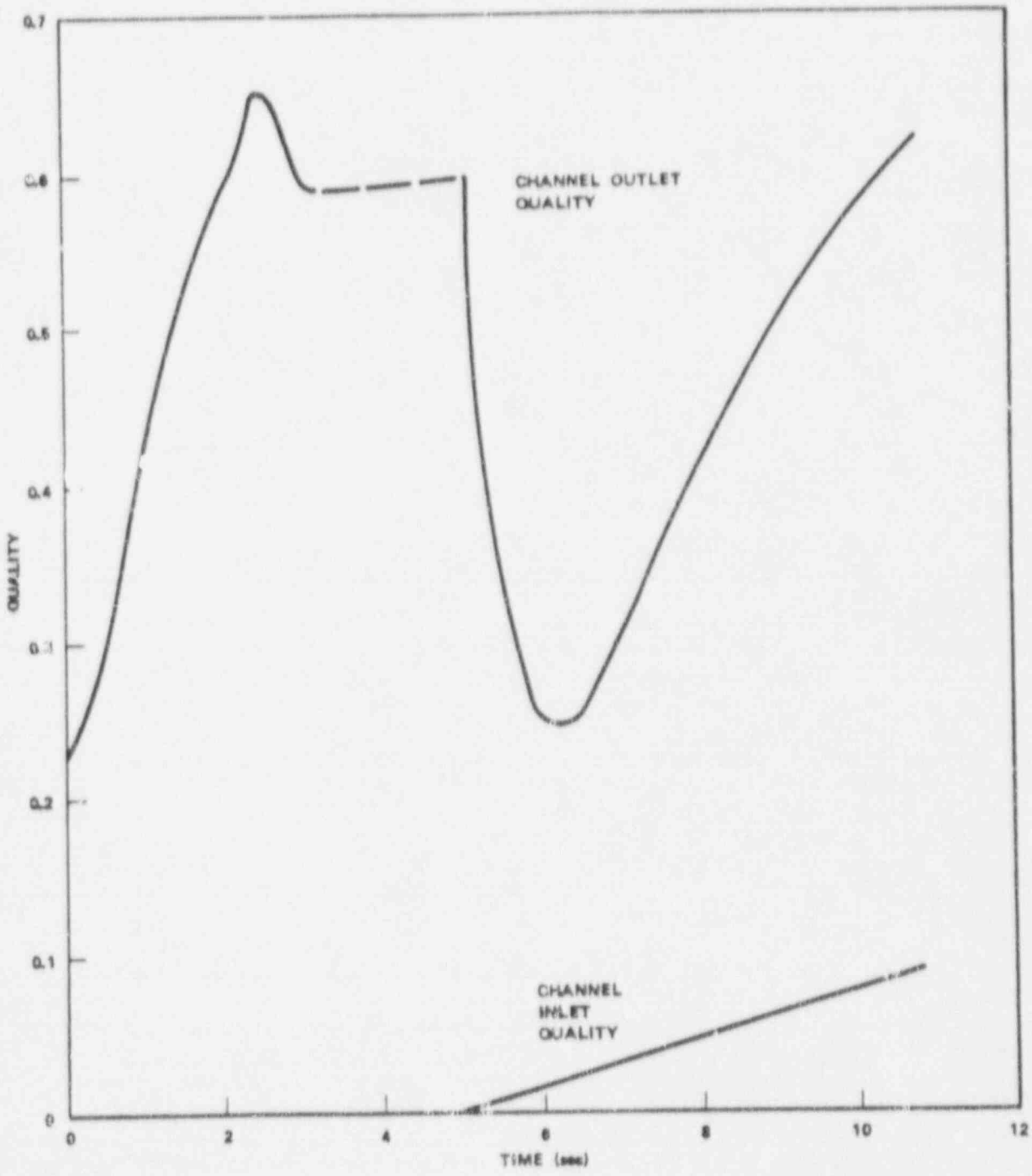

Figure 6-14. Quality vs. Time for DBA at Monticello

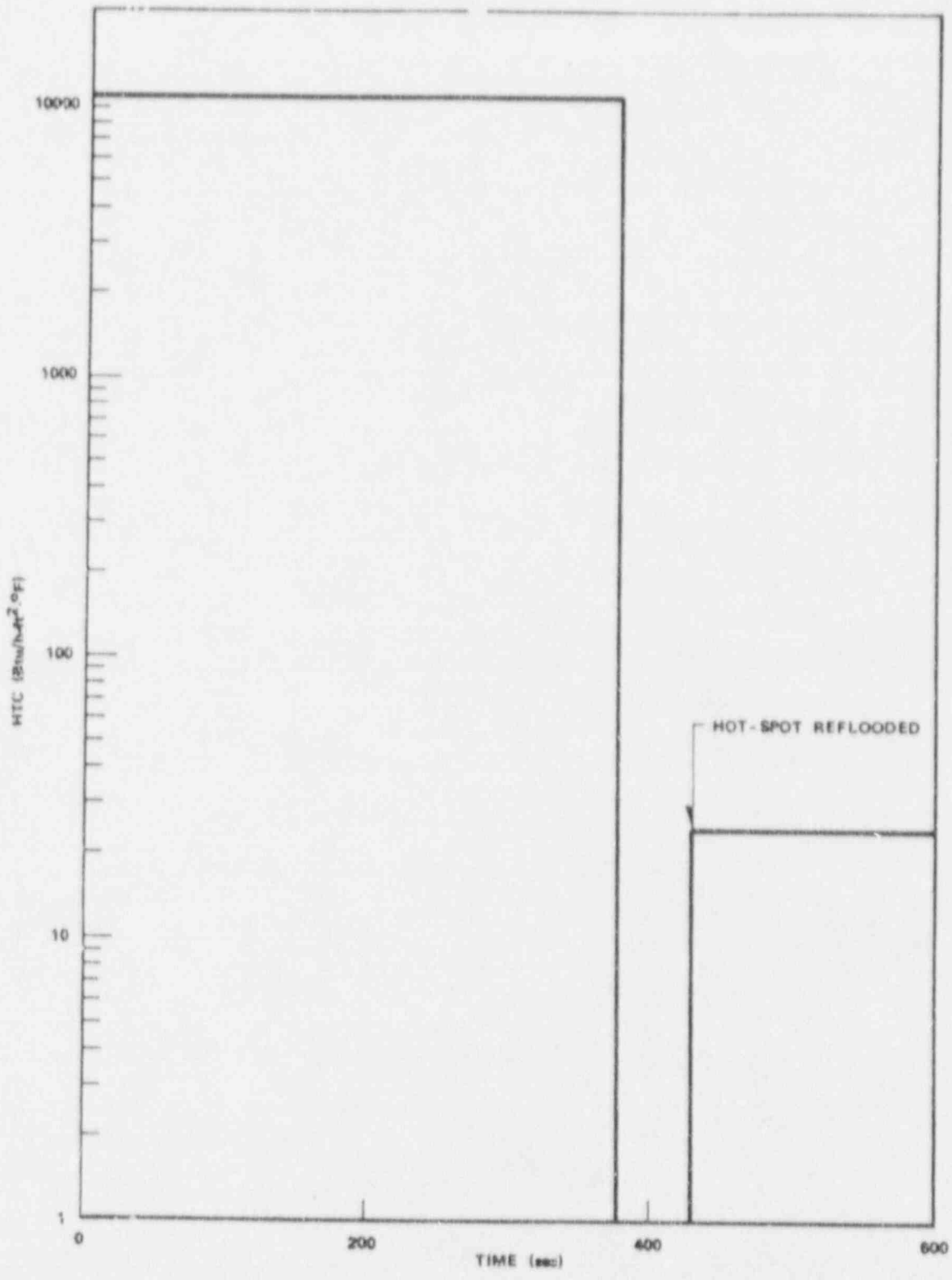

Figure 6-15. Heat Transfer Coefficient for a Small Break (0.02 ft^2) (4LPCI + 2CS + ADS) AEC Assumptions

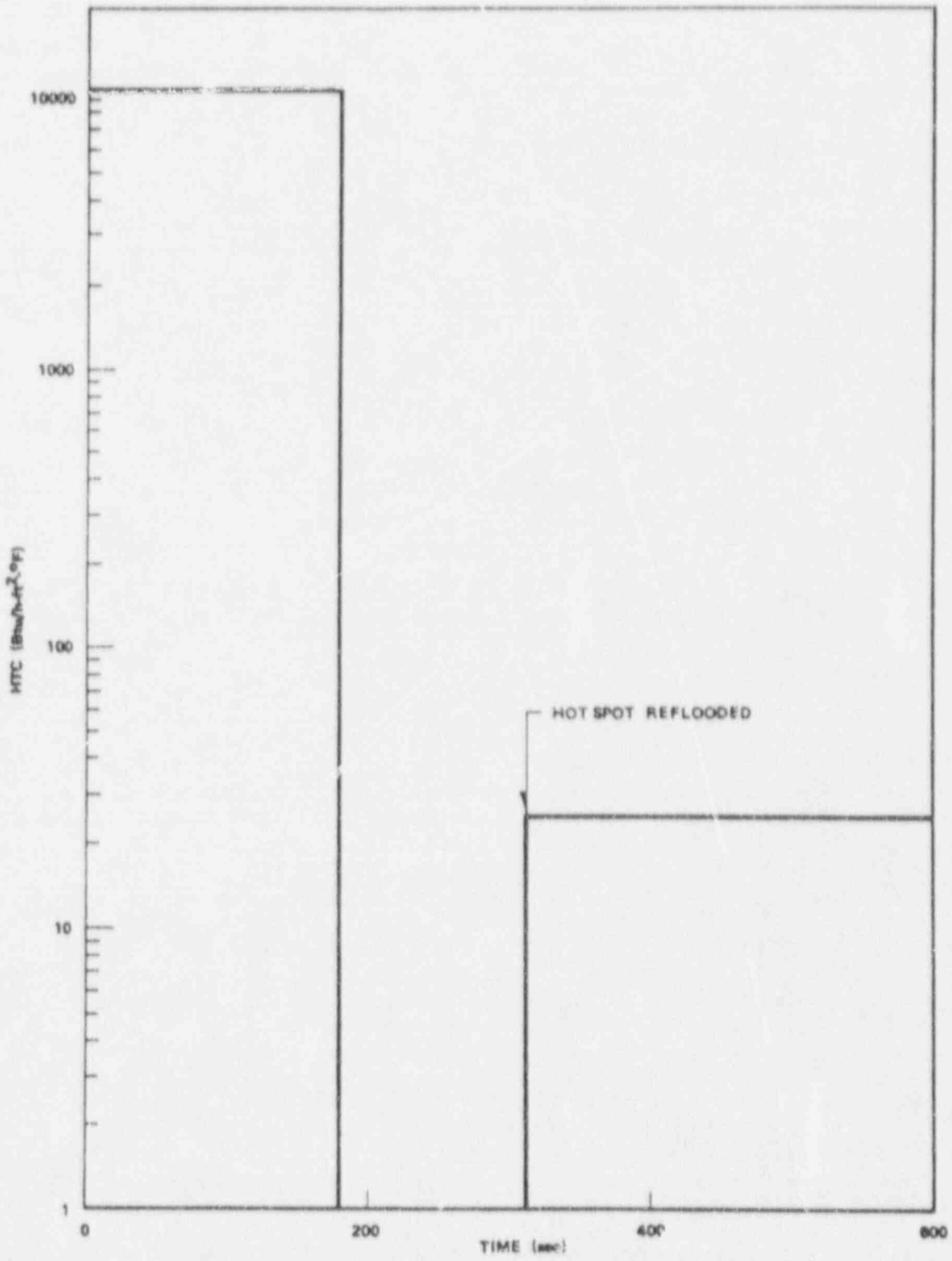

Figure 6-16. Heat Transfer Coefficient for an Intermediate Break (0.1 ft^2) (4LPCI + 2CS + ADS) AEC Assumptions

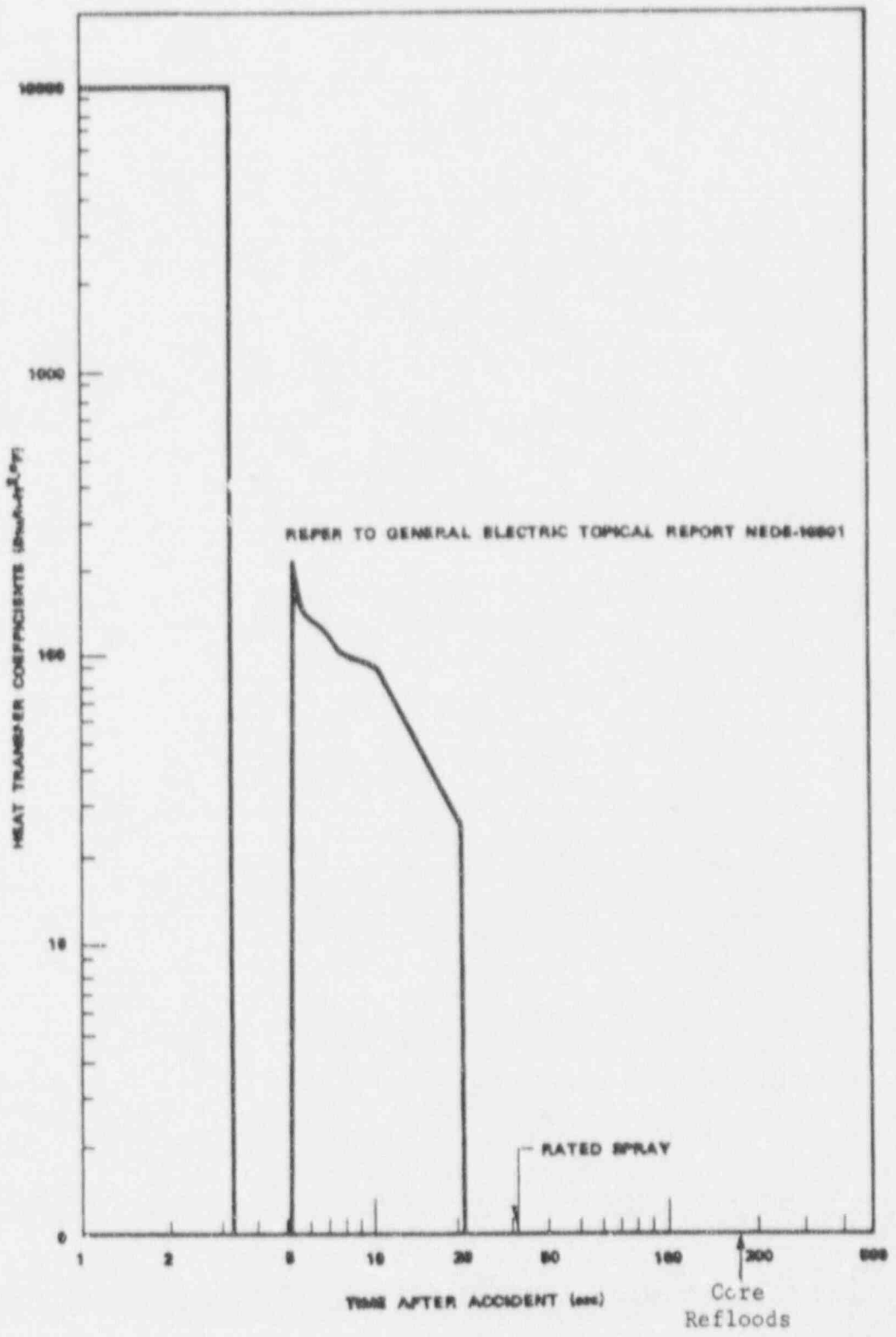

Figure 6-17. Montezuello Heat Transfer Coefficients for DBA with LPCI Injection Valve Failure – AEC Analysis No. 1 (CS + HPCI + ADS)

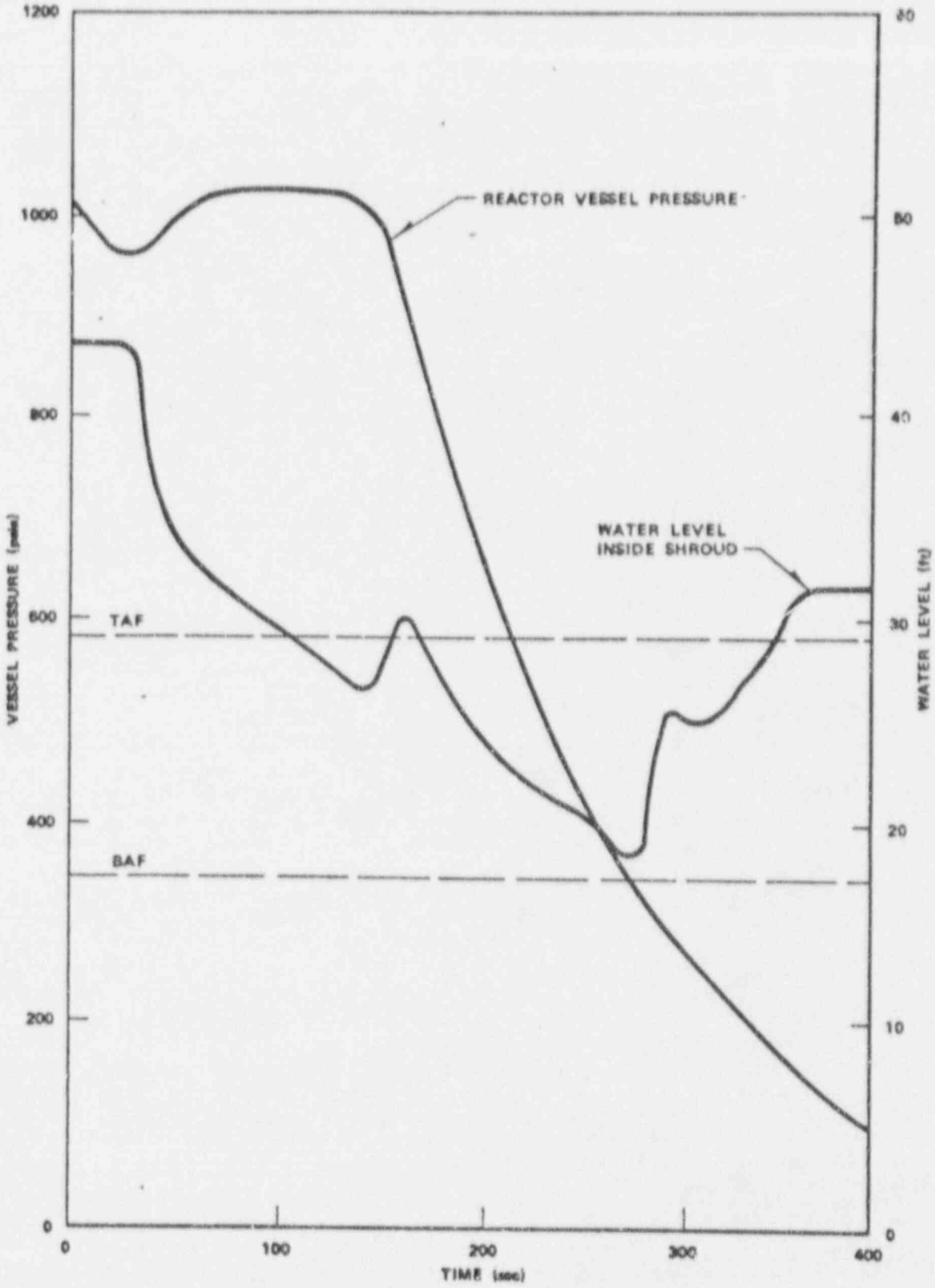

Figure 6-18. Performance of ECCS with failure of HPCI for Intermediate (0.1 ft^2) Liquid Break (2CS + 4LPCI + ADS) AEC Assumptions

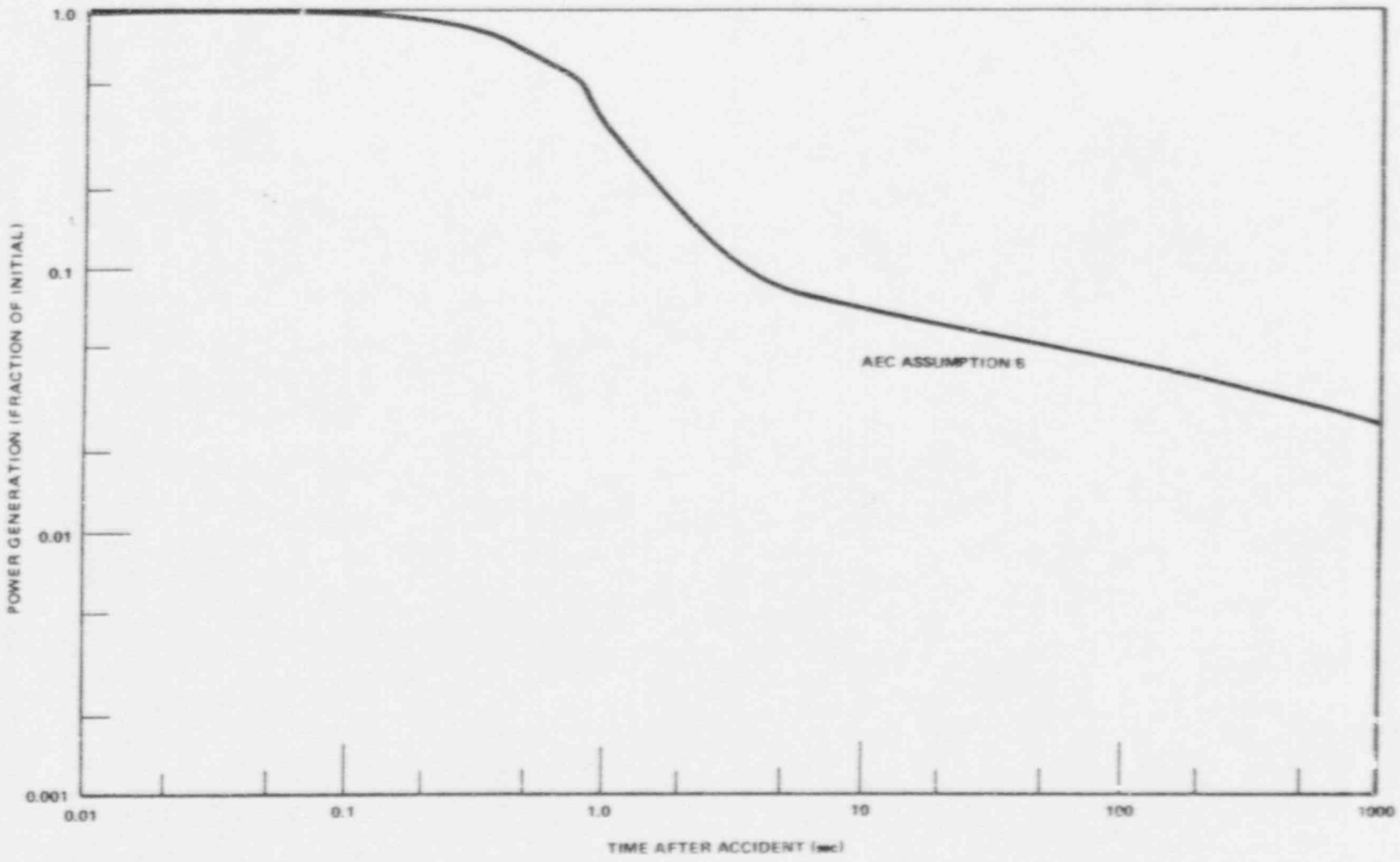

Figure 6-19. Power Generation Following a Design Basis Recirculation Line Break Accident

Long Term Core Cooling. Long term cooling is defined as cooling after the initial thermal transient has been terminated until the fuel can be safely removed. Long term cooling conditions have not changed with insertion of the reload fuel.

Peaking Factors

Figure 6-20 is a plot showing the typical behavior of cladding temperature versus exposure for the DBA. Peaking factors giving the highest peak cladding temperatures occur at ~15,000 MWd/T exposure. These peaking factors were then used in conjunction with the IAC calculational models to determine the stated peak cladding temperatures for Monticello.

Fuel Rod Perforations. The mechanism of fuel rod perforation during the LOCA has been studied extensively and is well understood. A fuel rod will perforate if the cladding hoop stress exceeds the ultimate strength of Zircaloy at the peak cladding temperature experienced during the LOCA. The number of fuel rods perforated is therefore a function of the predicted peak cladding temperatures as well as the experimentally determined internal gas pressure distribution and perforation stress data. A plot of stress at perforation and ultimate strength of Zircaloy at various temperatures is presented in Figure 6-21.

The calculated fission gas internal pressure distribution within the core is shown in Figure 6-22 for a typical 7x7 fuel design. The distribution is obtained by integrating the expected fission gas release rate for normal operation to the end of an equilibrium cycle when the accumulated fission products are maximum. In addition, the partial pressure of volatile materials and initial gas pressure is included. Because the 8x8 fuel design has lower operating fuel temperatures, a smaller diameter and thicker cladding relative to the 7x7, the stress distribution produced by Figure 6-22 for 7x7 fuel can be conservatively applied to 8x8 fuel. These data are used with the heatup analysis to determine the maximum percentage of fuel rod perforation for any size break and the worst single failure assumption (see Figure 6-23).

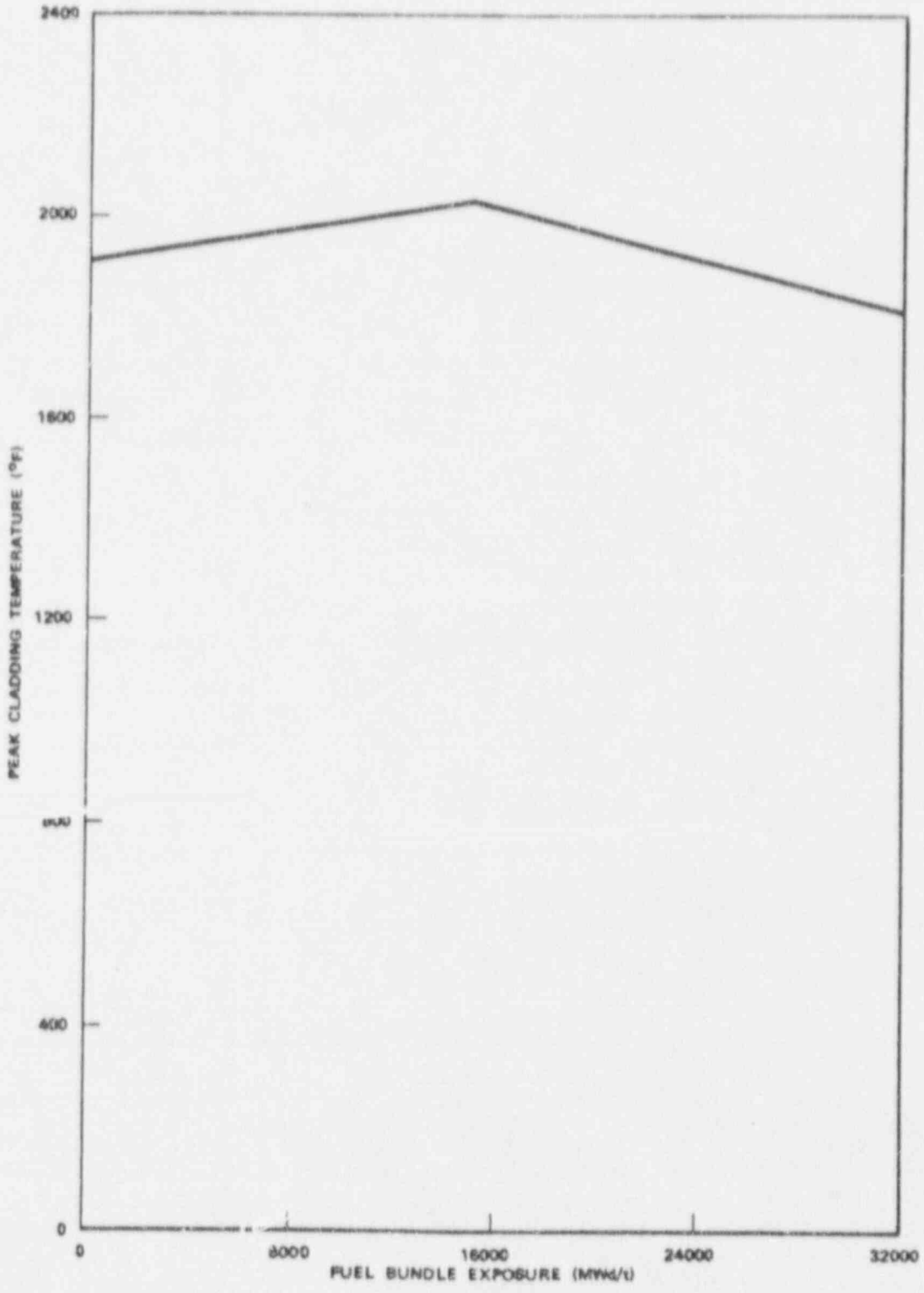

Figure 6-20. Effects of Exposure on Maximum Cladding Temperature

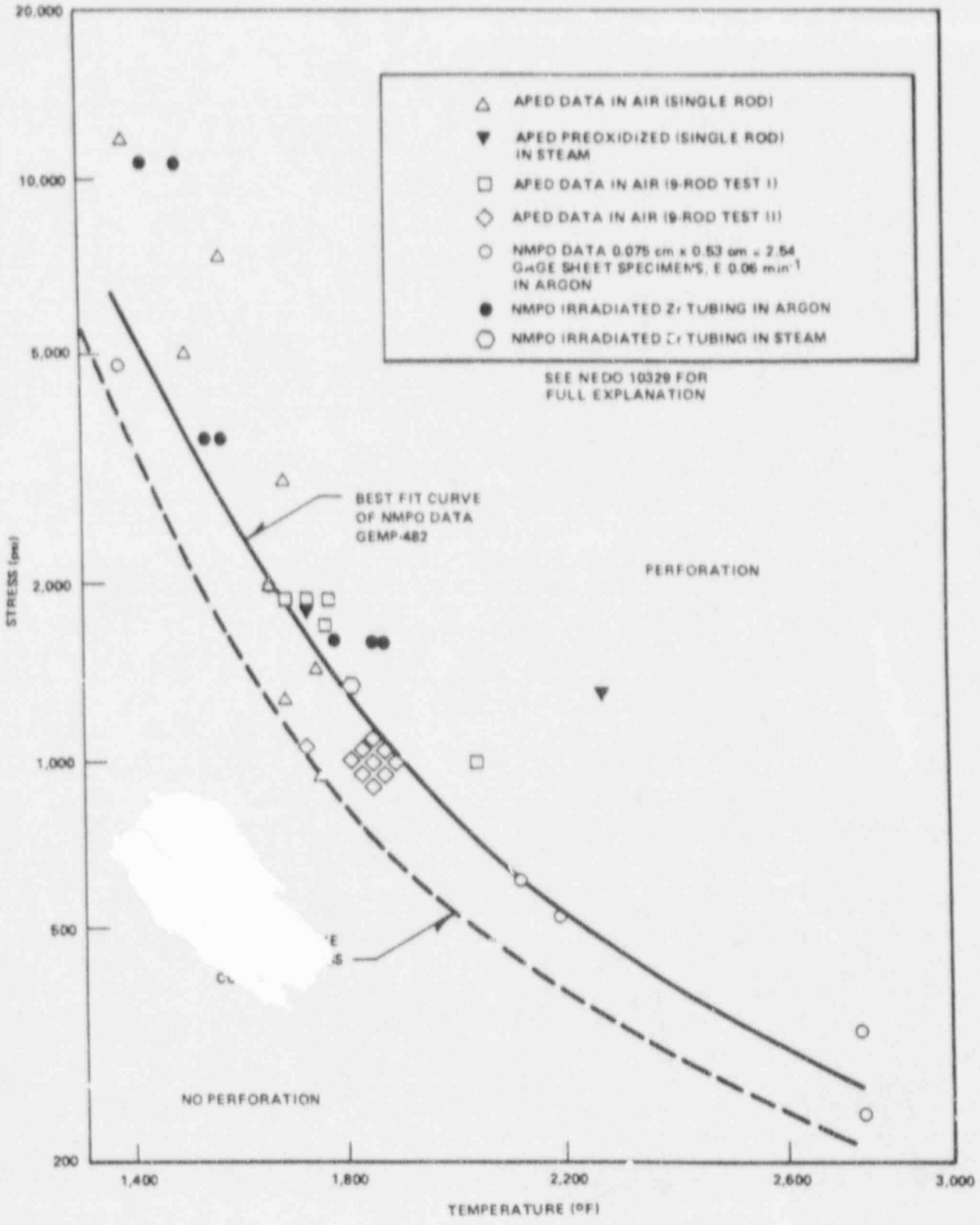

Figure 6-21. Fuel Rod Perforation Data

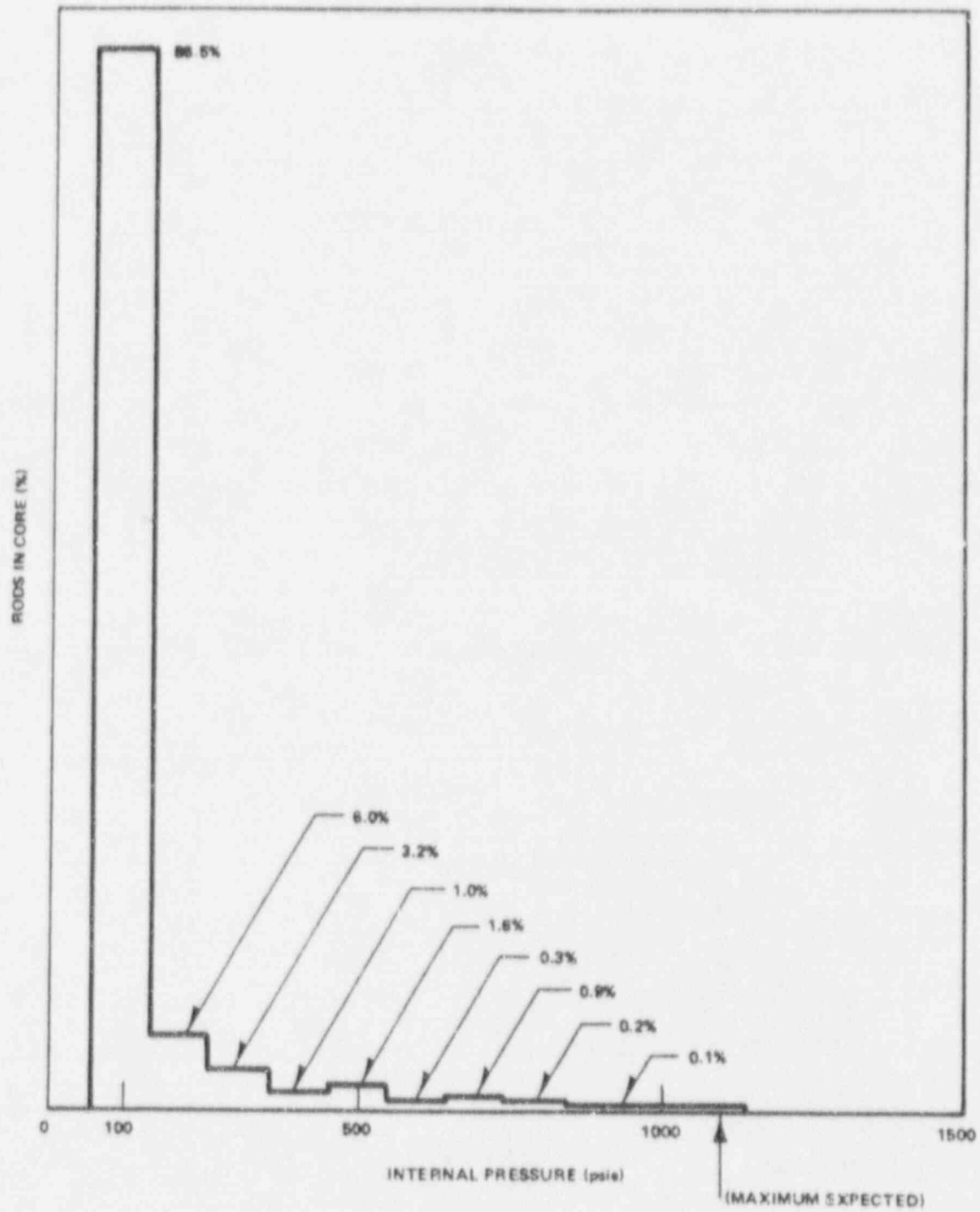

Figure 6-22. Distribution of Internal Pressure Within Rods

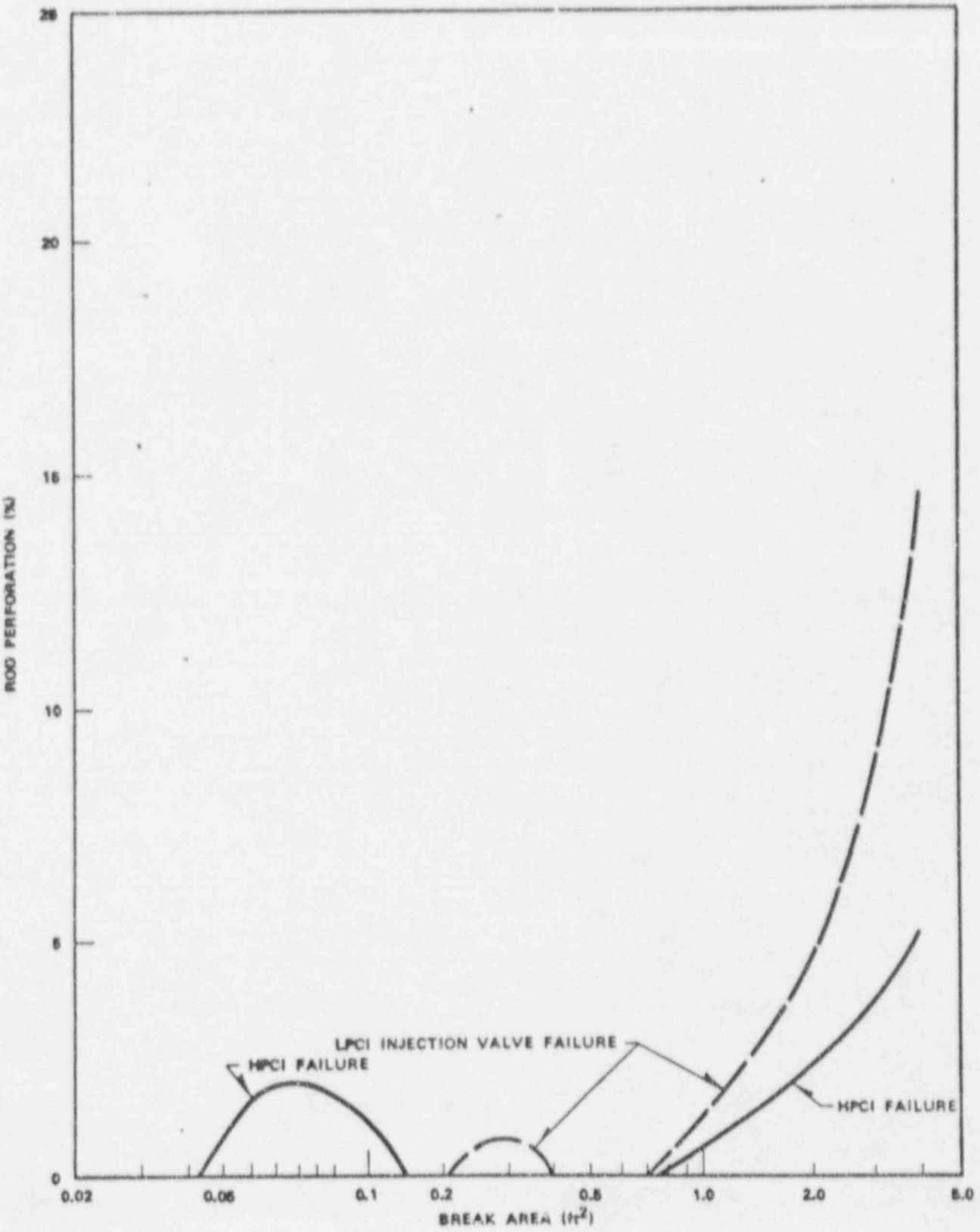

Figure 6-23. Percent Rod Perforation vs Break Area (AEC Assumptions)

Conformance With Interim Acceptance Criteria. In the analyses discussed above there have been no deviations from the evaluation model described in Appendix A, Part 2 of the AEC Interim Policy Statement.

Effects of ECCS Operation on the Core. The mechanical effects of ECCS operation on the core, reactor coolant system and ECCS are those associated with the thermal effect of injecting water into these systems which is cooler than these systems and components. These thermal stresses have been considered in the design of the core, reactor coolant system and ECCS.

There are no nuclear effects resulting from ECCS operation, since all control rods are inserted and the reactor remains subcritical during the injection of the cooler ECCS water.

There are no chemical additives in the ECCS water and therefore no chemical effects on the core, reactor coolant system or ECCS.

Lag Times. The system time delays assumed in the LOCA accident are as follows.

System	Maximum Allowable Time From Signal Receipt Until the Pumps Have Reached Rated Speed (sec)	Maximum Time Delay After Receipt of Signal Until All Valve Motion is Complete (sec)
HPCI	30	30
CS	30	30
LPCI	43	43
ADS	-	120

Fuel Densification

Actual fuel density data and a supplemental page to NEDM-10735 (Reference 13) will be provided so that Maximum Average Planar Linear Heat Generation Rate (MAPLHGR) and Power Spiking Penalties ($\Delta P/P$) for the 8x8 fuel can be determined. This information will be available prior to startup of the reloaded core. Appropriate changes to the densification models occurring in the interim will be similarly addressed.

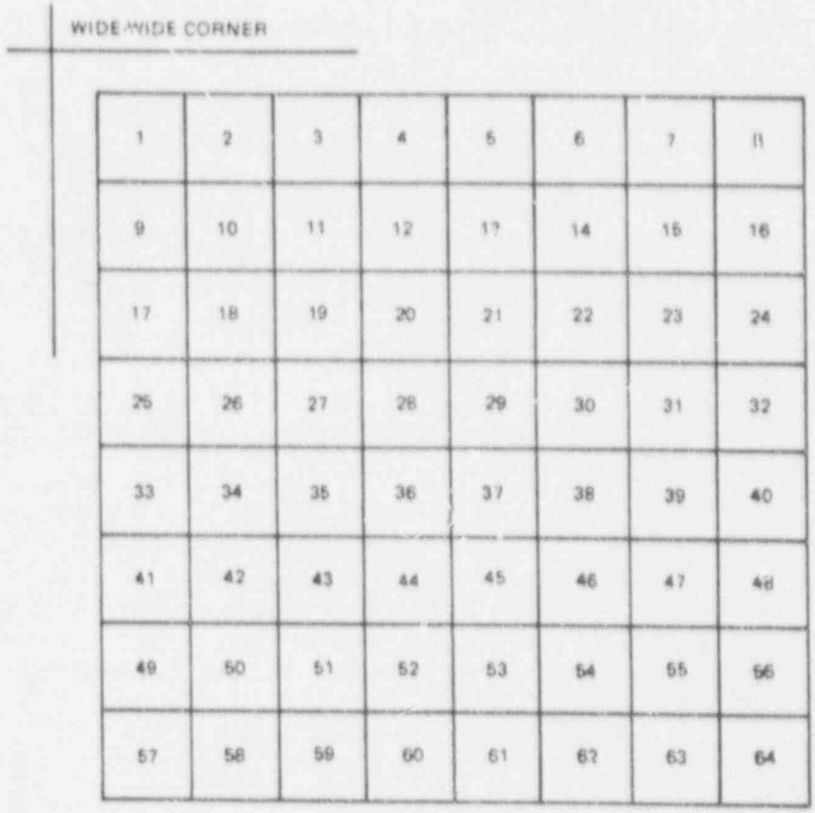

Figure 6-24. 8x8 Reload Fuel Rod Identification

6.2.3 Rod Withdrawal Error

6.2.3.1 Identification of Causes

Starting Conditions and Assumptions. The reactor is operating at a power level above hot standby at the time the control rod withdrawal error occurs. The reactor operator has followed procedures and up to the point of the withdrawal error is in a normal mode of operation (i.e., the control rod pattern, flow set point, etc., are all within normal operating limits). For these conditions it is assumed that the withdrawal error occurs with the maximum worth control rod. Therefore, the maximum positive reactivity insertion will occur.

Event Description. While operating in the power range in a normal mode of operation the reactor operator makes a procedural error and withdraws the maximum worth control rod to its fully withdrawn position. Due to this positive reactivity insertion, the core average power will increase. More importantly, the local power in the vicinity of the withdrawn control rod will increase and potentially could cause localized fuel failures due to either achieving critical heat flux (CHF) or by exceeding the 1% plastic strain limit imposed on the cladding as the transient failure threshold. The following list depicts the sequence of events for this transient.

	Event	Approximate Elapsed Time
(1)	Event begins; operator selects and withdraws at maximum rod speed the maximum worth control rod	0
(2)	Core average and local power increases	
(3)	LPRM's alarm	<5 sec
(4)	Event ends—rod block by RBM	<30 sec

Identification of Operator Actions. Under most normal operating conditions no operator action will be required since the transient which will occur will be very mild. If the peak linear power design limits are exceeded, the nearest local power range monitors (LPRM's) will detect this phenomenon and sound an alarm. The operator must acknowledge this alarm and take appropriate action to rectify the situation.

If the rod withdrawal error is severe enough, the rod block monitor (RBM) system will sound alarms at which tir the operator must acknowledge the alarm and take corrective action. Even for extremely severe conditions (i.e., for highly abnormal control rod patterns, operating conditions, and assuming that the operator ignores all alarms and warnings and continues to withdraw the control rod) the RBM system will block further withdrawal of the control rod before fuel damage occurs.

6.2.3.2 Analyses of Effects and Consequences

Methods, Assumptions, and Conditions. The analysis considers the continuous withdrawal of the maximum worth control rod at its maximum drive speed from the reactor which is operating at rated power with a control rod pattern which results in the core being placed on thermal design limits (i.e., MCHFR = 1.9 and a peak linear power of 13.4 kW/ft for the 8 X 8 fuel or 17.5 kW/ft for the 7 X 7 fuel). A worst case condition is analyzed to ensure that the results obtained are conservative. Also, this approach serves to demonstrate the function of the RBM system.

The worst case situation is established for the most reactive reactor state and assumes that no xenon is present. This ensures that the maximum amount of excess reactivity which must be controlled with the movable control rods is present. During a normal startup sufficient time would be available to achieve some xenon and samarium buildup, and after some short period of operation samarium will always be present. This assumption makes it possible to obtain a worst case situation in which the maximum worth control rod is fully inserted and the remaining control rod pattern is selected in such a way as to achieve design thermal limits in the fuel bundles directly adjacent to or diagonally adjacent to the inserted maximum worth control rod which is to be withdrawn. It should be pointed out that this control rod configuration would be highly abnormal and could only be achieved by deliberate operator action or by numerous operator errors during rod pattern manipulation prior to the selection and complete withdrawal of the maximum worth rod.

Figure 6-25 shows the locations of the initial, first reload and 8 X 8 fuel. Figure 6-26 indicates the rod withdrawn in the limiting case. Figure 6-27 is a composite MCHFR curve where the worst 7 X 7 and 8 X 8 bundles have been combined, thereby showing the rod position where further withdrawal of the control rod of interest could result in MCHFR <1.0 in one of the fuel bundles influenced by that rod. Figures 6-28 and 6-29 show the worst case MCHFR for 7 X 7 and 8 X 8 bundles, respectively. The most limiting case of each is used to establish the curve in Figure 6-27. Figure 6-30 shows the peak heat flux and relative bundle power for the limiting case considering both 7 X 7 and 8 X 8 fuel. The analyzed peaks occur at 22.4 kW/ft and 16.8 kW/ft well below the damage limits of 28.0 kW/ft and 25.4 kW/ft for 7 X 7 and 8 X 8, respectively.

From the composite MCHFR curve (Figure 6-27), the control rod maximum withdrawal point is shown to occur at 6.5 ft. From the diagrams in Figures 6-31 and 6-32 which reflect the various system responses to combinations of allowable LPRM failures, the RBM reading corresponding to withdrawal of the limiting rod is shown. In the case of Channels A and C (Figure 6-31), a rod block occurs at 5 ft., well below the limiting 6.5 ft. point.

For channels B and D, (Figure 6-32) the rod block occurs at 6.2 ft.; with the RBM setting of 108%, the RBM satisfies the analytical requirements.

The effects of continuous withdrawal of an in-sequence rod were also analyzed; as expected, no in-sequence event produces results more severe than the limiting cases described above.

6.2.4 Transient Analysis and Core Dynamics

This section describes the transient analysis for Monticello, Cycle 3, based on the analyses of the Final Safety Analysis Report (FSAR). This analysis considers the large reactor distrubances which serve as a basis for a comprehensive evaluation of the plant dynamic safeguards.

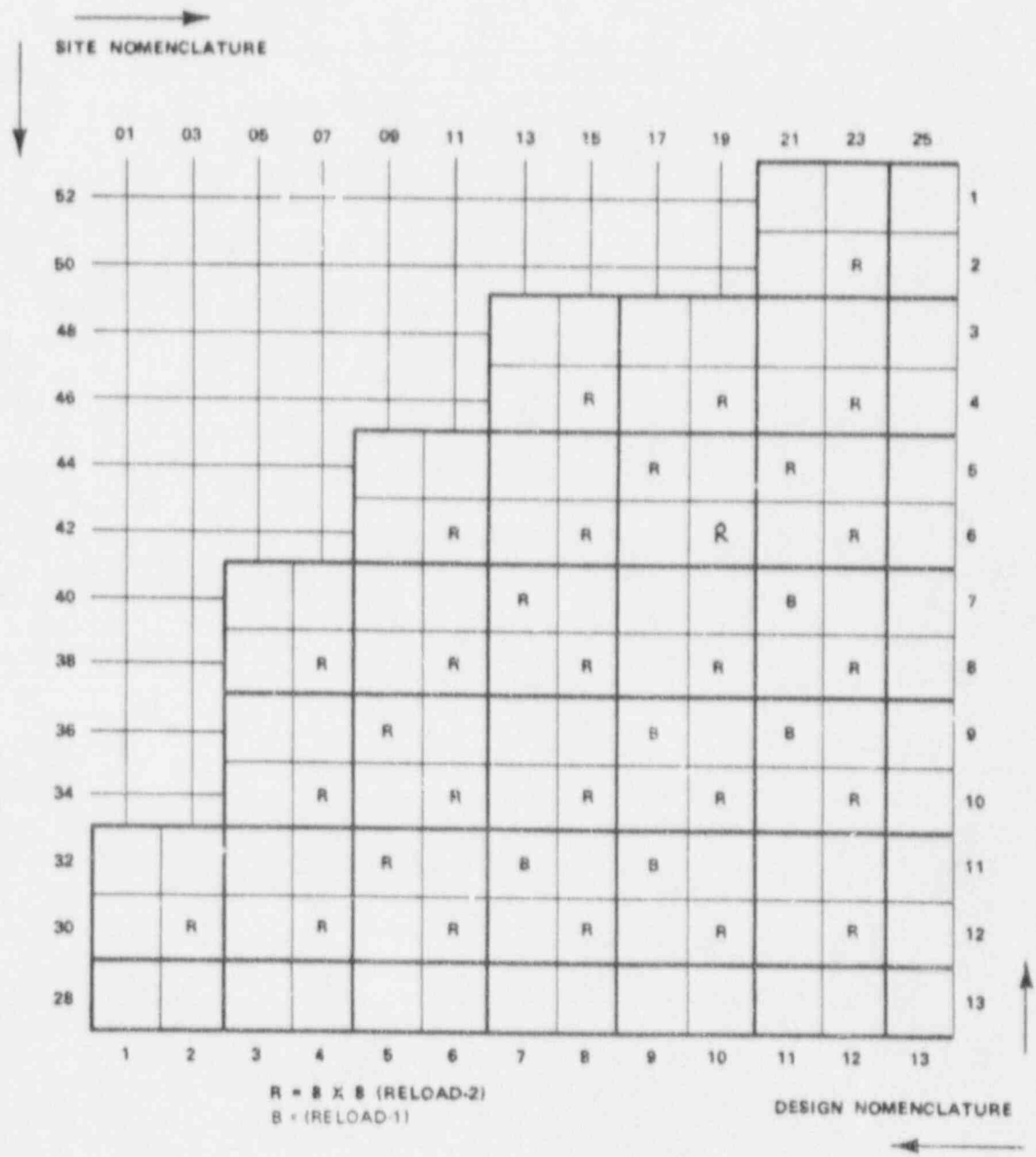

Figure 6-25. Fuel Type Locations

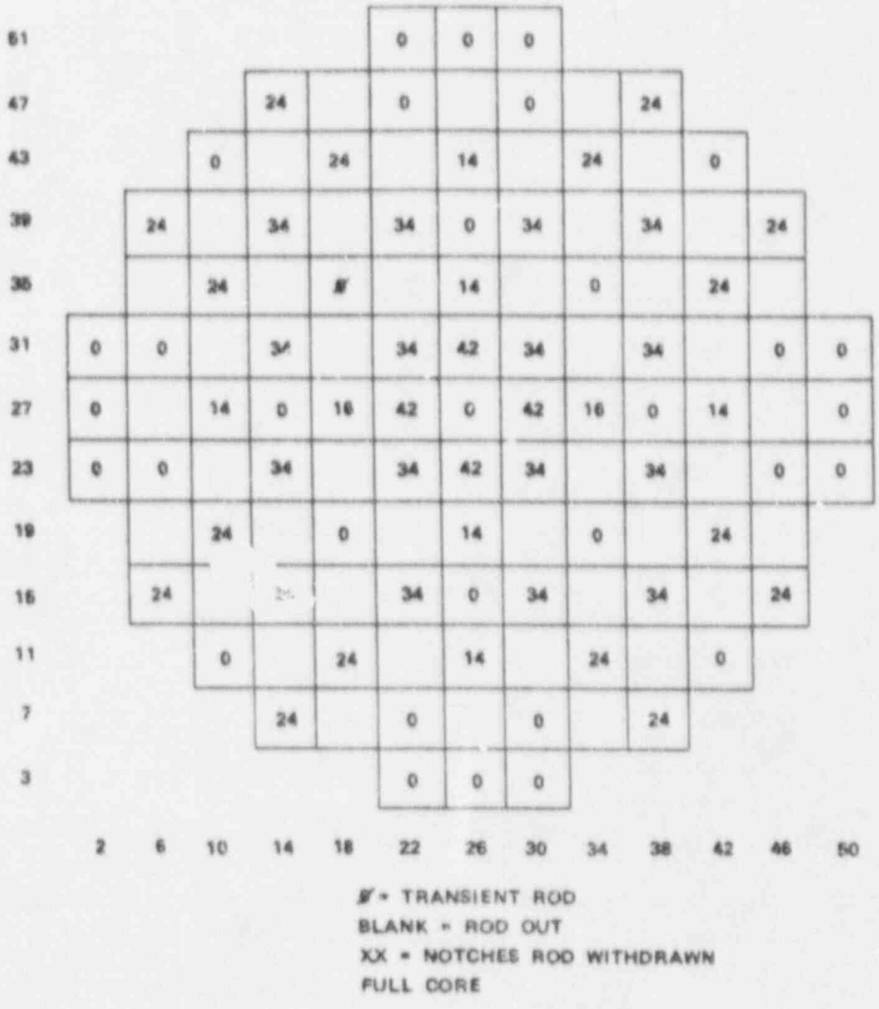

Figure 6-26. Base Rod Pattern for RWE

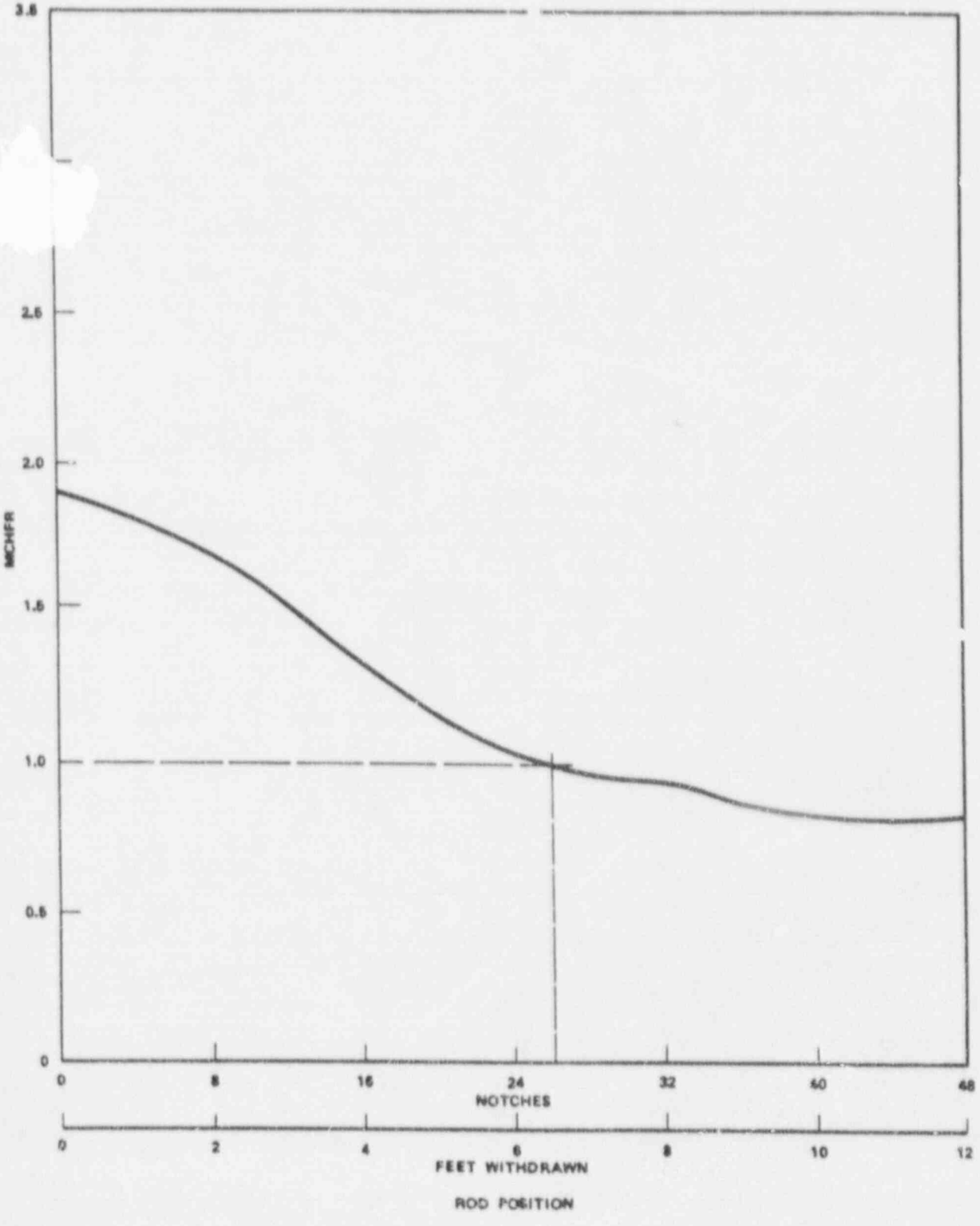

Figure 6-27. Monticello Composite MCHFR vs. Rod Position Limiting Rod Withdrawal

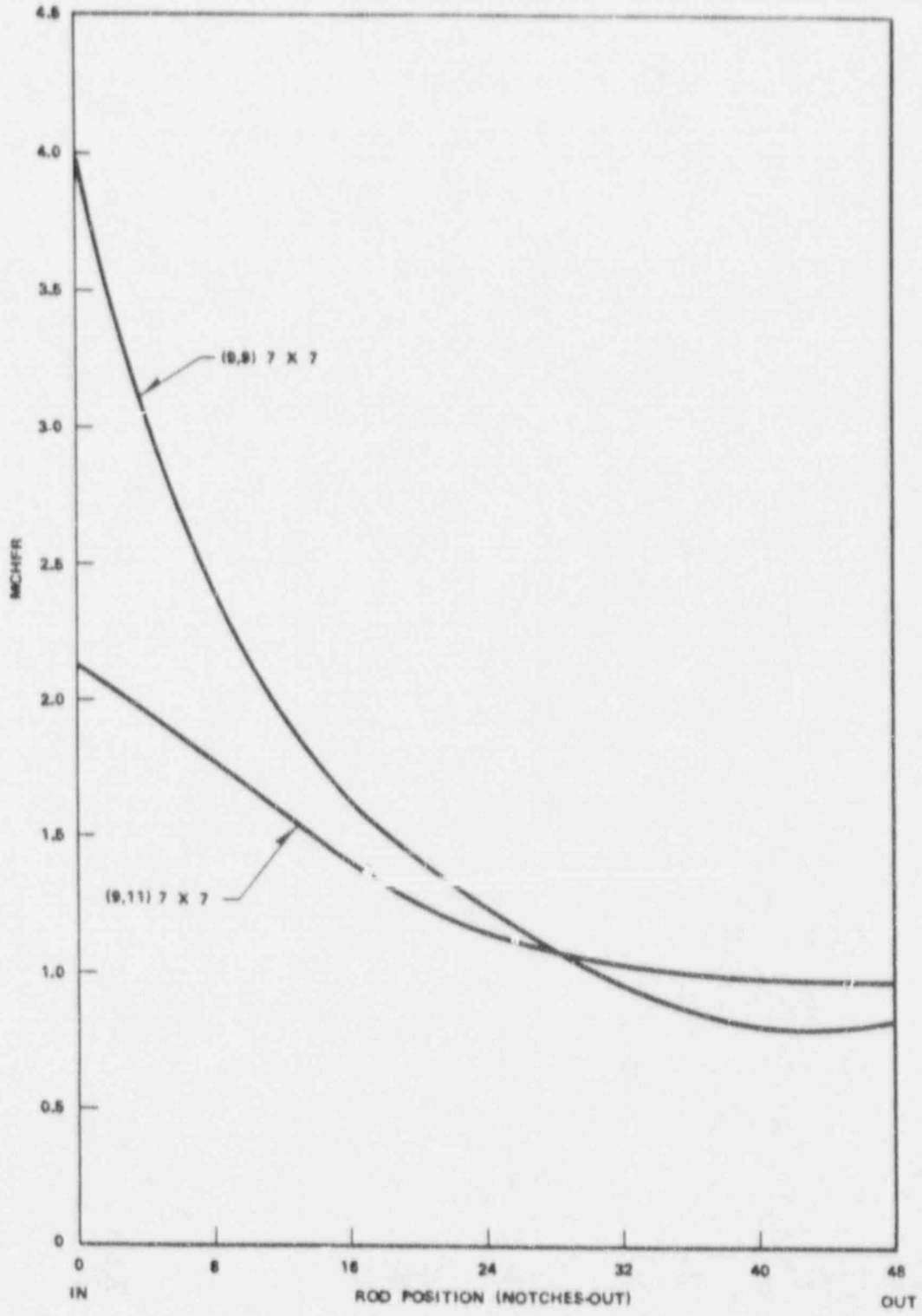

Figure 6-28. MCHFR vs Rod Position Limiting Rod Withdrawal 7 x 7

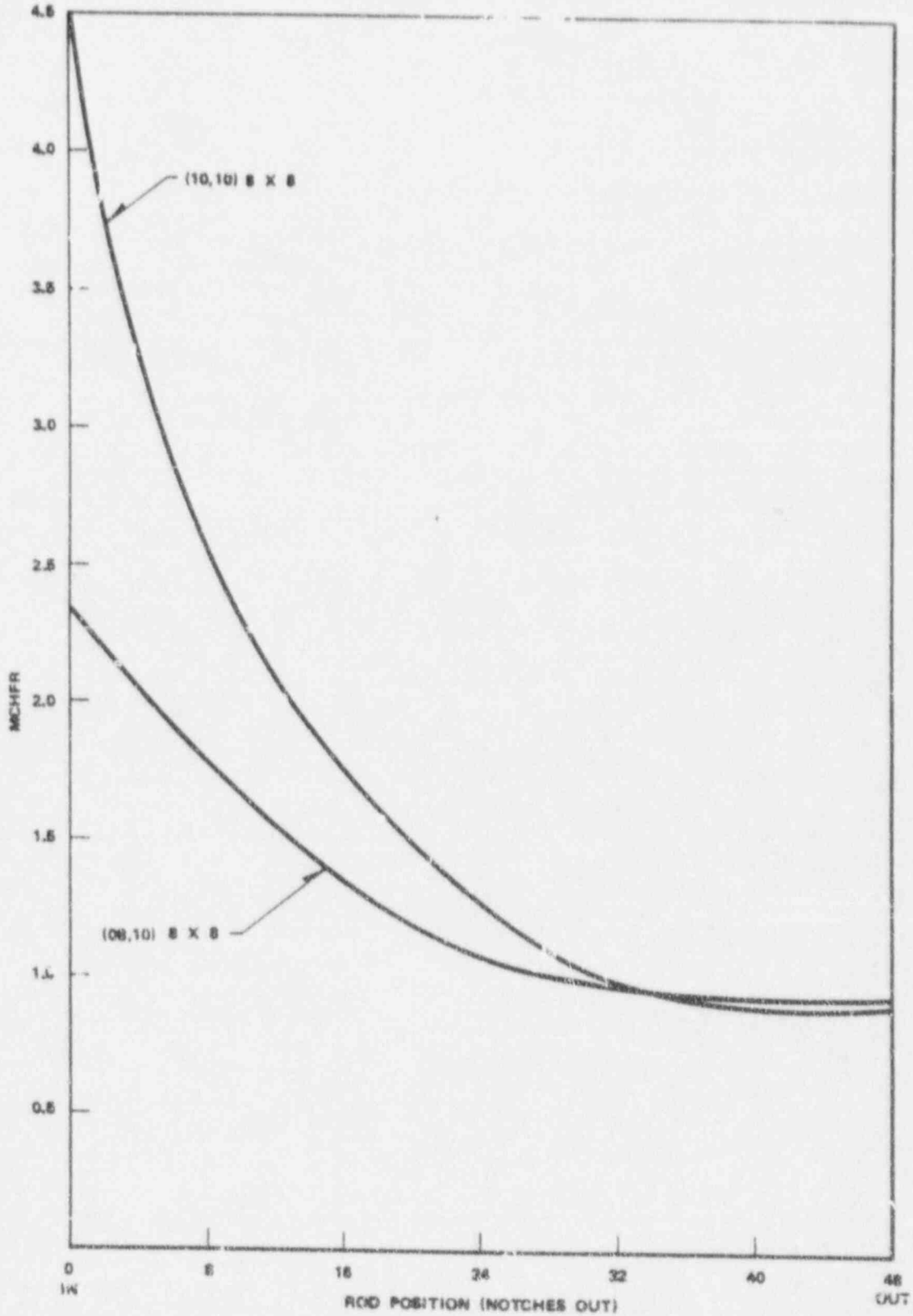

Figure 6-29. MCHFR vs. Rod Position Limiting Rod Withdrawal 8 X 8

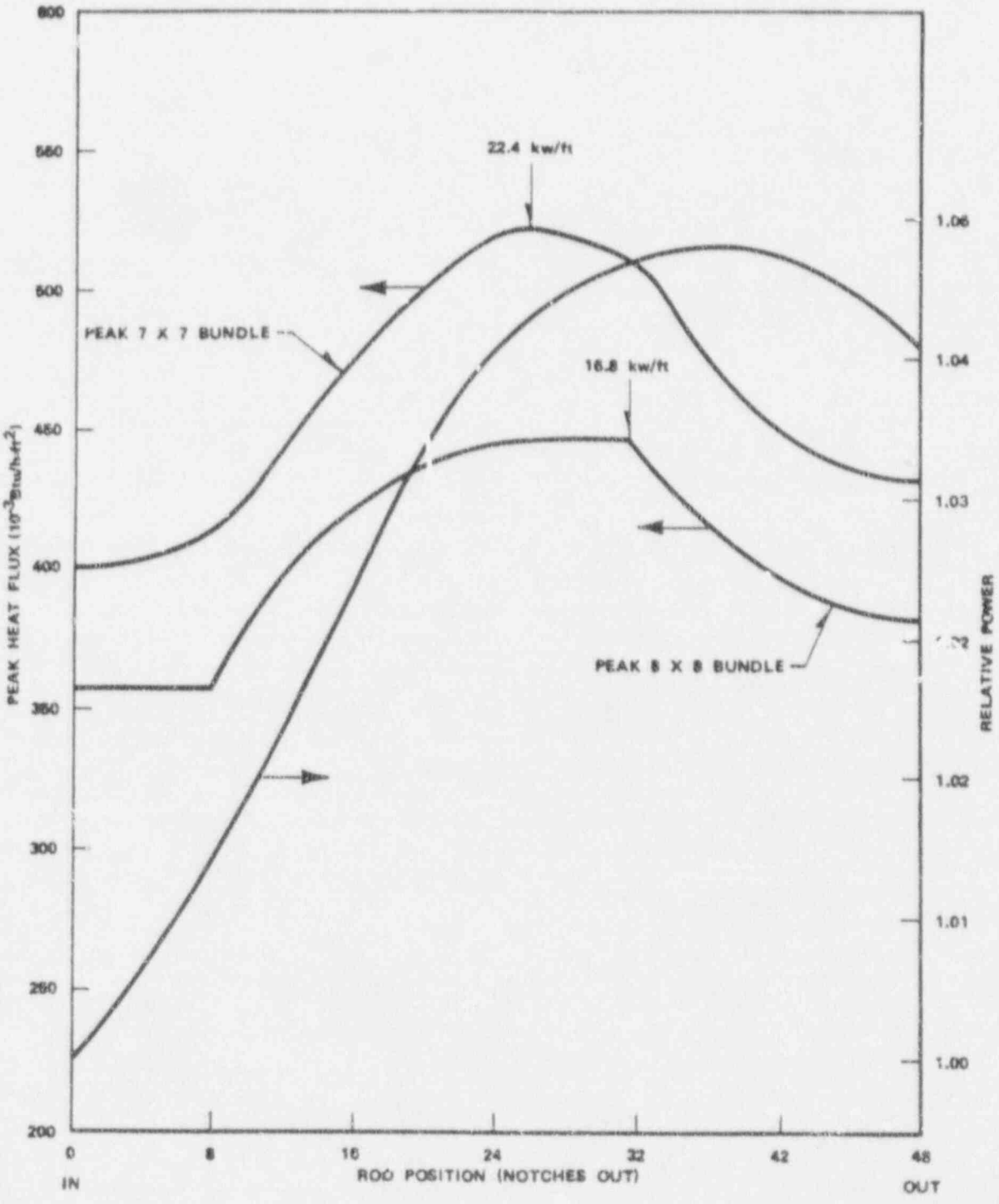

Figure 6-30. Peak Heat Flux and Relative Power vs. Rod Position Limiting Rod Withdrawal Monticello BOC3

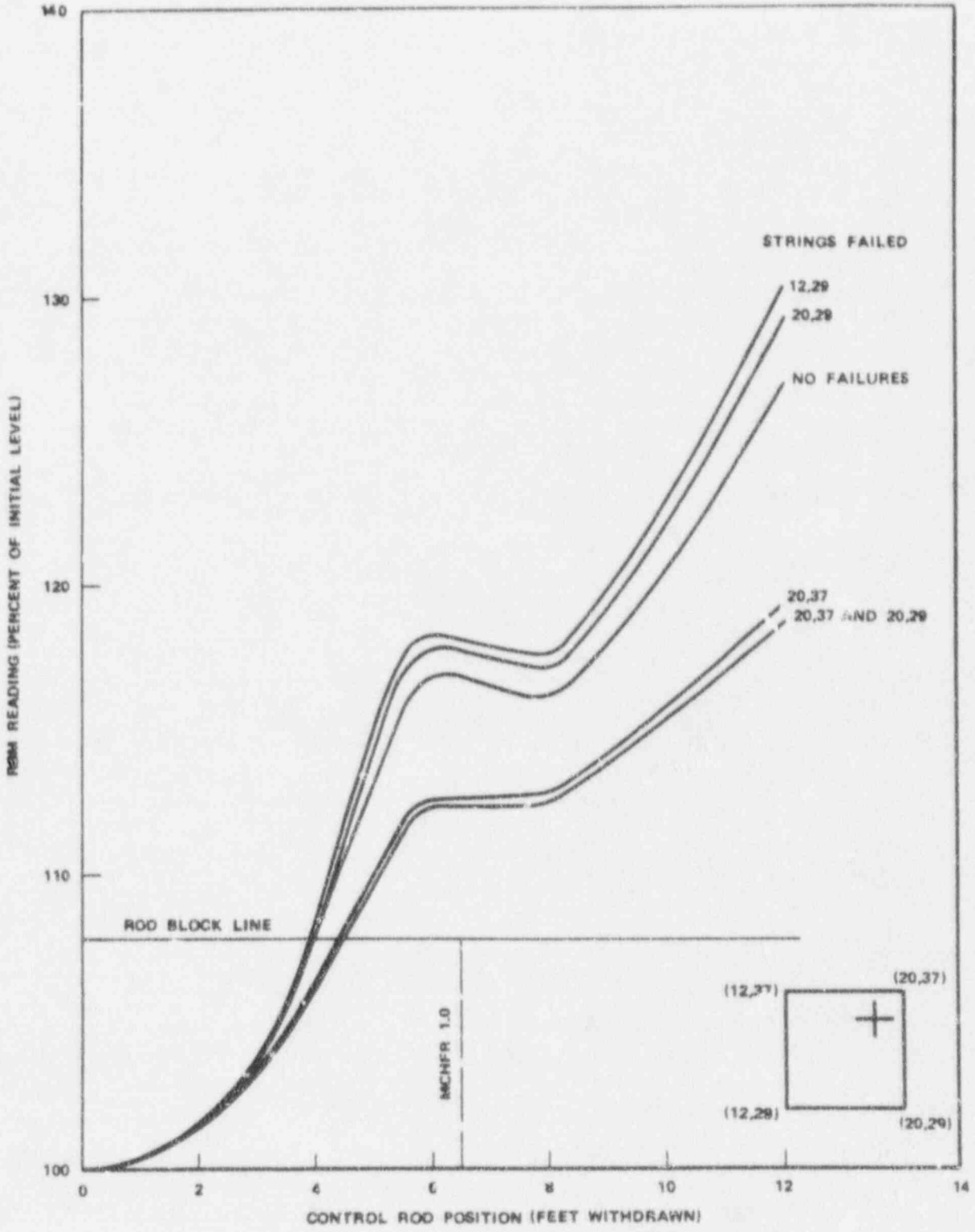

Figure 6-31. RBM Response to Control Rod Motion – Monticello Channel A + C Limiting Rod Withdrawal

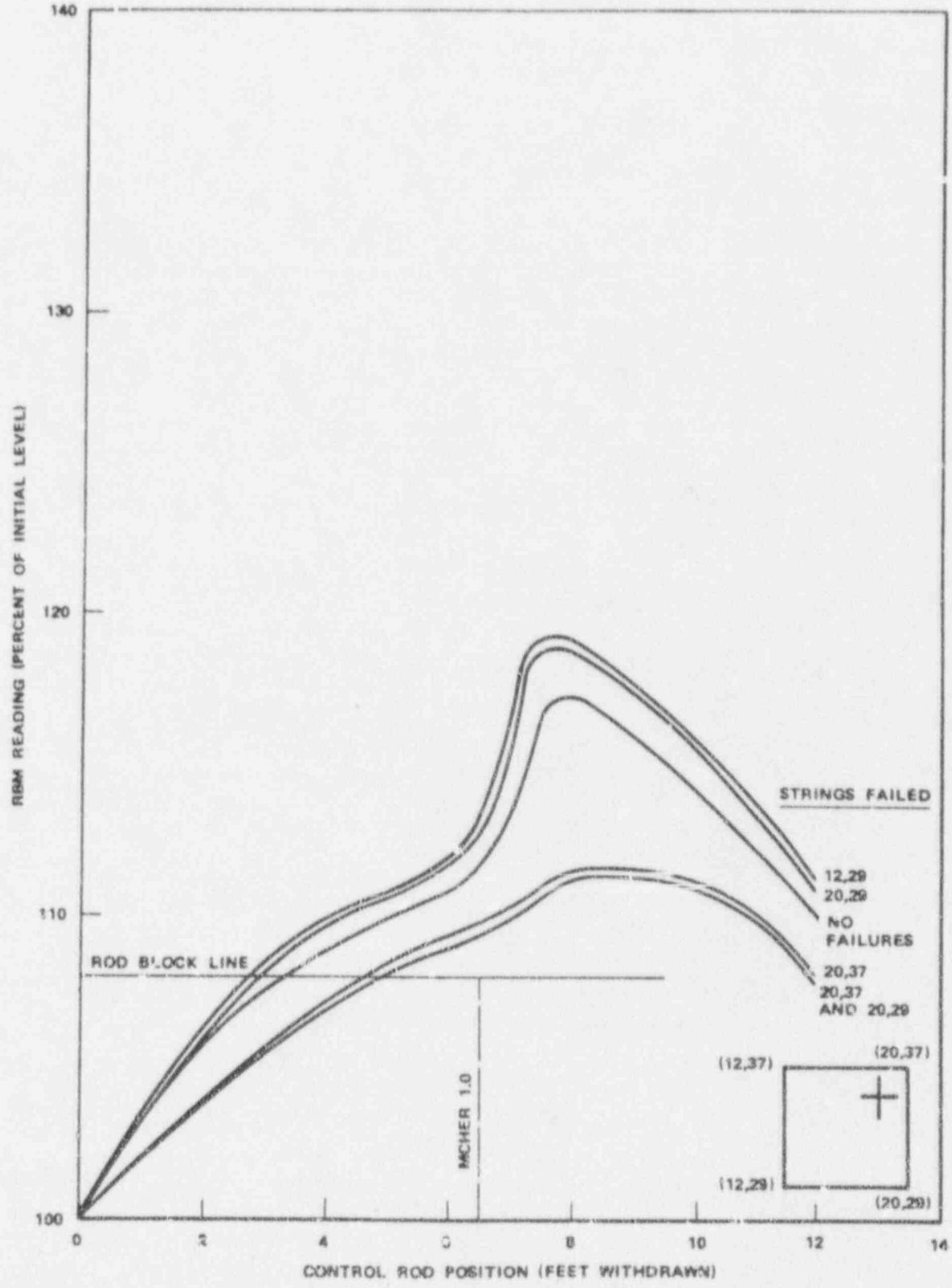

Figure 6-32. RBM Response to Control Rod Motion in Monticello Channel B + D Limiting Rod Withdrawal

Two major design changes, as well as the introduction of 8x8 fuel and modified control rod scram times, are being planned for Cycle 3 and have been incorporated in the digital model used for the analysis. The replacement of the four safety valves with combination safety/relief valves of the the same type as the existing RV's is a proposed change designed to improve pressure relief margins and eliminate the interaction of relief and safety valves. Six Target Rock combination safety/relief valves are considered in this analysis. A second major design change, a Prompt Relief Trip (PRT) system, is planned to increase the effectiveness of the safety/relief valves in maintaining pressure and thermal margins when the plant is subjected to severe steam flow disturbances.

The control rod scram time used was the same as the present Technical Specification scram time up to 50% insertion; a straight extension to the 90% insertion was used, changing that point from 5.0 seconds to 3.5 seconds. The analyses used the Design Basis Scram Reactivity Curve (D Curve) defining the generic outer bound scram reactivity function. The scram reactivity curve and scram time curve are shown in Figures 6-33 and 6-34.

The PRT system provides an immediate trip of six safety/relief valves in response to a turbine trip (stop valve closure) or a generator load rejection (fast closure of the control valves) from high reactor power levels. This system is a major improvement for the scram reactivity considerations discussed at length in earlier submittals.[11,15,16] The PRT system will be discussed in detail in a separate document to be submitted later; included will be a functional description of the system, its objectives, operating characteristics and other considerations. The reload analyses were based on the following operating conditions (except for special cases requiring initial conditions at less than rated power and flow):

Thermal Power	1670 MWt (T-G Design)
T-G Design Steam Flow	6.77×10^6 lb/hr

Turbine Inlet Pressure	980 psig
Jet Pump M Ratio	1.59
Bypass Capacity	15% - Design Flow
Safety/Relief Valve Capacity (6 valves at 1080 psig +1%)	71.1% - Design Flow
Safety/Relief Valve Time Delay	0.4 sec
Safety/Relief Valve Stroke Time	0.1 sec
Scram Rod Drive (Figure 6-33)	67B (3.5 seconds at 90% stroke)
Scram Curve (Figure 6-34)	Design Basis "D"
Feedwater Capacity	105% - Design Flow
Feedwater Temperature	376°F

6.2.4.1 Identification of Abnormal Operational Transients

A complete range of single-failure-caused events which are abnormal but reasonably expected to occur during the life of the plant were analyzed as part of the original licensing of the plant. These analyses were described in the FSAR. Subsequent submittals have, where appropriate, included additional consideration of those events of significance to the concept being reported (i.e., reloads, changes to transient analysis parameters, or plant modifications). [11,14,15,16]

A complete evaluation of all transient events (abnormal operational transients) was performed in support of this reload to ensure all previously established requirements were met. This extensive reanalysis was deemed necessary in view of the significant plant changes being concurrently applied to Monticello during the forthcoming refueling outage.

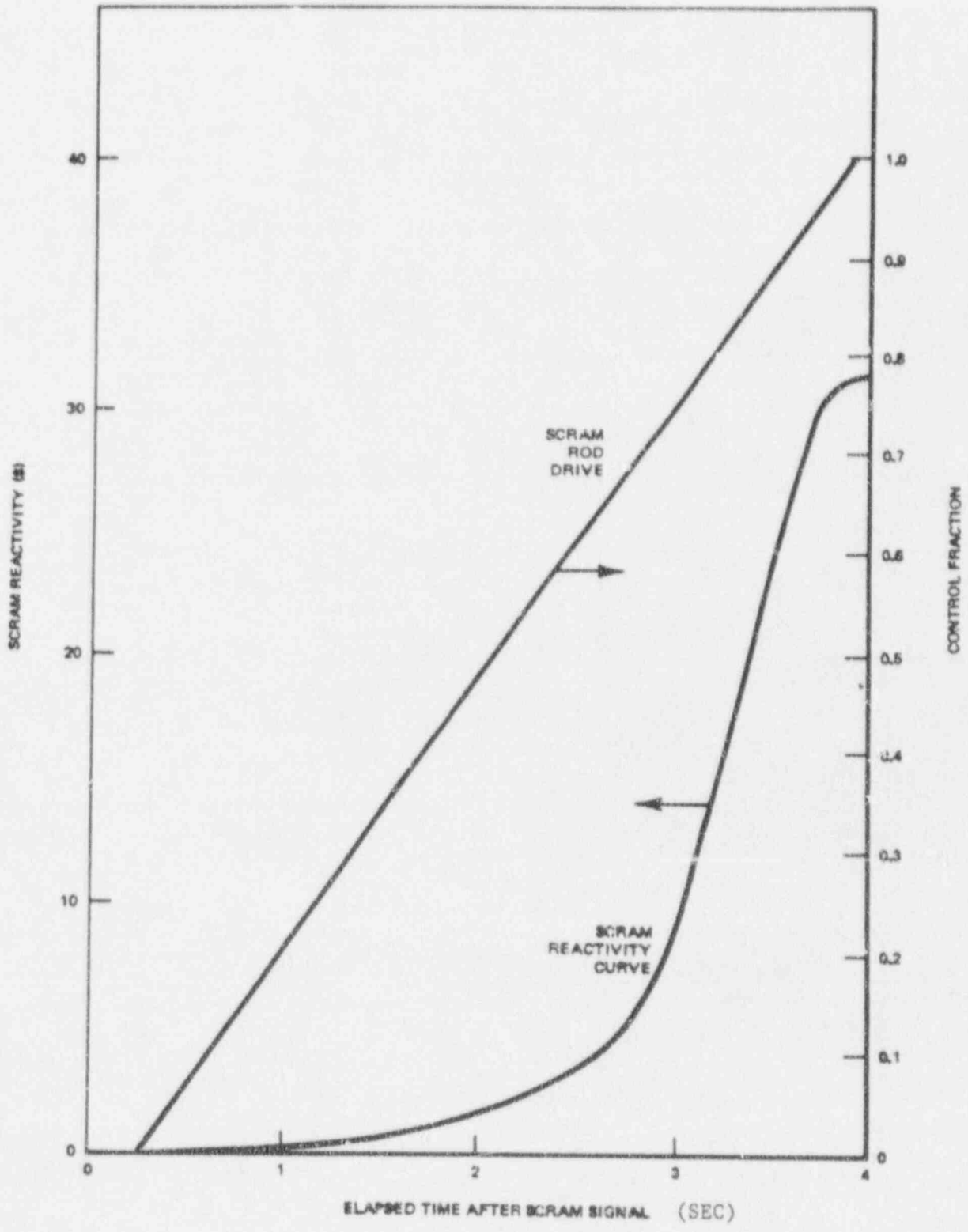

Figure 6-33. Scram Reactivity Curve

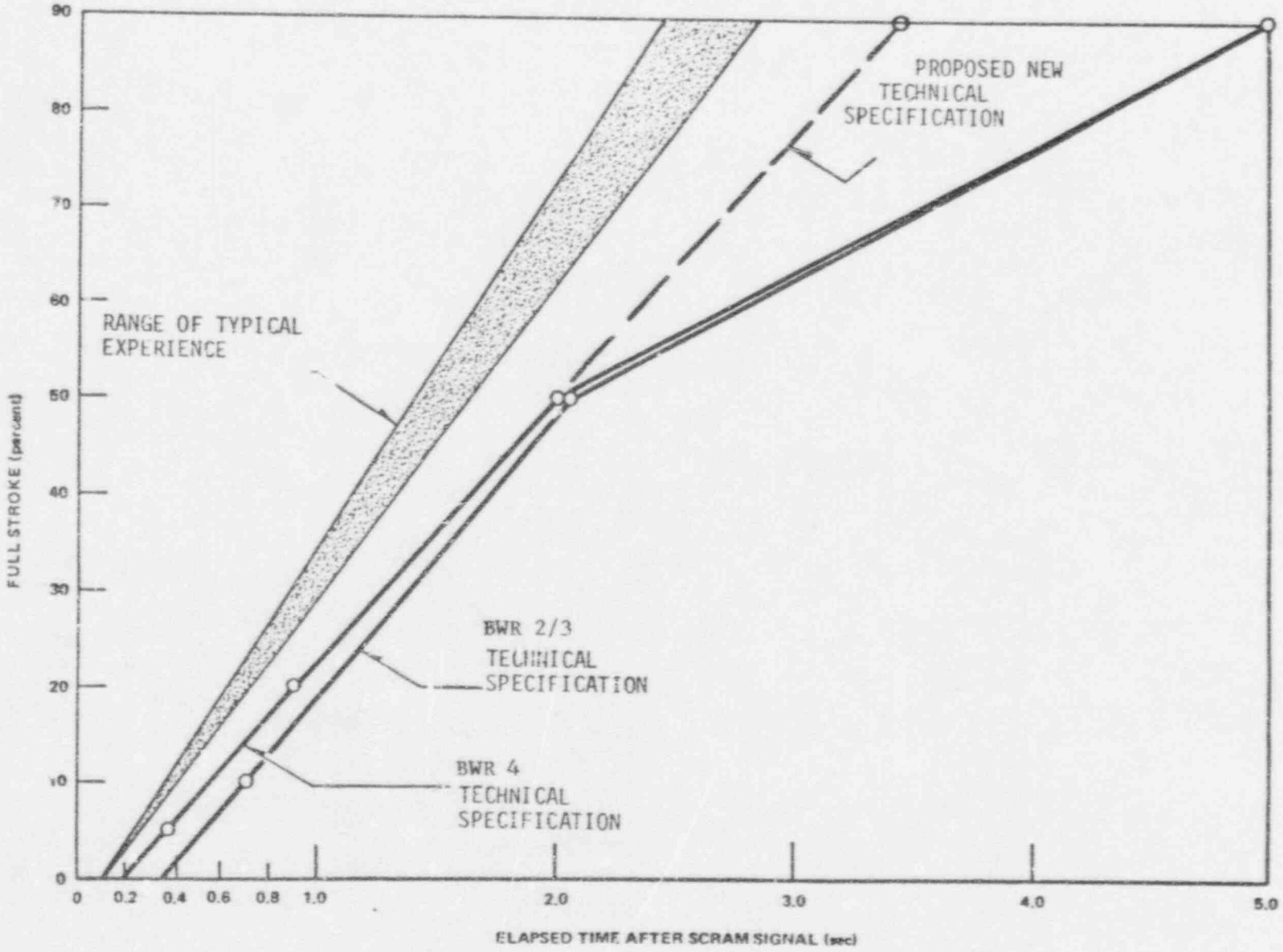

Figure 6-34. Control Rod Drive Scram Times

The transient reanalyses included the following nuclear system parameter variations:

1. nuclear system pressure increases;
2. reactor vessel water (moderator) temperature decreases;
3. positive reactivity insertions;
4. reactor vessel coolant inventory decreases;
5. reactor core coolant flow increases; and
6. reactor core coolant flow decreases.

The complete reanalysis of the affected FSAR abnormal operational transients shows that the reload core satisfies MCHFR, heat flux and over pressure requirements as described here and in Reference 10. Only those transients resulting in system pressure increases are significantly affected by the planned reactor pressure relief system modifications, the use of the D scram reactivity curve, and the new scram times. The detailed results of all Abnormal Operational Transients will be presented in the forthcoming analysis based on these permanent solutions to changing scram reactivity conditions. While specific details of the modification may change prior to the installation, the basic operational aspects should not; the analyses are expected to remain essentially the same.

6.2.5 Loading Error

The worst case loading error for the reference core configuration occurs when a reload bundle is rotated 180 degrees in a location near the center of the core.

Proper orientation of fuel assemblies in the reactor is readily verified by visual observation and is assured by verification procedures during core loading. Five separate visual indications of proper fuel assembly orientation exist:

1. The channel fastener assemblies, including the spring and guard used to maintain clearances between channels, are located at one corner of each fuel assembly adjacent to the center of the control rod.

2. The identification boss on the fuel assembly handle points toward the adjacent control rod.

3. The channel spacing buttons are adjacent to the control rod passage area.

4. The assembly identification numbers on the fuel assembly handles are all readable from the direction of the center of the cell.

5. There is cell-to-cell replication.

Experience has demonstrated that these design features are clearly visible so that any misoriented fuel assembly would be readily distinguished during core loading verification.

If, however, through an error, a fuel assembly were installed rotated 180° from the proper orientation, which is the worst case rotational error for any exposure level, no fuel damage would be incurred during the subsequent power operation, even if the misoriented assembly were operating at the maximum permitted power. Analysis shows that this error would result in a MLHGR $\leq$16.3 kW/ft and a MCHFR $\geq$1.51 for a rotated R2 bundle. These are less than the damage limits established for this fuel. Should the loading error involve one of the irradiated assemblies, the analysis in Reference 11 (reporting that no fuel damage would be incurred) is applicable for the Cycle 3 core.

REFERENCES - SECTION 6

1. Paone, C. J., and Woolley, J. A., "Rod Drop Accident Analysis for Large Boiling Water Reactors," Licensing Topical Report, March 1972 (NEDO-10527).

2. Stirn, R. C., Paone, C. J and Young, R. M., "Rod Drop Accident Analysis for Large BWRs," Licensing Topical Report, July 1972 (NEDO-10527, Supplement 1).

3. Stirn, R. C., Paone, C. J., and Haun, J. M., "Rod Drop Accident Analysis for Large Boiling Water Reactors Addendum No. 2 Exposed Cores," Licensing Topical Report, January 1973 (NEDO-10527, Supplement 2).

4. "Technical Basis for Changes to Allowable Rod Worth Specified in Technical Specification 3.3.8.3 (a)," submitted to AEC October 4, 1973, Dkt. 50-263.

5. Slifer, B. C., and Rogers, A. E., "Loss-of-Coolant Accident and Emergency Core Cooling Models for General Electric Boiling Water Reactors," Licensing Topical Report, April 1971 (NEDO-10329 and NEDO-10329 Supplement 1).

6. Duncan, J. D., and Leonard, J. E., "Modeling the BWR/6 Loss-of-Coolant Accident: Core Spray and Bottom Flooding Heat Transfer Effectiveness," March 1973 (NEDE-10801).

7. Linford, R. B., "Analytical Methods of Plant Transient Evaluations for the General Electric Boiling Water Reactor," February 1973 (NEDO-10802).

8. "In-Core Nuclear Instrumentation Systems for Oyster Creek Unit 1 and Nine Mile Point Unit 1 Reactors," August 1968 (APED-5456).

9. Morgan, W. R., "In-Core Neutron Monitoring System for General Electric Boiling Water Reactors," November 1968, revised April 1969 (APED-5706).

10. Monticello Nuclear Generating Plant, FSAR, Dkt. 50-263.

11. Monticello Nuclear Generating Plant, First Reload License Submittal, February 1973.

12. Millstone Unit 1, FSAR Amendment 14, Dkt. 50-245.

13. "Fuel Densification Effects on General Electric Boiling Water Reactor Fuel, Supplement 6, 7, and 8, Composite," August 1973 (NEDM-10735).

14. "Results of Transient Reanalysis for Monticello Nuclear Generating Plant with End-of-Cycle Core Dynamic Characteristics," February, 1973.

15. "Monticello - Safety Valve Setpoint Increase Analysis," Change request dated September 3, 1973.

16. "Monticello - Cycle 2 Scram Reactivity Considerations, Analyses and Modifications," October 1973.

7. TECHNICAL SPECIFICATIONS

There are four areas of the Technical Specifications affected by the preceeding information. Changes made necessary by the reactor pressure relief system modifications discussed in Section 6.2.4 will be outlined in the forthcoming submittal on that subject. The formal request for Technical Specification changes will be a separate, subsequent submittal. Specifications affected by this submittal include the following:

Section 2 - The heat flux of a 7x7 fuel assembly operating up to 17.5 kw/ft results in a 3.08 total peaking factor. Changes should reflect the use of 8x8 fuel operating up to 13.4 kw/ft resulting in a 3.04 total peaking factor.

Section 3.3.C - The transient analysis (Section 6.2.4) was done based on a control rod scram time to 90% insertion of 3.5 seconds rather that 5.0 seconds as presently allowed. The Specification will be changed accordingly.

Section 3.5.K - The 8x8, R-2 fuel will have unique properties for consideration of postulated fuel densification phenomena. Since the AEC staff model requires the use of measured pellet theoretical density, this information can not be finalized until the fuel is fabricated.

Section 5.2 - The facility description states that fuel assemblies have 49 fuel rods each. This must be changed to allow the use of 8x8, 63 fuel rod assemblies.